(2)

AD-A239 175

MENTATION PAGE

Form Approved
OMB No. 0704-0188

estimated to average 1 hour per response, including the time for reviewing instructions, searching existing data sources, g and reviewing the collection of information. Send comments regarding this burden estimate or any other aspect of this collection of information, including suggestions for reducing this burden, to Washington Headquarters Services, Directorate for information Operations and Reports, 1215 Jefferson Davis Highway, Suite 1204, Arlington, VA 22202-4302, and to the Office of Management and Budget, Paperwork Reduction Project (0704-0188), Washington, DC 20503.

1. AGENCY USE ONLY (Leave blank)	2. REPORT DATE	3. REPORT TYPE AND DATES COVERED
		FINAL 15 Aug 87 to 14 Aug 90

4. TITLE AND SUBTITLE

DIGITAL CONTROL AND IDENTIFICATION OF DISTRIBUTED SYSTEMS

5. FUNDING NUMBERS

AFOSR-87-0373
61102F 2304/A1

6. AUTHOR(S)

J.S. GIBSON

7. PERFORMING ORGANIZATION NAME(S) AND ADDRESS(ES)

MECHANICAL, AEROSPACE AND NUCLEAR ENGINEERING
UNIVERSITYOF CALIFORNIA
LOS ANGELES,CA 90024-1597

8. PERFORMING ORGANIZATION REPORT NUMBER

AFOSR-TR-90

9. SPONSORING/MONITORING AGENCY NAME(S) AND ADDRESS(ES)

AFOSR/NM
Bldg 410
Bolling AFB DC 20332-6448

10. SPONSORING/MONITORING AGENCY REPORT NUMBER

AFOSR-87-0373

11. SUPPLEMENTARY NOTES

12a. DISTRIBUTION/AVAILABILITY STATEMENT

Approved for public release;
distribution unlimited.

12b. DISTRIBUTION CODE

13. ABSTRACT *(Maximum 200 words)*

Research has been conducted in the following general areas; Optimal Control of Distributed Parameter System, Adaptive Identification and Control, and Robust Control. Work includes research in approximation theory and numerical methods for the design of finite dimensional compensators for optimal control of systems represented by partial differential equations, and adaptive control and tracking problems for flexible structures and manipulators with flexible links and joints.

14. SUBJECT TERMS	15. NUMBER OF PAGES
	16. PRICE CODE

17. SECURITY CLASSIFICATION OF REPORT	18. SECURITY CLASSIFICATION OF THIS PAGE	19. SECURITY CLASSIFICATION OF ABSTRACT	20. LIMITATION OF ABSTRACT
UNCLASSIFIED	UNCLASSIFIED	UNCALSSIFIED	SAR

A-1

FINAL REPORT
AFOSR GRANT 87-0373
August 15, 1987—August 14, 1990

Digital Control and Identification of Distributed Systems

J.S. Gibson
Mechanical, Aerospace and Nuclear Engineering
University of California, Los Angeles 90024-1597

91-06924

This grant has supported research in the following areas:

- Optimal Control of Distributed Systems
- Adaptive Identification
- Adaptive Control
- Robust Control

The Publications section of this report lists six PhD dissertations and sixteen research papers produced by research supported in whole or in part by this grant. Most of these publications have been provided to AFOSR previously. The Appendix to this report contains five of the research papers, which are representative of the project.

Optimal Control of Distributed Systems

The main focus of this component of the research is approximation theory and numerical methods for design of finite dimensional compensators for optimal control of systems represented by linear partial and functional differential equations. The primary class of applications is large flexible space structures. Papers dealing mainly with approximation theory and numerical methods for optimal control of distributed systems are [1, 2, 3, 4]. The paper [5] has substantial results on approximation of digital input/output models, as well as results on infinite dimensional system theory that are useful in adaptive identification and control of distributed systems. The paper [6], which deals exclusively with stability theory for a class of wave equations, is motivated by certain stability issues that arise in approximation theory for control of equations governing many flexible structures.

Adaptive Identification

This segment of the research has dealt with fast methods for real-time adaptive identification and prediction of systems with unknown parameters and unknown order. The class of such methods to which this research has contributed most is least-squares lattice filters. The paper [7] demonstrated the application of a lattice filter for adaptive identification and prediction of an experimental flexible structure. The paper [8] and the PhD dissertation [9] developed a new lattice filter, called an unwindowed lattice, which achieves much faster convergence to parameter estimates and accurate prediction than prewindowed lattices.

Adaptive Control

This part of the research has concentrated on adaptive control and tracking problems for flexible structures and manipulators with flexible links and joints. The papers [10, 11, 12, 13, 14] and the PhD dissertations [15, 16, 17] have developed adaptive control methods that appear to have wide application to flexible space structures and high-speed manipulators.

Robust Control

The goal of this part of the research has been to develop numerically efficient methods for determining robustness margins for control systems with uncertain parameters and for designing plants and controllers that have desired robustness margins. For parameter values within these robustness margins, the systems are guaranteed to be asymptotically stable. The papers [18, 19] presented new robustness margins along with numerically efficient methods for computing these margins, and the paper [20] presented a method for numerical design of robust control systems. These papers were based on the PhD dissertations [21, 22].

Publications Supported by This Grant

[1] J.S. Gibson, I.G. Rosen, and G. Tao, "Approximation in Control of Thermoelastic Systems," in *Proceedings of 1989 American Control Conference*, (Pittsburgh, PA), pp. 1171–1176, June 1989.

[2] J.S. Gibson, I.G. Rosen, and G. Tao, "Approximation in LQG Optimal Control of a Thermoelastic Rod," in *Proceedings of 3rd Annual Conference on Aerospace Computational Control*, (Oxnard, CA), August 1989.

[3] J.S. Gibson, I.G. Rosen, and G. Tao, "Approximation in Control of Thermoelastic Systems,". *SIAM Journal on Control and Optimization*, to appear.

[4] J.S. Gibson and A. Adamian, "A comparison of three approximation schemes for optimal control of a flexible structure," 1990. To appear in *SIAM Frontiers Edition on Control of Distributed Parameter Systems.*

[5] J.S. Gibson and F. Jabbari, "A digital input/output model for trace class systems," *Journal of Mathematical Analysis and Applications*, vol. 144, pp. 89–108, November 1989.

[6] J.S. Gibson, "Uniform Exponential Stability of Solutions to Abstract Linear Wave Equations with Coercive Damping,". Submitted to *Quarterly of Applied Mathematics.*

[7] F. Jabbari and J.S. Gibson, "Adaptive Identification of a Flexible Structure by Lattice Filters," *AIAA Journal of Guidance, Control, and Dynamics*, vol. 12, pp. 548–554, July 1989.

[8] S.W. Chen and J.S. Gibson, "A new unwindowed lattice filter for RLS estimation," . To appear in *IEEE Transactions on Acoustics, Speech, and Signal Processing.*

[9] S.W. Chen, *Unwindowed Lattice Filters and Application to Variable-order Adaptive Control.* PhD thesis, University of California, Los Angeles, 1991.

[10] J.S. Gibson and F. Jabbari, "A variable-order adaptive controller for a flexible system," in *1989 American Control Conference*, (Pittsburgh, PA), June 1989.

[11] Y.P. Yang and J.S. Gibson, "Adaptive Control of a Manipulator with a Flexible Link," *Journal of Robotic Systems*, vol. 6, pp. 217–232, June 1989.

[12] Y.K. Kim and J.S. Gibson, "A variable-order adaptive controller for a manipulator with a sliding flexible link," . To appear in *IEEE Transactions on Robotics and Automation.*

[13] S.M. Kim and J.S. Gibson, "Adaptive LQ tracking with efficient use of future reference signals," 1989. Submitted to *International Journal of Control.*

[14] S.M. Kim and J.S. Gibson, "Digital adaptive control of robotic manipulators with flexible joints," 1990. Submitted to *IEEE Journal of Robotics and Automation.*

[15] Y.K. Kim, *Adaptive control of a robotic manipulator with a sliding flexible link.* PhD thesis, University of California, Los Angeles, 1988.

[16] Y.P. Yang, *Adaptive control of a robotic manipulator with a flexible link.* PhD thesis, University of California, Los Angeles, 1988.

[17] S.M. Kim, *Adaptive LQ Tracking of MIMO systems and its application to robotic manipulators with flexible joints.* PhD thesis, University of California, Los Angeles, 1990.

[18] M.A. Leal and J.S. Gibson, "A first-order Lyapunov robustness method for linear systems with uncertain parameters," *IEEE Trans. AC*, vol. 35, pp. 1068–1070, September 1990.

[19] U.L. Chen and J.S. Gibson, "A Lyapunov robustness bound for linear systems with periodic coefficients," 1991. To appear in *Automatica.*

[20] M.A. Leal and J.S. Gibson, "Design of a robust control system by optimizing a Lyapunov robustness criterion," in *American Automatic Control Conference*, (Boston, MA), p. , June 1991.

[21] M.A. Leal, *Objective and constraint functions for the analysis and design of robust control systems.* PhD thesis, University of California, Los Angeles, 1988.

[22] U.L. Chen, *Analysis and design of robust control systems: a first-order Lyapunov approach.* PhD thesis, University of California, Los Angeles, 1990.

APPENDIX

Approximation in Control of Thermoelastic Systems

J.S. Gibson *
Mechanical, Aerospace and Nuclear Engineering
University of California, Los Angeles 90024

I.G. Rosen †
Center for Applied Mathematical Sciences
Department of Mathematics
University of Southern California, Los Angeles 90089

G. Tao
Department of Electrical Engineering
Washington State University, Pullman, WA 99164

June 1, 1991

Abstract

This paper develops an abstract framework for analysis and approximation of linear thermoelastic control systems, and for design of finite-dimensional compensators. The thermoelastic systems in this paper consist of abstract wave and diffusion equations coupled in a skew self-adjoint fashion. Linear semigroup theory is used to establish that the abstract thermoelastic models are well posed and to prove convergence of generic approximation schemes. Open-loop uniform exponential stability for a subclass of thermoelastic systems is proved via a Lyapunov function. An example involving the design of an optimal LQG compensator for a thermoelastic rod illustrates the application of the abstract theory. Results of an extensive numerical study, including a comparison of the closed-loop performance of different compensator designs, are presented and discussed.

*This author was supported by AFOSR Grant 87-0373.
†This author was supported by AFOSR Grant 87-0356.

1 Introduction

The transfer of energy between its mechanical form and heat generally has been ignored as a source of both structural damping and excitation in the vast literature on control of flexible structures. Only a few recent papers have considered control of thermoelastic structures [1, 2, 3, 4, 5], [6, 7, 8, 9]. However, the thermally induced vibrations that hampered the recently launched Hubble space telescope have highlighted the coupling between mechanical vibration and heat transfer and the need to model and control thermoelastic phenomena in flexible structures.

This paper has two main objectives: first, to develop a theoretical framework for analysis and approximation in the design of feedback control systems for a broad class of linear thermoelastic systems; second, to illustrate the application of the theory by presenting the most interesting results from an extensive numerical study of LQG optimal control of a thermoelastic rod. Both the theory and the example focus on numerical methods and convergence analysis for the design of finite-dimensional compensators based on finite-dimensional approximations of distributed models of thermoelastic systems.

By a thermoelastic system, we mean an abstract wave equation coupled in a skew self-adjoint fashion with a diffusion equation. While some of the theory developed here pertains specifically to problems in which the generalized wave equation is second-order (in time), much of the theory applies to a broader class of problems, including, for example, problems in which a Schrodinger equation is coupled with a diffusion equation. In this paper, we are particularly interested in second-order generalized wave equations because they are common in flexible structures, but the results here that allow a more general class of wave equations are intended to apply also to problems such as thermal blooming in lasers [10]. Although the theoretical framework developed in this paper handles a wide variety of thermoelastic systems, it is not clear whether our hypotheses hold for the thermo-viscoelastic systems with memory studied by Burns et al. [1, 2, 3].

Our philosophy in the abstract formulation of thermoelastic control systems in Section 2 and in the approximation theory in Section 4 is to base the results on hypotheses that require as little as possible beyond conditions that normally hold for the individual wave and diffusion equations. This means that, in analyzing a particular application, most of the work is done on the uncoupled wave and diffusion equations, and the work required to couple the systems is minimized. For example, in verifying the hypotheses for Theorem 4.6, which concerns convergence of approximations to the open-loop thermoelastic system, once the convergence conditions for independent approximations to the uncoupled wave and diffusion equations are verified, no further work is necessary to guarantee convergence of the approximations to the thermoelastic system when the straightforward Galerkin scheme that we assume for approximating the coupling operator is used.

The approach to compensator design in Sections 3 and 4.1 of this paper is to approximate an ideal infinite-dimensional LQG compensator with a sequence of finite-dimensional compensators. However, the abstract formulation of thermoelastic control systems in Section 2, the approximation and convergence theory in Section 4.2, and the result in Section 5 on open-loop uniform exponential stability should be useful in any method for analysis and design of controllers for thermoelastic systems.

An important issue in both convergence of the approximating compensators and performance of the closed-loop systems is uniform exponential stability of the open-loop thermoelastic system. While several authors [6, 11, 4, 12, 13] have proved strong stability for various linear and nonlinear thermoelastic systems, few results have been published on uniform exponential stability. A result in [12] on integrability of the energy, when applied to the linear case, yields uniform exponential stability for thermoelastic rods with certain sets of boundary conditions. Also, a recent eigenvalue analysis in [6] yields uniform exponential stability for linear thermoelastic rods with the same sets of boundary conditions to which the result in [12] applies. The proof of our Theorem 5.1 uses a Lyapunov function to establish uniform exponential stability for a large class of linear thermoelastic systems, but does not improve on the results in [6] and [12] for the rod. The results in [6, 12] and

our Section 5 do not apply to the set of boundary conditions for which uniform exponential stability has been proved recently in [14].

In Section 6, we apply the theory developed in Sections 2–5 to design finite dimensional compensators for a thermoelastic rod. We present numerical results for the functional control and estimator gains that represent the compensators graphically. We also compare the closed-loop eigenvalues produced by three of the finite-dimensional compensators based on different damping models. These eigenvalues were obtained from simulations in which each compensator was connected to a model of the rod with dimension significantly higher than the dimension of the compensator. This comparison illustrates the importance of modelling even very light thermoelastic damping, or possibly an artificial viscous equivalent, if no stronger damping mechanism is present.

2 Abstract Thermoelastic Systems

Throughout this paper, H or $H_j\,(j = 0,1,2)$ will be a Hilbert space with inner product $\langle\cdot,\cdot\rangle$ or $\langle\cdot,\cdot\rangle_j$ and corresponding induced norm $|\cdot|$ or $|\cdot|_j$. Also, V or V_j will be a reflexive Banach space with norm $\|\cdot\|$ or $\|\cdot\|_j$. The continuous dual of V will be denoted by V', and

$$V \hookrightarrow H \hookrightarrow V' \tag{2.1}$$

will mean that V is embedded densely and continuously in H, which implies that H is embedded densely and continuously in V' (see, for example, [15, 16]). In this case, $\langle\cdot,\cdot\rangle$ will denote both the H-inner product and the duality pairing on $V \times V'$.

Lemma 2.1 *Let V and H be related as in (2.1), let $\mathcal{A}$ be a linear isomorphism (i.e., a continuous linear bijection with continuous inverse) from V to V' such that $\mathcal{A}$ is dissipative in the sense that*

$$\mathrm{Re}\langle v, \mathcal{A}v\rangle \le 0 \;\; \forall v \in V, \tag{2.2}$$

and define

$$\mathrm{Dom}(A) = \mathcal{A}^{-1}H, \qquad A = \mathcal{A}|_{\mathrm{Dom}(A)}. \tag{2.3}$$

Then $\mathrm{Dom}(A)$ is dense in H and $A^{-1} \in \mathcal{B}(H,H)$. Also, A is a maximal dissipative operator on H.

Proof That $\mathrm{Dom}(A)$ is dense in H follows from the fact that H is dense in V' and $\mathcal{A}^{-1}$ is bounded from V' to H. To see that A is maximal dissipative, suppose that there exists a dissipative linear operator $\tilde{A} : \mathrm{Dom}(\tilde{A}) \subset H \to H$ that is a proper extension of A. Since $\mathcal{R}(A) = H$, there exists $h \in \mathrm{Dom}(\tilde{A})\backslash\mathrm{Dom}(A)$ and $v \in \mathrm{Dom}(A)$ such that $h \neq 0$, $\tilde{A}h = 0$, and $Av = h$. Then, for any real α, $\langle v + \alpha h, \tilde{A}(v + \alpha h)\rangle = \langle v, Av\rangle + \alpha|h|^2$, and, for sufficiently large $\alpha > 0$, $\mathrm{Re}\langle v + \alpha h, \tilde{A}(v + \alpha h)\rangle > 0$, contradicting the dissipativity of $\tilde{A}$. □

Theorem 2.2 *Let the Hilbert space H_1, the reflexive Banach space V_1 and the operator $\mathcal{A}_1$ be as in* Lemma 2.1. *Let the Hilbert space H_2 and the reflexive Banach space V_2 be as in* Lemma 2.1, *and let $\mathcal{A}_2$ be a linear isomorphism from V_2 to V_2' that is V_2-coercive; i.e., there exists a positive real number α such that*

$$\mathrm{Re}\langle \phi, \mathcal{A}_2\phi\rangle_2 \ge \alpha\|\phi\|_2^2, \qquad \phi \in V_2. \tag{2.4}$$

Also, let $\mathcal{L} \in \mathcal{B}(V_1, V_2')$. Define

$$H = H_1 \times H_2, \qquad V = V_1 \times V_2 \tag{2.5}$$

and

$$\mathcal{A} = \begin{bmatrix} \mathcal{A}_1 & -\mathcal{L}^* \\ \mathcal{L} & -\mathcal{A}_2 \end{bmatrix} \tag{2.6}$$

where $\mathcal{L}^* \in \mathcal{B}(V_2, V_1')$ is defined by

$$\langle \psi, \mathcal{L}^*\phi\rangle_1 = \overline{\langle \phi, \mathcal{L}\psi\rangle}_2, \qquad \psi \in V_1,\ \phi \in V_2 \tag{2.7}$$

(i.e., $\mathcal{L}^*$ is the Banach-space adjoint of $\mathcal{L}$). Then H, V, V' and $\mathcal{A}$ are as in Lemma 2.1.

Proof Since $\mathcal{A}_1$ is dissipative and $\mathcal{A}_2$ is V_2-coercive, the operator $(\mathcal{A}_2 - \mathcal{L}\mathcal{A}_1^{-1}\mathcal{L}^*) \in \mathcal{B}(V_2, V_2')$ is V_2-coercive. Hence, for $f_1 \in V_1'$ and $f_2 \in V_2'$, the pair $(v_1, v_2) \in V$ given by

$$v_2 = (\mathcal{A}_2 - \mathcal{L}\mathcal{A}_1^{-1}\mathcal{L}^*)^{-1}(\mathcal{L}\mathcal{A}_1^{-1}f_1 - f_2), \qquad v_1 = \mathcal{A}_1^{-1}(\mathcal{L}^*v_2 + f_1) \tag{2.8}$$

is the unique solution to

$$\mathcal{A}\begin{pmatrix} v_1 \\ v_2 \end{pmatrix} = \begin{pmatrix} f_1 \\ f_2 \end{pmatrix}. \tag{2.9}$$

The mapping that takes (f_1, f_2) to (v_1, v_2) is clearly bounded from $V' = V_1' \times V_2'$ to V. □

Remark 2.3 *We define the adjoint operators $\mathcal{A}_1^* \in \mathcal{B}(V_1, V_1')$, $\mathcal{A}_2^* \in \mathcal{B}(V_2, V_2')$ and $\mathcal{A}^* \in \mathcal{B}(V, V')$ as in* (2.7) *with the appropriate duality pairing in each case. Under the hypotheses of* Theorem 2.2, *$\mathcal{A}_1^*$, $\mathcal{A}_2^*$ and $\mathcal{A}^*$ have the same properities, respectively, as $\mathcal{A}_1$, $\mathcal{A}_2$ and $\mathcal{A}$.*

Remark 2.4 *We define the operator $L : \mathrm{Dom}(L) \subset H_1 \to H_2$ to be the restriction of $\mathcal{L}$ to $\mathrm{Dom}(L) = \{\psi \in V_1 : \mathcal{L}\psi \in H_2\}$. If $\mathrm{Dom}(L)$ is dense in V_1, we define the operator $L^* : \mathrm{Dom}(L^*) \subset H_2 \to H_1$ to be the Hilbert space adjoint of L with respect to the H_1 and H_2 inner products. It can be shown that L^* is the restriction of $\mathcal{L}^*$ to $\mathrm{Dom}(L^*) = \{\phi \in V_2 : \mathcal{L}^*\phi \in H_1\}$.*

For the class of systems of primary interest in this paper, there exist Hilbert spaces H_0 and H_2 and reflexive Banach spaces V_0 and V_2 such that $V_0 \hookrightarrow H_0 \hookrightarrow V_0'$ and $V_2 \hookrightarrow H_2 \hookrightarrow V_2'$ (with each injection continuous and dense). The thermoelastic evolution equations have the form

$$\ddot{w}(t) + \mathcal{D}_0\dot{w}(t) + \mathcal{A}_0 w(t) + \mathcal{L}_0^*\theta(t) = f_0(t), \qquad t > 0, \tag{2.10}$$

$$\dot{\theta}(t) + \mathcal{A}_2\theta(t) - \mathcal{L}_0\dot{w}(t) = f_2(t), \qquad t > 0, \tag{2.11}$$

where $\mathcal{D}_0, \mathcal{A}_0 \in \mathcal{B}(V_0, V_0')$, $\mathcal{L}_0 \in \mathcal{B}(V_0, V_2')$, $\mathcal{A}_2 \in \mathcal{B}(V_2, V_2')$, $f_i \in L_1(0, \tilde{t}; H_i)$ for $i = 0, 2$ and all $\tilde{t} > 0$.

We assume that $\mathcal{A}_0$ is symmetric in the sense that

$$\langle \psi, \mathcal{A}_0\phi\rangle_0 = \overline{\langle \phi, \mathcal{A}_0\psi\rangle}_0, \qquad \phi, \psi \in V_0, \tag{2.12}$$

and that $\mathcal{A}_0$ is V_0-coercive and $\mathcal{A}_2$ is V_2-coercive. We assume that $\mathcal{D}_0$ is nonnegative in the sense that

$$\mathrm{Re}\langle \psi, \mathcal{D}_0\psi\rangle_0 \geq 0, \qquad \psi \in V_0. \tag{2.13}$$

To derive a semigroup generator for the thermoelastic system in (2.10) and (2.11), we first consider the semigroup generator corresponding to (2.10) for the case $\mathcal{L}_0 = 0$. We make V_0 into a Hilbert space by defining

$$\langle \psi, \phi\rangle_{V_0} = \langle \psi, \mathcal{A}_0\phi\rangle_0, \qquad \phi, \psi \in V_0. \tag{2.14}$$

Our hypotheses on $\mathcal{A}_0$ imply that the norm induced by the inner product in (2.14) is equivalent to the original V_0 norm. We define

$$H_1 = V_0 \times H_0, \qquad V_1 = V_0 \times V_0, \tag{2.15}$$

and we identify V_0 with V_0' in the first component of H_1 and V_1 and write $V_1' = V_0 \times V_0'$. It follows that $V_1 \hookrightarrow H_1 \hookrightarrow V_1'$.

Next we define

$$\mathcal{A}_1 = \begin{bmatrix} 0 & I \\ -\mathcal{A}_0 & -\mathcal{D}_0 \end{bmatrix} \in \mathcal{B}(V_1, V_1'). \tag{2.16}$$

That $\mathcal{A}_1$ is an isomorphism from V_1 to V_1' follows from

$$\mathcal{A}_1^{-1} = \begin{bmatrix} -\mathcal{A}_0^{-1}\mathcal{D}_0 & -\mathcal{A}_0^{-1} \\ I & 0 \end{bmatrix} \in \mathcal{B}(V_1', V_1). \tag{2.17}$$

We define A_1 by (2.3) with A, $\mathcal{A}$ and H replaced by A_1, $\mathcal{A}_1$ and H_1, respectively. According to Lemma 2.1, A_1 generates a contraction semigroup on H_1. (See [15, 16, 17, 18] for similar approaches to obtaining semigroup generators of the form in (2.16).) Also, we note that the restriction of $-\mathcal{A}_2$ to $\mathcal{A}_2^{-1}H_2$ generates a uniformly exponentially stable analytic contraction semigroup on H_2. For the thermoelastic system, we define

$$\mathcal{L} = [0 \quad \mathcal{L}_0] \in \mathcal{B}(V_1, V_2') \tag{2.18}$$

to obtain the situation in Theorem 2.2 with $\mathcal{A}_1$ defined by (2.16). The corresponding $\mathcal{A}$ defined by (2.6) is

$$\mathcal{A} = \begin{bmatrix} 0 & I & 0 \\ -\mathcal{A}_0 & -\mathcal{D}_0 & -\mathcal{L}_0^* \\ 0 & \mathcal{L}_0 & -\mathcal{A}_2 \end{bmatrix} \in \mathcal{B}(V, V') \tag{2.19}$$

where

$$V = V_0 \times V_0 \times V_2 \hookrightarrow H = V_0 \times H_0 \times H_2 \hookrightarrow V' = V_0 \times V_0' \times V_2'. \tag{2.20}$$

The semigroup generator A for the thermoelastic system in (2.10) and (2.11) then is defined by (2.3). Explicitly, the domain of this semigroup generator is

$$\mathrm{Dom}(A) = \{(\phi, \psi, \theta) \in V : \mathcal{A}(\phi, \psi, \theta) \in H\}. \tag{2.21}$$

The system in (2.10) and (2.11) now can be written as

$$\dot{x}(t) = Ax(t) + f(t), \qquad t > 0, \tag{2.22}$$

where $x(t) = (w(t), \dot{w}(t), \theta(t)) \in H$ and $f = (0, f_0, f_2) \in L_1(0, \bar{t}; H)$ for all $\bar{t} > 0$. If $\{T(t) : t \geq 0\}$ is the semigroup generated by A, the *mild solution* to the initial value problem consisting of (2.22) and an initial condition $x(0) = (w(0), \dot{w}(0), \theta(0)) \in H$ is

$$x(t) = T(t)x(0) + \int_0^t T(t-s)f(s)ds, \qquad t \geq 0. \tag{2.23}$$

3 The LQG Optimal Control Problem

In the abstract thermoelastic system (2.10)–(2.11), we consider inputs of the form

$$f(t) = Bu(t) + \tilde{B}\gamma(t), \qquad t > 0 \tag{3.1}$$

and an output given by

$$y(t) = Cx(t) + \nu(t), \qquad t > 0, \tag{3.2}$$

where x is the mild solution to (2.22), $u(t) \in R^m$, $\gamma(t) \in R^l$, $y(t) \in R^p$, $\nu(t) \in R^p$, $B \in \mathcal{B}(R^m, H)$, $\tilde{B} \in \mathcal{B}(R^l, H)$, and $C \in \mathcal{B}(H, R^p)$. Also, γ and ν are stationary zero-mean Gaussian white noise processes with covariance matrices Γ and $\hat{R}$, respectively, and $\hat{R}$ is positive definite.

The linear-quadratic-Gaussian (LQG) optimal control problem is: given the output y in (3.2), choose u to minimize

$$J(u) = \lim_{t_f \to \infty} E\{\frac{1}{t_f}\int_0^{t_f} [(Qx(t), x(t)) + u(t)^T Ru(t)]dt\} \tag{3.3}$$

where $Q \in \mathcal{B}(H, H)$ and $R \in R^{m\times m}$ are self-adjoint with Q nonnegative and R positive definite; as in (3.2), x is the mild solution to the thermoelastic system (2.10)–(2.11) (or, equivalently, (2.22)) for the input of the form (3.1).

In view of (2.10) and (2.11), the operator B has the form

$$B = \begin{bmatrix} 0 \\ B_0 \\ B_2 \end{bmatrix} \tag{3.4}$$

where

$$B_i = [b_{i1} b_{i2} \ldots b_{im}], \qquad b_{ij} \in H_i, \quad j = 1, 2, \ldots m, \qquad i = 0, 2. \tag{3.5}$$

The operator $\tilde{B}$ has the same form. The operator C in (3.2) has the form

$$C = [C_{01}\ C_{02}\ C_2], \tag{3.6}$$

where $C_{01} \in \mathcal{B}(V_0, R^p)$, $C_{02} \in \mathcal{B}(H_0, R^p)$ and $C_2 \in \mathcal{B}(H_2, R^p)$.

Theory for the infinite dimensional LQG optimal control problem with bounded input and output operators can be found in [19, 20, 21, 22, 18]. We briefly summarize the relevant results and essential features of the theory here. As in finite dimensions, the LQG problem separates into a deterministic linear-quadratic regulator problem on the infinite interval and a dual state estimator, or filtering, problem.

First, we consider the regulator problem, which is to choose the control u to minimize the integral in (3.3) when both noise processes in (3.1) and (3.2) are zero, the output operator C is the identity, and $t_f = \infty$. If the operator pair (A, B) is uniformly exponentially stabilizable (i.e., there exists a bounded linear operator K such that $A - BK$ generates a uniformly exponentially stable semigroup on H) and the pair (Q, A) is uniformly exponentially detectable (i.e., the pair (A^*, Q) is uniformly exponentially stabilizable), then there exists a unique nonnegative self-adjoint solution $\Pi \in \mathcal{B}(H, H)$ to the operator algebraic Riccati equation

$$A^*\Pi + \Pi A - \Pi B R^{-1} B^* \Pi + Q = 0, \tag{3.7}$$

with $\Pi(\mathrm{Dom}(A)) \subset \mathrm{Dom}(A^*)$. The optimal control for the infinite-time linear-quadratic regulator problem has the feedback form

$$u(t) = -Kx(t), \qquad t \geq 0, \tag{3.8}$$

where

$$K = R^{-1} B^* \Pi \in \mathcal{B}(H, R^m). \tag{3.9}$$

For the filtering problem, we define

$$\hat{Q} = \tilde{B}\Gamma\tilde{B}^*. \tag{3.10}$$

If the pair (C, A) is uniformly exponentially detectable and the pair $(A, \hat{Q})$ is uniformly exponentially stabilizable, the operator algebraic Riccati equation

$$A\hat{\Pi} + \hat{\Pi}A^* - \hat{\Pi}C^*\hat{R}^{-1}C\hat{\Pi} + \hat{Q} = 0 \tag{3.11}$$

admits a unique nonnegative self-adjoint solution $\hat{\Pi} \in \mathcal{B}(H, H)$ with $\hat{\Pi}(\mathrm{Dom}(A^*)) \subset \mathrm{Dom}(A)$. The minimum-variance estimate of $x(t)$ given $y(\tau)$ $(\tau \leq t)$ is a mild solution $\hat{x}(t)$ to the evolution equation

$$\dot{\hat{x}}(t) = A\hat{x}(t) + Bu(t) + \hat{K}\{y(t) - C\hat{x}(t)\} \tag{3.12}$$

where

$$\hat{K} = \hat{\Pi}C^*\hat{R}^{-1} \in \mathcal{B}(R^p, H). \tag{3.13}$$

The optimal LQG compensator consists of the filter, or state estimator, in (3.12) and the control law

$$u(t) = -K\hat{x}(t), \qquad t \geq 0, \tag{3.14}$$

with the control and filter gain operators given by (3.9) and (3.13), respectively.

The optimal closed-loop system then takes the form

$$z(t) = S_{cl}(t - s)z(s), \qquad 0 \leq s \leq t \tag{3.15}$$

where $z(t) = (x(t), \hat{x}(t)) \in Z = H \times H$ and $\{S_{cl}(t) : t \geq 0\}$ is the C_0-semigroup of bounded linear operators on Z with infinitesimal generator

$$A_{cl} = \begin{bmatrix} A & -BK \\ \hat{K}C & A - BK - \hat{K}C \end{bmatrix}, \qquad \mathrm{Dom}(A_{cl}) = \mathrm{Dom}(A) \times \mathrm{Dom}(A). \tag{3.16}$$

If $\{S(t) : t \geq 0\}$ and $\{\hat{S}(t) : t \geq 0\}$ are the semigroups of bounded linear operators generated on H by infinitesimal generators $A - BK$ and $A - \hat{K}C$, respectively, then it is easy to show that

$$e(t) = \hat{S}(t)e(0), \qquad t \geq 0, \tag{3.17}$$

where $e(t) = x(t) - \hat{x}(t)$. Moreover, if for some real a and M,

$$\|S(t)\| \leq Me^{-at}, \quad t \geq 0, \tag{3.18}$$

$$\|\hat{S}(t)\| \leq Me^{-at}, \quad t \geq 0, \tag{3.19}$$

then for each $b < a$, there exists a constant $M_{cl} > 0$ for which

$$\|S_{cl}(t)\| \leq M_{cl}e^{-bt}, t \geq 0. \tag{3.20}$$

Finally, as in the finite dimensional case, it can be shown that

$$\sigma(A_{cl}) = \sigma(A - BK) \cup \sigma(A - \hat{K}C) \tag{3.21}$$

where $\sigma(A_{cl})$ denotes the spectrum of the closed-loop semigroup generator in (3.16).

We note that the uniform exponential stabilizability and detectability conditions stated in this section are sufficient for the existence of unique nonnegative self-adjoint solutions to the operator algebraic Riccati equations (3.7) and (3.11). These conditions are not necessary for some problems with finite rank Q and $\hat{Q}$. A sufficient and usually necessary condition for uniform exponential stabilizability and detectability is that the open-loop system be uniformly exponentially stable except possibly on a controllable and observable finite-dimensional subspace.

It is convenient to note that, since $\mathcal{R}(K) \subset R^m$ and $\mathrm{Dom}(\hat{K}) = R^p$, there exist $k = (k_1, \ldots, k_m)$ and $\hat{k} = (\hat{k}_1, \ldots, \hat{k}_p)$ with k_j and $\hat{k}_j$ in H such that

$$[Kx]_j = \langle x, k_j \rangle, \qquad x \in H, \qquad j = 1, 2, \ldots, m, \tag{3.22}$$

and

$$\hat{K}r = \sum_{j=1}^{p} \hat{k}_j r_j = [\hat{k}_1 \ \hat{k}_2 \ \ldots \ \hat{k}_p]r, \qquad r \in R^p. \tag{3.23}$$

Also, $k_j, \hat{k}_j \in H$ implies that $k_j = (k_{j,1}, k_{j,2}, k_{j,3})$ and $\hat{k}_j = (\hat{k}_{j,1}, \hat{k}_{j,2}, \hat{k}_{j,3})$ with $k_{j,1}, \hat{k}_{j,1} \in V_0$, $k_{j,2}, \hat{k}_{j,2} \in H_0$, and $k_{j,3}, \hat{k}_{j,3} \in H_2$. It follows that

$$\langle x, k_j \rangle = \langle \phi, \mathcal{A}_0 k_{j,1} \rangle_0 + \langle \psi, k_{j,2} \rangle_0 + \langle \theta, k_{j,3} \rangle_2 \tag{3.24}$$

for $x = (\phi, \psi, \theta) \in H$. The vectors k_j and $\hat{k}_j$ and their components, $k_{j,i}$ and $\hat{k}_{j,i}$, are referred to as *functional control and estimator (or observer) gains*, respectively.

4 Approximation and Convergence

4.1 Approximation Theory for the LQG Control Problem

An approximation and convergence theory for the optimal LQG problem for infinite-dimensional systems was developed in [21, 23, 24, 18]. Here, we shall first briefly summarize the generic theory and then take a closer look at it in the context of abstract thermoelastic control systems.

Hypothesis 4.1 *There exists a sequence of finite-dimensional subspaces H^n $(n = 1, 2, ...)$ of H, and sequences of operators $A^n \in \mathcal{B}(H^n, H^n), B^n \in \mathcal{B}(R^m, H^n), \hat{B}^n \in \mathcal{B}(R^l, H^n)$ $Q^n \in \mathcal{B}(H^n, H^n), C^n \in \mathcal{B}(H^n, R^p)$. The operators Q^n are nonnegative and self-adjoint for each n.*

From here on, we take $\hat{Q}^n = \tilde{B}^n \Gamma (\tilde{B}^n)^* \in \mathcal{B}(H^n)$.

Hypothesis 4.2 *The finite dimensional algebraic Riccati equations*

$$(A^n)^* \Pi^n + \Pi^n A^n - \Pi^n B^n R^{-1} (B^n)^* \Pi^n + Q^n = 0 \tag{4.1}$$

and

$$A^n \hat{\Pi}^n + \hat{\Pi}^n (A^n)^* - \hat{\Pi}^n (C^n)^* \hat{R}^{-1} C^n \hat{\Pi}^n + \hat{Q}^n = 0 \tag{4.2}$$

admit unique nonnegative self-adjoint solutions $\Pi^n \in \mathcal{B}(H^n, H^n)$ and $\hat{\Pi}^n \in \mathcal{B}(H^n, H^n)$, respectively.

We define gain operators

$$K^n = R^{-1} (B^n)^* \Pi^n \in \mathcal{B}(H^n, R^m), \tag{4.3}$$

and

$$\hat{K}^n = \hat{\Pi}^n (C^n)^* \hat{R}^{-1} \in \mathcal{B}(R^p, H^n), \tag{4.4}$$

for a sequence of finite-dimensional compensators for the control system (2.10)–(2.11) with input of the form (3.1) and output of the form (3.2). The n-th compensator is given by

$$u^n(t) = -K^n \hat{x}^n(t), \tag{4.5}$$

$$\dot{\hat{x}}^n(t) = A^n \hat{x}^n(t) + B^n u(t) + \hat{K}^n [y(t) - C^n \hat{x}^n(t)]. \tag{4.6}$$

The resulting closed-loop system is then given by

$$z^n(t) = S_{cl}^n(t - s) z(s), \qquad 0 \le s \le t < \infty \tag{4.7}$$

where $z^n(t) = (x^n(t), \hat{x}^n(t)) \in Z^n \equiv H \times H^n$, and $\{S_{cl}^n(t) : t \ge 0\}$ is the C_0-semigroup of bounded linear operators on Z^n with infinitesimal generator $A_{cl}^n : \mathrm{Dom}(A_{cl}^n) \subset Z^n \to Z^n$ given by

$$A_{cl}^n = \begin{bmatrix} A & -BK^n \\ \hat{K}^n C & [A^n - B^n K^n - \hat{K}^n C^n] \end{bmatrix}, \qquad \mathrm{Dom}(A_{cl}^n) = \mathrm{Dom}(A) \times H^n. \tag{4.8}$$

Since $K^n \in \mathcal{B}(H^n, R^m)$ and $\hat{K}^n \in \mathcal{B}(R^p, H^n)$ we have

$$[K^n x^n]_j = \langle k_j^n, x^n \rangle_H, \quad j = 1, 2, \cdots, m \tag{4.9}$$

for $x^n \in H^n$ and

$$\hat{K}^n r = \sum_{j=1}^{p} \hat{k}_j^n r_j = [\hat{k}_1^n \ \hat{k}_2^n \ \ldots \hat{k}_p^n] r \tag{4.10}$$

for $r \in R^p$ with $k_i^n, \hat{k}_j^n \in H^n$, $i = 1, 2, \ldots, m$, $j = 1, 2, \cdots, p$.

The convergence theory can be summarized as follows. We will refer to the following finite dimensional semigroups:

$$T^n(t) = e^{A^n t}, \qquad S^n(t) = e^{[A^n - B^n K^n]t}, \qquad \hat{S}^n(t) = e^{[A^n - \hat{K}^n C^n]t}, \tag{4.11}$$

and their adjoints $T^n(t)^*$, $S^n(t)^*$ and $\hat{S}^n(t)^*$.

Hypothesis 4.3 *For each n, there exists a linear mapping P^n from H onto H^n such that*

$$\lim_{n\to\infty} P^n x = x, \qquad x \in H. \tag{4.12}$$

For each $x \in H$ and each $t \geq 0$,

$$\lim_{n\to\infty} T^n(t)P^n x = T(t)x, \tag{4.13}$$

$$\lim_{n\to\infty} T^n(t)^* P^n x = T(t)^* x. \tag{4.14}$$

where, in each case, the convergence is uniform in t for t in bounded intervals. Also,

$$\lim_{n\to\infty} B^n u = Bu, \qquad u \in R^m, \tag{4.15}$$

$$\lim_{n\to\infty} Q^n P^n x = Qx, \qquad x \in H, \tag{4.16}$$

and

$$\lim_{n\to\infty} CP^n x = Cx, \qquad x \in H. \tag{4.17}$$

If

$$\sup_n \|\Pi^n\| < \infty \qquad \text{and} \qquad \sup_n \|\hat{\Pi}^n\| < \infty \tag{4.18}$$

and there exist positive constants M and α, independent of n, for which

$$\|S^n(t)\| \leq Me^{-\alpha t}, \qquad \text{and} \qquad \|\hat{S}^n(t)\| \leq Me^{-\alpha t}, \qquad t \geq 0, \tag{4.19}$$

then the algebraic Riccati equations (3.7) and (3.11) admit bounded nonnegative self-adjoint solutions Π and $\hat{\Pi}$, and

$$\lim_{n\to\infty} \Pi^n P^n x = \Pi x, \qquad x \in H, \tag{4.20}$$

$$\lim_{n\to\infty} \hat{\Pi}^n P^n x = \hat{\Pi} x, \qquad x \in H. \tag{4.21}$$

Also,

$$\lim_{n\to\infty} S^n(t)P^n x = S(t)x, \qquad x \in H, \tag{4.22}$$

and

$$\lim_{n\to\infty} \hat{S}^n(t)P^n x = \hat{S}(t)x, \qquad x \in H, \tag{4.23}$$

with the convergence uniform in t in bounded t-intervals. If, in addition, the operators Q^n and $\hat{Q}^n$ are coercive and bounded away from 0 uniformly in n, then the uniform boundedness of $\|\Pi^n\|$ and $\|\hat{\Pi}^n\|$ yields the existence of positive constants M and α independent of n for which (4.19) holds.

The easiest way to guarantee (4.18) and (4.19) is to show that there exist positive constants M and α, independent of n, for which

$$\|T^n(t)\| \leq Me^{-\alpha t}, \qquad t \geq 0, \tag{4.24}$$

although such a uniform decay rate for the approximating open-loop semigroups does not always exist. When (4.18) holds but the semigroups $\{S^n(t) : t \geq 0\}$ and $\{\hat{S}^n(t) : t \geq 0\}$ are not necessarily uniformly exponentially stable, uniformly in n, then bounded nonnegative self-adjoint solutions Π and $\hat{\Pi}$ to (3.7) and (3.11) exist, but Π_n and $\hat{\Pi}_n$ are guaranteed only to converge weakly to Π and $\hat{\Pi}$, respectively, as $n \to \infty$.

When the strong convergence in (4.20) and (4.21) holds, we obtain

$$\lim_{n\to\infty} \|K^n P^n - K\|_{\mathcal{B}(H,R^m)} = 0, \tag{4.25}$$

$$\lim_{n\to\infty} \|\hat{K}^n - \hat{K}\|_{\mathcal{B}(R^p,H)} = 0, \tag{4.26}$$

and therefore

$$\lim_{n\to\infty} k_j^n = k_j, \qquad j = 1,2,\cdots,m, \tag{4.27}$$

and

$$\lim_{n\to\infty} \hat{k}_j^n = \hat{k}_j, \qquad j = 1,2,\cdots,p, \tag{4.28}$$

in H. If we define $P_{cl}^n : Z \to Z^n$ by

$$P_{cl}^n = \begin{bmatrix} I & 0 \\ 0 & P^n \end{bmatrix}, \tag{4.29}$$

then we obtain further that

$$\lim_{n\to\infty} S_{cl}^n(t) P_{cl}^n z = S_{cl}(t) z, \qquad z \in Z, \tag{4.30}$$

uniformly on bounded $t-$intervals.

4.2 Abstract Approximation Theory for Linear Thermoelastic Systems

Now we condiser the construction of the approximating finite dimensional subepaces H^n, the mappings P^n and the operators A^n, B^n, Q^n, etc. We establish a generic approximation theory for abstract linear thermoelastic systems that includes relatively easily verified sufficient conditions for the convergence in Hypothesis 4.3.

We assume the hypotheses of Theorem 2.2.

Hypothesis 4.4 *For $j = 1, 2$, and $n = 1, 2, 3, \ldots$, H_j^n is a finite dimensional subspace of V_j and $A_j^n \in B(H_j^n, H_j^n)$ such that the followng conditions hold.*

(i) *For each $v_j \in V_j$ $(j = 1, 2)$, there exists a sequence $v_j^n \in H_j^n$ such that*

$$v_j^n \xrightarrow{V_j} v_j. \tag{4.31}$$

(ii) *For each n, A_1^n is dissipative; i.e.,*

$$\mathrm{Re}\langle v, A_1^n v\rangle_1 \le 0, \qquad v \in H_1^n. \tag{4.32}$$

(iii) *For each $f \in V_1'$ and each real $\lambda > 0$,*

$$(\lambda - A_1^n)^{-1} P_1^{n\prime} f \xrightarrow{V_1} (\lambda - \mathcal{A}_1)^{-1} f \tag{4.33}$$

and

$$(\lambda - A_1^{n*})^{-1} P_1^{n\prime} f \xrightarrow{V_1} (\lambda - \mathcal{A}_1^*)^{-1} f, \tag{4.34}$$

where $P_j^{n\prime} \in B(V_j', H_j^n)$ is defined by

$$\langle v, \tilde{P}_j^n f\rangle_j = \langle v, f\rangle_j, \qquad v \in H_j^n, \qquad j = 1, 2. \tag{4.35}$$

(iv) *There exsits a positive constant α such that, for all n,*

$$\mathrm{Re}\langle v, A_2^n v\rangle_2 \ge \alpha \|v\|_2^2, \qquad v \in H_2^n. \tag{4.36}$$

(v) *For each $f \in V_2'$ and each real $\lambda > 0$,*

$$(\lambda + A_2^n)^{-1} \tilde{P}_2^n f \xrightarrow{V_2} (\lambda + \mathcal{A}_2)^{-1} f \tag{4.37}$$

and

$$(\lambda + A_2^{n*})^{-1} \tilde{P}_2^n f \xrightarrow{V_2} (\lambda + \mathcal{A}_2^*)^{-1} f. \tag{4.38}$$

Remark 4.5 *The operator $\tilde{P}_j^n$ restricts a functional $f \in V_j'$ to H_j^n and identifies $f|_{H_j^n}$ with an element of H_j^n via the Riesz map for H_j^n. If f can be identified with an element of H_j (via the Riesz map for H_j), then $\tilde{P}_j^n f$ is the H_j- projection of f onto H_j^n.*

With $\tilde{P}_j^n$ defined by (4.35), we define $L^n \in B(H_1^n, H_2^n)$ and $L^{n*} \in B(H_2^n, H_1^n)$ by

$$L^n = \tilde{P}_2^n \mathcal{L}\,|_{H_1^n} \qquad \text{or} \qquad \langle v_2, L^n v_1\rangle_2 = \langle v_2, \mathcal{L} v_1\rangle_2, \qquad v_1 \in H_1^n, v_2 \in H_2^n, \tag{4.39}$$

$$L^{n*} = \tilde{P}_1^n \mathcal{L}^*\,|_{H_2^n} \qquad \text{or} \qquad \langle v_1, L^{n*} v_2\rangle_1 = \langle v_1, \mathcal{L}^* v_2\rangle_1, \qquad v_1 \in H_1^n, v_2 \in H_2^n. \tag{4.40}$$

Hence L^{n*} is the Hilbert-space adjoint of L^n. The operator L^n is a straightforward Galerkin approximation of $\mathcal{L}$. On the other hand, Hypothesis 4.4 does not require that A_1^n and A_2^n be Galerkin approximations. Next, we define

$$H^n = H_1^n \times H_2^n \tag{4.41}$$

and

$$A^n = \begin{bmatrix} A_1^n & -L^{n*} \\ L^n & -A_2^n \end{bmatrix} \in B(H^n, H^n). \tag{4.42}$$

Theorem 4.6 *For $f_1 \in V_1'$, $f_2 \in V_2'$ and $\lambda > 0$,*

$$(\lambda - A^n)^{-1} \begin{pmatrix} \tilde{P}_1^n f_1 \\ \tilde{P}_2^n f_2 \end{pmatrix} \xrightarrow{v} (\lambda - \mathcal{A})^{-1} \begin{pmatrix} f_1 \\ f_2 \end{pmatrix} \quad \text{as } n \to \infty \tag{4.43}$$

and

$$(\lambda - A^{n*})^{-1} \begin{pmatrix} \tilde{P}_1^n f_1 \\ \tilde{P}_2^n f_2 \end{pmatrix} \xrightarrow{v} (\lambda - \mathcal{A}^*)^{-1} \begin{pmatrix} f_1 \\ f_2 \end{pmatrix} \quad \text{as } n \to \infty. \tag{4.44}$$

Proof For $f_1 \in V_1'$ and $f_2 \in V_2'$, we set

$$v = \begin{pmatrix} v_1 \\ v_2 \end{pmatrix} = (\lambda - \mathcal{A})^{-1} \begin{pmatrix} f_1 \\ f_2 \end{pmatrix}, \tag{4.45}$$

and

$$v^n = \begin{pmatrix} v_1^n \\ v_2^n \end{pmatrix} = (\lambda - A^n)^{-1} \begin{pmatrix} \tilde{P}_1^n f_1 \\ \tilde{P}_2^n f_2 \end{pmatrix}. \tag{4.46}$$

We note that (4.46) is equivalent to

$$v_1^n = (\lambda - A_1^n)^{-1}(\tilde{P}_1^n f_1 - L^{n*} v_2^n) = (\lambda - A_1^n)^{-1} \tilde{P}_1^n (f_1 - \mathcal{L}^* v_2^n) \tag{4.47}$$

and

$$v_2^n = (\lambda + A_2^n)^{-1}(\tilde{P}_2^n f_2 + L^n v_2^n) = (\lambda + A_2^n)^{-1} \tilde{P}_2^n (f_2 + \mathcal{L} v_2^n). \tag{4.48}$$

Substituting (4.47) into (4.48) yields

$$[(\lambda + A_2^n) + L^n(\lambda - A_1^n)^{-1} L^{n*}] v_2^n = \tilde{P}_2^n f_2 + L^n(\lambda - A_1^n)^{-1} \tilde{P}_1^n f_1. \tag{4.49}$$

From (4.32), (4.36), (4.39) and (4.49), we have

$$\begin{aligned} \alpha \|v_2^n\|_2^2 &\le \mathrm{Re}(\langle v_2^n, [(\lambda + A_2^n) + L^n(\lambda - A_1^n)^{-1} L^{n*}] v_2^n \rangle_2) \\ &= \mathrm{Re}(\langle v_2^n, \tilde{P}_2^n f_2 \rangle_2 + \langle v_2^n, L^n(\lambda - A_1^n)^{-1} \tilde{P}_1^n f_1 \rangle_2) \\ &= \mathrm{Re}(\langle v_2^n, f_2 \rangle_2 + \langle v_2^n, \mathcal{L}(\lambda - A_1^n)^{-1} \tilde{P}_1^n f_1 \rangle_2) \\ &\le \|v_2^n\|_2 (|f_2|_{V_2'} + \|\mathcal{L}\| \cdot \|(\lambda - A_1^n)^{-1} \tilde{P}_1^n f_1\|_1). \end{aligned} \tag{4.50}$$

Since (4.33) implies that $\|(\lambda - A_1^n)^{-1} \tilde{P}_1^n f_1\|_1$ is bounded in n, (4.50) shows that $\|v_2^n\|_2^2$ is bounded in n. Then, it follows from (4.33) and (4.47) that $\|v_1^n\|_1$ is bounded in n.

Next, we note that, for $z = (z_1, z_2) \in H^n$,

$$\mathrm{Re}\langle z, (\lambda - A^n) z \rangle = \mathrm{Re}\langle z_1, (\lambda - A_1^n) z_1 \rangle_1 + \langle z_2, (\lambda + A_2^n) z_2 \rangle_2) \ge \alpha \|z_2\|_2^2 + \lambda |z|^2. \tag{4.51}$$

We set

$$\tilde{v}^n = \begin{pmatrix} \tilde{v}_1^n \\ \tilde{v}_2^n \end{pmatrix} = \begin{pmatrix} (\lambda - A_1^n)^{-1} \tilde{P}_1^n (f_1 - \mathcal{L}^* v_2) \\ (\lambda + A_2^n)^{-1} \tilde{P}_2^n (f_2 + \mathcal{L} v_1) \end{pmatrix} \tag{4.52}$$

and

$$x^n = \begin{pmatrix} x_1^n \\ x_2^n \end{pmatrix} = v^n - \bar{v}^n. \tag{4.53}$$

Then, recalling (4.47) and (4.52) yields

$$\begin{aligned} \langle x_1^n, (\lambda - A_1^n) x_1^n \rangle_1 &= \langle x_1^n, (\lambda - A_1^n) v_1^n - (\lambda - A_1^n) \bar{v}_1^n \rangle_1 \\ &= -\langle x_1^n, \mathcal{L}^*(v_2^n - v_2) \rangle_1 = -\langle x_1^n, \mathcal{L}^* x_2^n \rangle_1 - \langle x_1^n, \mathcal{L}^*(\bar{v}_2^n - v_2) \rangle_1 \end{aligned} \tag{4.54}$$

and similarly (4.48) gives

$$\begin{aligned} \langle x_2^n, (\lambda + A_2^n) x_2^n \rangle_2 &= \langle x_2^n, (\lambda + A_2^n) v_2^n - (\lambda + A_2^n) \bar{v}_2^n \rangle_2 \\ &= \langle x_2^n, \mathcal{L}(v_1^n - v_1) \rangle_2 = \langle x_2^n, \mathcal{L} x_1^n \rangle_2 + \langle x_2^n, \mathcal{L}(\bar{v}_1^n - v_1) \rangle_2. \end{aligned} \tag{4.55}$$

Hence,

$$\mathrm{Re}(\langle x_1^n, (\lambda - A_1^n) x_1^n \rangle_1 + \langle x_2^n, (\lambda + A_2^n) x_2^n \rangle_2) = \mathrm{Re}(-\langle x_1^n, \mathcal{L}^*(\bar{v}_2^n - v_2) \rangle_1 + \langle x_2^n, \mathcal{L}(\bar{v}_1^n - v_1) \rangle_2). \tag{4.56}$$

In view of (4.51) then,

$$\alpha \|v_2^n - \bar{v}_2^n\|_2^2 \le \|x_1^n\|_1 \cdot \|\mathcal{L}\| \cdot \|\bar{v}_2^n - v_2\|_2 + \|x_2^n\|_2 \cdot \|\mathcal{L}\| \cdot \|\bar{v}_1^n - v_1\|_1 \tag{4.57}$$

According to (2.6), (4.45), (4.52) and conditions (*iii*) and (*v*) of Hypothesis 4.4,

$$\lim_{n \to \infty} \|\bar{v}_1^n - v_1\|_1 = 0 \qquad \text{and} \qquad \lim_{n \to \infty} \|\bar{v}_2^n - v_2\|_2 = 0. \tag{4.58}$$

Hence, $\|\bar{v}^n\|$ is bounded in n, and we have seen that $\|v^n\|$ is bounded in n. Hence $\|x^n\|$ is bounded in n. Therefore, (4.57) and (4.58) show that v_2^n converges in V_2 to v_2. Then (4.47), condition (*iii*) of Hypothesis 4.4 and (4.58) show that v_1^n converges in V_1 to v_1, and (4.43) is proven. The proof of (4.44) is the same except that all operators except $\tilde{P}_1^n$ and $\tilde{P}_2^n$ are replaced by their adjoints. □

Hypothesis 4.4 holds for most common approximation schemes, Galerkin schemes, in particular. The following theorem establishes conditions (*iv*) and (*v*) of Hypothesis 4.4 when A_2^n represents a Galerkin approximation of $\mathcal{A}_2$.

Theorem 4.7 *Assume the hypotheses of* Theorem 2.2 *regarding H_2, V_2 and $\mathcal{A}_2$, and assume condition (i) of* Hypothesis 4.4 *for $j = 2$. Define $A_2^n \in \mathcal{B}(H_2^n, H_2^n)$ by*

$$A_2^n = \tilde{P}_2^n \mathcal{A}_2 |_{H_2^n} \qquad \text{or} \qquad \langle v, A_2^n w \rangle_2 = \langle v, \mathcal{A}_2 w \rangle_2, \qquad v, w \in H_2^n. \tag{4.59}$$

Then conditions (iv) and (v) of Hypothesis 4.4 *hold.*

Proof condition (*iv*) is immediate. To prove (4.37), let $f \in V_2'$ and set

$$v = (\lambda + \mathcal{A}_2)^{-1} f, \tag{4.60}$$

$$v^n = (\lambda + A_2^n)^{-1} \tilde{P}_2^n f. \tag{4.61}$$

Also, let $\bar{v}^n \in H_2^n$ such that $\|\bar{v}^n - v\|_2$ converges to 0. Then

$$\alpha \|v^n\|_2^2 \le |\langle v^n, (\lambda + A_2^n) v^n \rangle_2| = |\langle v^n, \tilde{P}_2^n f \rangle_2| = |\langle v^n, f \rangle_2| \le \|v^n\|_2 |f|_{V_2'}. \tag{4.62}$$

Hence $\|v^n\|_2$ is bounded in n. Next,

$$\begin{aligned} \alpha \|v^n - \bar{v}^n\|_2^2 &\le |\langle v^n - \bar{v}^n, (\lambda + A_2^n)(v^n - \bar{v}^n) \rangle_2| \\ &= |\langle v^n - \bar{v}^n, \tilde{P}_2^n f \rangle_2 - \langle v^n - \bar{v}^n, (\lambda + A_2^n) \bar{v}^n \rangle_2| = |\langle v^n - \bar{v}^n, f - (\lambda + \mathcal{A}_2) \bar{v}^n \rangle_2|. \end{aligned} \tag{4.63}$$

Since $\tilde{v}^n$ converges in V_2 to v and $\mathcal{A}_2 \in \mathcal{B}(V_2, V_2')$, it follows that $\|\tilde{v}^n\|_2$ is bounded in n and $(\lambda+\mathcal{A}_2)\tilde{v}^n$ converges in V_2' to $(\lambda+\mathcal{A}_2)v = f$. Therefore, (4.63) shows that $\|v^n - \tilde{v}^n\|_2$ converges to 0 as $n \to \infty$, so that v^n converges in V_2 to v.

The proof is the same when $\mathcal{A}_2$ and A_2^n are replaced by their adjoints. □

When $\mathcal{A}_1$ has the form (2.16) and A_1^n is a Galerkin approximation of $\mathcal{A}_1$, condition (*iii*) of Hypothesis 4.4 can be proved either by arguments similar to the proof of Theorem 4.7 or by projection arguments like those in [18]. Also, see [17].

Usually, the operator P^n in Hypothesis 4.3 is the H-projection onto $H^n = H_1^n \times H_2^n$, so that condition (*i*) of Hypothesis 4.4 guarantees (4.12). In this case, if $f_j \in H_j$, then $P^n(f_1, f_2) = (\tilde{P}_1^n f_1, \tilde{P}_2^n f_2)$ (recall Remark 4.5). Hence, it follows from Theorem 4.6 and the Trotter-Kato theorem [25] that the approximating open-loop semigroups $T_n(t)$ and $T_n^*(t)$ converge as in Hypothesis 4.3.

Also, when P^n is the H^n-projection, it is most common to define the approximating input, state-weighting and output operators by

$$B^n = P^n B \tag{4.64}$$

$$Q^n = P^n Q|_{H^n}, \tag{4.65}$$

and

$$C^n = C|_{H^n}, \tag{4.66}$$

so that (4.15), (4.16) and (4.17) follow from (4.12).

4.3 Matrix Representations of Approximating Operators

We assume now that A_1^n has the form in (2.16), that $\mathcal{L}$ has the form in (2.18) and that H_1 and V_1 have the forms in (2.15). Then H_1^n has the form $H_0^n \times H_0^n$ with $H_0^n \subset V_0$. We assume that, for each n, H_0^n is the span of a finite number of basis vectors $e_{0,i}^n$ and H_2^n is the span of a finite number of basis vectors $e_{2,i}^n$. (The spaces H_0^n and H_2^n may have different dimensions.)

Also, we use Galerkin approximations of both $\mathcal{A}_1$ and $\mathcal{A}_2$. The matrix representation of the operator A^n in (4.42) is then

$$\text{matrix representation of } A^n = [A^n] = \begin{bmatrix} 0 & I & 0 \\ -M_0^{n\,-1} K_0^n & -M_0^{n\,-1} K_4^n & -M_0^{n\,-1} \overline{K_3^n}^T \\ 0 & M_2^{n\,-1} K_3^n & -M_2^{n\,-1} K_2^n \end{bmatrix} \tag{4.67}$$

where

$$\begin{aligned} M_0^n &= [(e_{0,i}^n, e_{0,j}^n)_0] & M_2^n &= [(e_{2,i}^n, e_{2,j}^n)_2] \\ K_0^n &= [(e_{0,i}^n, \mathcal{A}_0 e_{0,j}^n)_0] & K_2^n &= [(e_{2,i}^n, \mathcal{A}_2 e_{2,j}^n)_2] \\ K_3^n &= [(e_{2,i}^n, \mathcal{L}_0 e_{0,j}^n)_2] & K_4^n &= [(e_{0,i}^n, \mathcal{D}_0 e_{0,j}^n)_0]. \end{aligned} \tag{4.68}$$

The matrix representation of the operator B^n in (3.1) and (3.4) is

$$[B^n] = \begin{bmatrix} 0 \\ M_0^{n\,-1}[(e_{0,i}^n, b_{0j})_0] \\ M_2^{n\,-1}[(e_{2,i}^n, b_{2j})_2] \end{bmatrix}, \tag{4.69}$$

and the matrix representation of the operator $\tilde{B}^n$ is similar. The matrix representation of the operator C in (3.2) and (3.6) is

$$[C^n] = [\,[C_{01} e_{0,i}^n]\ [C_{02} e_{0,i}^n]\ [C_2 e_{2,i}^n]\,]. \tag{4.70}$$

To discuss the matrix representations of the operators Q^n, $\hat{Q}^n$, Π^n and $\hat{\Pi}^n$, it is convenient to define basis vectors

$$\vec{e}^n_{0,i} = (e^n_{0,i}, 0, 0) \qquad \vec{e}^n_{1,i} = (0, e^n_{0,i}, 0) \qquad \vec{e}^n_{2,i} = (0, 0, e^n_{2,i}) \tag{4.71}$$

and the block-diagonal matrix

$$M^n = \mathrm{diag}\{M^n_0, K^n_0, M^n_2\}. \tag{4.72}$$

The matrix representations of Q^n and $\hat{Q}^n$ are

$$[Q^n] = M^{n^{-1}}[(\vec{e}^n_{i',i}, Q\vec{e}^n_{j',j})], \qquad [\hat{Q}^n] = M^{n^{-1}}[(\vec{e}^n_{i',i}, \hat{Q}\vec{e}^n_{j',j})], \qquad i', j' = 0, 1, 2. \tag{4.73}$$

The matrix representations $[\Pi^n]$ and $[\hat{\Pi}^n]$ of Π^n and $\hat{\Pi}^n$, respectively, are determined by solving Riccati matrix equations equivalent to the operator equations (4.1) and (4.2). The form of $[\Pi^n]$ is like that of $[Q^n]$, and in general neither of these matrices is symmetric. Hence, rather than solving the matrix representation of (4.1) directly, it is preferable to premultiply the matrix representation of (4.1) by M^n to obtain a Riccati matrix equation that can be solved for the symmetric matrix $M^n[\Pi^n]$. Also, instead of solving the matrix representation of (4.2), it is preferable to postmultiply the matrix representation of (4.2) by $M^{n^{-1}}$ to obtain a Riccati matrix equation that can be solved for the symmetric matrix $[\hat{\Pi}^n]M^{n^{-1}}$. (See [18].)

Finally, it follows from (4.3) and (4.4) that the approximating functional control and estimator gains in (4.9) and (4.10) are given by

$$[k^n_1\ k^n_2\ \ldots k^n_m] = \vec{e}^n M^{n^{-1}}[\Pi^n]M^n[B^n]R^{-1}, \tag{4.74}$$

$$[\hat{k}^n_1\ \hat{k}^n_2\ \ldots \hat{k}^n_p] = \vec{e}^n[\hat{\Pi}^n]M^{n^{-1}}[C^n]^T\hat{R}^{-1}, \tag{4.75}$$

where

$$\vec{e}^n = [\,[\vec{e}^n_{0,i}]\,[\vec{e}^n_{1,i}]\,[\vec{e}^n_{1,i}]\,] \tag{4.76}$$

and $[\vec{e}^n_{0,i}]$, for example, is the row matrix containing the basis vectors $\vec{e}^n_{0,i}$ in order. See [18] for details on computing similar functional gains.

5 Stability of the Open-loop System

We consider the system in (2.10) and (2.11), and we define

$$\mathrm{Dom}(A_0) = \mathcal{A}_0^{-1} H_0, \qquad A_0 = \mathcal{A}_0|_{\mathrm{Dom}(A_0)}. \tag{5.1}$$

Since $\mathcal{A}_0$ is symmetric and V_0-coercive, A_0 is self-adjoint and V_0-coercive. We recall the operators $\mathcal{L}$ and $\mathcal{L}_0$ in (2.18) and note that $\mathcal{L}_0 \in \mathcal{B}(V_0, V_2')$.

In this section, we assume that

$$\mathcal{L}_0 = L_0 \in \mathcal{B}(V_0, H_2), \tag{5.2}$$

and we assume that there exists a positive real number α such that

$$\mathrm{Dom}(A_0) = \{v \in \mathrm{Dom}(L_0) : L_0 v \in \mathrm{Dom}(L_0^*)\} \quad \text{and} \quad A_0 = \alpha L_0^* L_0, \tag{5.3}$$

where L_0^* is the Hilbert-space adjoint of L_0 with respect to the H_0 and H_2 inner products (recall Remark 2.4). In this case,

$$\langle v, w \rangle_{V_0} = \alpha \langle L_0 v, L_0 w \rangle_0, \qquad v, w \in V_0. \tag{5.4}$$

The conditions (5.2) and (5.3) are common in thermoelastic structures because the thermal stress enters the equation governing mechanical vibrations in the same way as the stress due to elastic deformation [26, 27].

Theorem 5.1 *Assume the conditions stated so far in this section and that the damping operator $\mathcal{D}_0$ is symmetric (in the sense of (2.12)). If the range of the operator*

$$\Lambda_0 = L_0 A_0^{-1} \tag{5.5}$$

is in V_2 or if $\mathcal{D}_0$ is H_0-coercive, then the semigroup generated on the space H in (2.20) by the operator A defined in (2.19)–(2.21) is uniformly exponentially stable.

Proof First consider the case where $\mathcal{R}(\Lambda_0) \subset V_2$ but $\mathcal{D}_0$ is not necessarily H_0-coercive. It is clear that $\Lambda_0 \in \mathcal{B}(H_0, H_2)$ and $\Lambda_0^* \in \mathcal{B}(H_2, H_0)$. Hence, $\mathcal{R}(\Lambda_0) \subset V_2$ implies $\Lambda_0 \in \mathcal{B}(H_0, V_2)$. Furthermore, it can be shown that $\Lambda_0^* \in \mathcal{B}(H_2, V_0)$ and $\alpha L_0 \Lambda_0^*$ is the H_2-projection onto $\mathcal{R}(L_0)$.

Now define the following self-adjoint bounded linear operator on H:

$$Q = \begin{bmatrix} \sigma I & \mathcal{A}_0^{-1} & 0 \\ I & \sigma I & -2\alpha\Lambda_0^* \\ 0 & -2\alpha\Lambda_0 & \sigma I \end{bmatrix} \tag{5.6}$$

where σ is a positive real number. For σ sufficiently large, Q is H-coercive. Also, since $\mathcal{R}(\Lambda_0) \subset V_2$ and $\mathcal{R}(\Lambda_0^*) \subset V_0$, $QV \subset V$. For $\mathcal{D}_0 = 0$ and $z = (v, h, \theta) \in \mathrm{Dom}(A) \subset V$,

$$\mathrm{Re}\,\langle Qz, Az \rangle = \mathrm{Re}\,\langle Qz, \mathcal{A}z \rangle =$$

$$-\|v\|_0^2 - |h|_0^2 - \sigma \mathrm{Re}\langle \theta, \mathcal{A}_2\theta \rangle_2 + (2\alpha - 1)\mathrm{Re}\langle \theta, L_0 v \rangle_2 + 2\alpha \langle L_0 \Lambda_0^* \theta, \theta \rangle_2 + 2\alpha \mathrm{Re}\langle \Lambda_0 h, \mathcal{A}_2\theta \rangle_2. \tag{5.7}$$

Since

$$|\langle \Lambda_0 h, \mathcal{A}_2\theta \rangle_2| \le \|\Lambda_0 h\|_2 \cdot \|\mathcal{A}_2\|_{\mathcal{B}(V_2, V_2')} \cdot \|\theta\|_2, \tag{5.8}$$

and $\Lambda_0 \in \mathcal{B}(H_0, V_2)$, it follows from (5.7) that, for σ sufficiently large, there exists a positive real number β such that

$$\mathrm{Re}\langle Qz, Az \rangle \le -\beta |z|^2, \qquad z \in \mathrm{Dom}(A). \tag{5.9}$$

When $\mathcal{D}_0 \neq 0$, the right side of (5.7) has more terms, but (5.9) can be obtained in a similar manner. The generalized Schwarz inequality $|\langle v, \mathcal{D}_0 h\rangle_0|^2 \leq |\langle v, \mathcal{D}_0 v\rangle_0| \cdot |\langle h, \mathcal{D}_0 h\rangle_0|$ is useful.

If $\mathcal{D}_0$ is H_0-coercive, then replacing α with 0 in (5.6) allows (5.9) to be obtained for σ sufficiently large and some positive β. □

Remark 5.2 *The condition $\mathcal{R}(\Lambda_0) \subset V_2$ is equivalent to the following two conditions combined:*

$$\mathrm{Dom}(L_0^*) \cap \mathcal{N}(L_0^*)^\perp \subset V_2 \tag{5.10}$$

and there exists a real number μ such that

$$\|v\|_2 \leq \mu |L_0^* v|_0, \qquad v \in \mathrm{Dom}(L_0^*) \cap \mathcal{N}(L_0^*)^\perp. \tag{5.11}$$

Remark 5.3 *To generalize* Theorem 5.1 *to the case where $\mathcal{D}_0$ is not symmetric, we would have to impose further conditions on $\mathcal{D}_0$, which would take us beyond the focus of this paper.*

The hypotheses of Theorem 5.1 hold for many but not all linear thermoelastic systems that seem likely to be uniformly exponentially stable. In most applications, the conditions (5.10) and (5.11) restrict the combinations of boundary conditions. For example, if (2.10) and (2.11) represent a thermoelastic rod, as in the example in the next section, (5.10) and (5.11) hold for Dirichlet boundary conditions on the wave equation at both ends of the rod and Nuemann boundary conditions on the heat equation at both ends, and for various other combinations. However, (5.10) and (5.11) do not hold for Dirichlet boundary conditions on both equations at both ends of the rod.

Recently, J.U. Kim [14] has proved that the linear thermoelastic rod with all Dirichlet boundary conditions is uniformly exponentiall stable. We have tried without success to modify the hypotheses of Theorem 5.1 to cover this case. Also, it might be possible to apply the methods used by Slemrod in [12] for nonlinear thermoelasticy to prove uniform exponential stability for the linear all-Dirichlet case, but (5.10) and (5.11) hold for the boundary conditions treated in [12]. Hansen [6] has shown that all of the eigenvalues are bounded strictly to the left of the imaginary axis for the linear thermoelastic rod with all Dirichlet boundary conditions, but Hansen's analysis suggests that the eigenvectors do not form a Riesz basis.

The conditions (5.10) and (5.11) say that the operator $\mathcal{A}_2$ in the diffusion equation is bounded in a certain sense with respect to the stiffness operator A_0. We believe that some such relative boundedness is necessary for uniform exponentially stability. A numerical experiment in which we used the one-dimensional wave equation for (2.10) and a fourth-order one-dimensional partial differential operator for $\mathcal{A}_2$ in (2.11) yielded a sequence of complex eigenvalues that appeared to approach the imaginary axis asymptotically.

6 An Example and Numerical Results

6.1 Linear Model of a Thermoelastic Rod

We consider the axial vibrations of a visco-thermoelastic rod that is clamped and insulated at both ends. The length of the rod is normalized to 1. Control actuation is produced by a single force directed parallel to the rod and distributed uniformly over the rod segment $\eta_1 \le \eta \le \eta_2$. A sensor measures axial displacement at $\eta = \eta_1$ (i.e., the left end of the rod segment over which the actuator force is distributed). Finally we assume that both the actuator input and sensor output are corrupted by zero-mean Gaussian white noise with unit intensities.

The dynamics of the plant are described by the equations of one-dimensional linear thermoelasticity (see, for example, [26, 28, 13]), which consist of coupled one dimensional wave and heat equations. If the rod has Kelvin-Voigt viscoelastic damping in addition to thermoelastic damping, then the state equations, boundary conditions, and output equation are

$$\rho\frac{\partial^2 w}{\partial t^2}(t,\eta) - \alpha_D(\lambda+2\mu)\frac{\partial^3 w}{\partial\eta^2\partial t}(t,\eta) - (\lambda+2\mu)\frac{\partial^2 w}{\partial\eta^2}(t,\eta) \tag{6.1}$$
$$+\alpha_L(3\lambda+2\mu)\frac{\partial\theta}{\partial\eta}(t,\eta) = b_0(\eta)u(t) + b_0(\eta)\gamma(t), \qquad 0<\eta<1, \quad t>0,$$

$$\rho c\frac{\partial\theta}{\partial t}(t,\eta) - \kappa\frac{\partial^2\theta}{\partial\eta^2}(t,\eta) + \tilde{\theta}\alpha_L(3\lambda+2\mu)\frac{\partial^2 w}{\partial\eta\partial t}(t,\eta) = 0 \qquad 0<\eta<1, \quad t>0, \tag{6.2}$$

$$w(t,0) = 0 = w(t,1), \qquad t>0, \tag{6.3}$$

$$\frac{\partial\theta}{\partial\eta}(t,0) = 0 = \frac{\partial\theta}{\partial\eta}(t,1), \qquad t>0, \tag{6.4}$$

$$y(t) = w(t,\eta_1) + \nu(t), \qquad t>0, \tag{6.5}$$

where w and θ are respectively the axial displacement and absolute temperature, ρ is the mass density, λ and μ are the Lamé (elasticity) parameters, c is the specific heat and κ is the thermal conductivity. The positive constant $\tilde{\theta}$ is a reference temperature–the absolute temperature of a stress-free reference state for the rod. The nonnegative constants α_D and α_L are respectively the viscoelastic coefficient and the coefficient of thermal expansion, γ and ν are the noise processes, and the function $b_0 \in L_2(0,1)$ is given by

$$b_0(\eta) = \begin{cases} 1, & \eta_1 \le \eta \le \eta_2 \\ 0, & \text{otherwise.} \end{cases} \tag{6.6}$$

Because of the insulated, or Neumann, boundary conditions in (6.4) on the temperature distribution, the open-loop system corresponding to (6.1)–(6.2) has a zero eigenvalue for which the associated eigenvector consists of zero displacement and velocity and nonzero uniform temperature distribution. This eigenvector is orthogonal (in $L_2(0,1)$) to the control input function b_0 and is in the null space of the output operator corresponding to the measurement in (6.5), so that the span of this eigenvector is uncontrollable and unobservable. It follows that (i) the only part of the temperature distribution that can be controlled or observed is the part that is orthogonal to uniform temperature distributions; (ii) the average (over η) temperature in the rod, which we denote by θ_{ave}, is neither stabilizable nor detectable; (iii) θ_{ave} is a constant function of t.

Consequently, in the thermoelastic control problem, we replace the temperature distribution $\theta(t,\eta)$ with

$$\tilde{\theta}(t,\eta) = \theta(t,\eta) - \theta_{ave}. \tag{6.7}$$

The state equations, then, are (6.1)–(6.5) with θ replaced by $\tilde{\theta}$. The state space H has the structure in (2.20) with

$$H_0 = L_2(0,1), \qquad V_0 = H_0^1(0,1), \tag{6.8}$$

$$H_2 = \{\phi \in L_2(0,1) : \int_0^1 \phi \, d\eta = 0\}, \qquad V_2 = H^1(0,1) \cap H_2. \tag{6.9}$$

All of the spaces in this example are real. We use the standard L_2 inner product for H_0, but we use

$$\langle \phi, \psi \rangle_2 = \frac{c}{\theta} \int_0^1 \phi\psi \, d\eta \tag{6.10}$$

for the inner product on H_2. This inner product on H_2 is required to get the $\mathcal{L}_0^*$ for which the semigroup generator in this example has the form in (2.19). For V_0 and V_2, we use the norms

$$\|\phi\|_0 = (\int_0^1 |\phi'|^2 \, d\eta)^{1/2}, \qquad \|\phi\|_2 = (\int_0^1 |\phi'|^2 \, d\eta)^{1/2}. \tag{6.11}$$

We define the operators $\mathcal{A}_j \in \mathcal{B}(V_j, V_j')$, $j = 0, 2$, $\mathcal{D}_0 \in \mathcal{B}(V_0, V_0')$ and $\mathcal{L}_0 \in \mathcal{B}(V_0, V_2')$ by

$$\langle \phi, \mathcal{A}_0 \psi \rangle_0 = \int_0^1 \frac{\lambda + 2\mu}{\rho} \phi'\psi' \, d\eta, \qquad \phi, \psi \in V_0, \tag{6.12}$$

$$\langle \phi, \mathcal{A}_2 \psi \rangle_2 = \int_0^1 \frac{\kappa}{\rho\theta} \phi'\psi' \, d\eta, \qquad \phi, \psi \in V_2, \tag{6.13}$$

$$\langle \phi, \mathcal{D}_0 \psi \rangle_0 = \int_0^1 \frac{\alpha_D(\lambda + 2\mu)}{\rho} \phi'\psi' \, d\eta, \qquad \phi, \psi \in V_0, \tag{6.14}$$

and

$$\langle \phi, \mathcal{L}_0 \psi \rangle_2 = -\int_0^1 \frac{\alpha_L(3\lambda + 2\mu)}{\rho} \phi\psi' \, d\eta, \qquad \phi \in V_2, \quad \psi \in V_0. \tag{6.15}$$

With these operators, the system in (6.1) and (6.2), with θ replaced by $\tilde{\theta}$, has the form in (2.22) with a semigroup generator of the form in (2.19).

From (6.12)–(6.15), it follows that we have all of the conditions in Section 5, including the hypotheses of Theorem 5.1 (assuming $\alpha_L > 0$, else we would not have a thermoelastic problem). Hence, the open-loop thermoelastic system is uniformly exponentially stable, even if $\alpha_D = 0$.

For the numerical studies in this paper, we chose the parameters in (6.1) and (6.2) for an aluminum rod of length 100in (see [27, 29]). With the length normalized to 1, the parameters take the values in Table 6.1.

$\rho = 9.82 \times 10^{-2}$	$\lambda = 2.064 \times 10^{-1}$	$\mu = 1.11 \times 10^{-1}$
$c = 5.40 \times 10^{-1}$	$\kappa = 7.02 \times 10^{-7}$	$\tilde{\theta} = 68$
$\alpha_L = 1.29 \times 10^{-3}$	$\alpha_D = 0$	
$\eta_1 = .385$	$\eta_2 = .486$	

Table 6.1: Parameters for (6.1)–(6.6)

The numerical results in this paper focus on the effects of thermoelastic damping. In [7], we presented numerical results for a similar example that included nonzero viscoelastic damping ($\alpha_D > 0$). The functional gains were much smoother than the gains for the case with thermoelastic damping only, and the approximating functional gains converged much faster. The numerical results in [7] indicate that, if Voigt-Kelvin viscoelastic damping is present, its effect dominates the effect of thermoelastic damping, but it is not clear whether Voigt-Kelvin viscoelastic damping is present at significant levels in common metals.

6.2 The Optimal Control Problem and the Approximation Scheme

We have $m = \ell = p = 1$ with the input operators given by

$$B_0 r = \bar{B}_0 r = (\frac{1}{\rho} b_0) r, \quad r \in R^1, \qquad B_2 = \bar{B}_2 = 0, \tag{6.16}$$

and the output operator given by

$$C(\phi, \psi, \theta) = \phi(\eta_1), \qquad (\phi, \psi, \theta) \in H = V_0 \times H_0 \times H_2. \tag{6.17}$$

In the quadratic performance index, we take the operator $Q \in \mathcal{B}(H)$ to be given by

$$Qx = Q(w, \dot{w}, \tilde{\theta}) = (w, \dot{w}, 0), \tag{6.18}$$

and we take $R = 1$. This Q penalizes the total mechanical energy in the rod but does not penalize temperature variations from the constant average value. The operator $\hat{Q} \in \mathcal{B}(H)$ is given by (3.10) with $\bar{B} = B$ given by (3.4) and (6.16). Since $\gamma(t)$ and $\nu(t)$ have unit intensities, $\Gamma = \hat{R} = 1$.

The optimal functional control and estimator gains have the form $k_1 = (k_{1,1}, k_{1,2}, k_{1,3})$ and $\hat{k}_1 = (\hat{k}_{1,1}, \hat{k}_{1,2}, \hat{k}_{1,3})$ with $k_{1,1}, \hat{k}_{1,1} \in H_0^1(0,1)$, $k_{1,2}, \hat{k}_{1,2} \in L_2(0,1)$, and $k_{1,3}, \hat{k}_{1,3} \in H_2 \subset L_2(0,1)$. If K and $\hat{K}$ are, respectively, the control and estimator gain operators, then

$$Kx = \int_0^1 k_{1,1}' \phi' \, d\eta + \int_0^1 k_{1,2} \psi \, d\eta + \frac{c}{\theta} \int_0^1 k_{1,3} \theta \, d\eta, \qquad x = (\phi, \psi, \theta) \in H, \tag{6.19}$$

and

$$\hat{K} r = (r\hat{k}_{1,1}, r\hat{k}_{1,2}, r\hat{k}_{1,3}) \in H, \qquad r \in R^1. \tag{6.20}$$

In [7], we compared two Galerkin approximations for solving a linear-quadratic regulator problem for the thermoelastic rod in this example. One scheme was a finite element approximation in which linear splines were the basis vectors; in the other approximation, the open-loop eigenvectors of the distributed systems were the basis vectors. The modal approximation gave faster convergence for the approximating functional control gains. In this paper, we use the modal approximation only.

It is easy to see that, for the boundary conditions in this example, the eigenspaces of the open-loop thermoelastic rod are three-dimensional subspaces each spanned by a two-dimensional subspace of the undamped wave equation and a one-dimensional eigenspace of the heat equation. The eigenvectors of the wave equation are sine waves, and the eigenvectors of the heat equation are cosine waves. The sequence of three-dimensional subspaces of the thermoelastic rod are mutually orthogonal and complete in the state space H. Thus it is easy to show that all the conditions of Hypothesis 4.4 hold.

The open-loop eigenvalues can be determined as the solutions to the cubic characteristic equations corresponding to the three-dimensional eigenspaces. For the values of the parameters that we used, the eigenvalues corresponding to each open-loop subspace consist of a complex conjugate pair and a real eigenvalue, all with negative real parts. It can be shown by analysis of the sequence of cubic equations that, asymptotically, the real eigenvalues approach $-\infty$ and the complex pairs of eigenvalues approach a vertical line strictly to the left of the imaginary axis. This, together with the orthogonality and completeness of the eigenspaces, guarantees (4.24); i.e., that the approximating open-loop semigroups are uniformly exponentially stable, with a decay rate uniform in n (the order of approximation, or number of modal subspaces). Hence (4.18) and (4.19) hold. Therefore, (4.20)–(4.30) are guaranteed.

To obtain the approximating control and estimator gains shown in Figures 6.1 and 6.2, we used the matrix sign function method in [30] to solve Riccati matrix equations equivalent to the finite dimensional Riccati operator equations (4.1) and (4.2), as discussed in Section 4.3. We used (4.74) and (4.75) with $m = p = 1$ to compute the approximating functional control gains $k_{1,i}^n (i = 1,2,3)$ and approximating functional estimator gains $\hat{k}_{1,i}^n (i = 1,2,3)$.

6.3 Numerical Results for Finite-Dimensional Compensators

In each of the figures, we have plotted the approximation to the particular functional gain for each n between 18 and 33, where n is the number of modal subspaces used. Because the damping produced by thermoelastic dissipation is so small in this example, we see nothing resembling gain convergence until we use at least $n = 15$. The convergence results for approximations to the infinite-dimensional LQG problem guarantee that all of the functional gains do converge, but the convergence theory does not indicate the rate at which the gains converge. Numerical experience has shown that, generally, greater damping causes faster gain convergence.

We are not sure that we are seeing convergence in Figure 6.1. Increasing n past 40 does not make the functional control gains look closer to any limit, and between $n = 40$ and $n = 50$, the numerical solution to the Riccati equation is so inaccurate in some cases that the corresponding gains do not resemble those in Figure 6.1. While the functional gains must converge, it is possible that the order of approximation required for convergence exceeds our capability to solve the Riccati equations accurately. Another reason that we question whether our plots of the functional control gains show convergence is that when we compute the control gains for both $\alpha_D = 0$ and $\alpha_L = 0$, the plots look identical to Figure 6.1. But with no damping for the wave equation and the coercive weighting that we place on the solution to the wave equation in the performance index, the norms of the finite dimensional Riccati operators are guaranteed to grow without bound as n increases [31, 18]. Indeed, when $\alpha_D = 0$ and $\alpha_L = 0$, our numerical solutions to the Riccati equations break down for smaller n than they do when $\alpha_D = 0$ and $\alpha_L > 0$. There is some difference between the finite-dimensional gain matrices that we compute with and without thermoelastic damping in the plant model, but that difference is too small to be seen in plots of the functional gains.

The question arises, then, whether the very light structural damping produced by the thermoelastic effect in the rod is significant in compensator design. To address this question, we computed eigenvalues for two closed-loop systems. Each closed-loop system was constructed by connecting a compensator based on a control model consisting of the first 20 modal subspaces to a simulation model, or truth model, consisting of the first 30 modal subspaces of the rod. Each compensator thus has dimension 60 while the simulation model has dimension 90. The 30-mode simulation model was the same in each case; it had the parameters in Table 6.1, including $\alpha_L = 1.29 \times 10^{-3}$. The 20-mode control model for Compensator 1 also had the parameters in Table 6.1. The control model for Compensator 2 had $\alpha_L = 0$, and all of the other parameters had the values in Table 6.1. This means that there is no damping for the mechanical vibrations of the rod in the open-loop control model for Compensator 2. Because the temperature distribution is not penalized in the performance index, the control gains $k_{1,3}$ and $k^n_{1,3}$ and estimator gains $\hat{k}_{1,3}$ and $\hat{k}^n_{1,3}$ are all zero in Compensator 2, and the gains $k_{1,1}$ and $k^n_{1,1}$, $\hat{k}_{1,1}$ and $\hat{k}^n_{1,1}$, $k_{1,2}$ and $k^n_{1,2}$, $\hat{k}_{1,2}$ and $\hat{k}^n_{1,2}$ are those that would be computed for a 20-mode model of the undamped wave equation alone.

Table 6.2 shows typical eigenvalues for the open-loop system and for the closed-loop system produced by each compensator. Since each compensator contains a copy of each of the first 20 modal subspaces, each closed-loop system contains six states, and six eigenvalues, corresponding to each of the first 20 modal subspaces. Each closed-loop system also contains the 30 states in twenty-first through thirtieth modal subspaces. While the closed-loop performance in the first ten or so modes is similar with both compensators, the closed-loop eigenvalues corresponding to several of the higher-frequency modes reveal important differences between the two compensators. In particular, we note the second complex pair of closed-loop eigenvalues listed for mode 18. The magnitude of the real part produced by Compensator 1 is more than 20 times the corresponding number produced by Compensator 2. The same is true for mode 19. In certain high-frequency closed-loop states, then, the decay rates produced by Compensator 1 are more than 20 times the decay rates produced by Compensator 2.

The eigenvalues in Table 6.2 for modes 21 and 22, the first modes not modelled in the compensators, are typical of the eigenvalues for all ten modes that are present in the simulation model

but not in the control models. These eigenvalues show that we have modelled enough modes in the compensators ') eliminate any significant spillover between modelled and unmodelled modes.

Because the magnitudes of the real eigenvalues, which correspond to the heat equation (6.2), are so much larger than the magnitudes of the complex eigenvalues, we suspected that it might be possible to eliminate the states corresponding to the real open-loop eigenvalues from the control model and base a compensator design on a control model consisting of a sequence of second-order modes with eigenvalues equal to the complex open-loop eigenvalues of the thermoelastic rod. This amounts to putting artificial viscous damping in the wave equation.

We carried out such a design with twenty second-order modes having eigenvalues equal to the first twenty pairs of complex open-loop thermoelastic eigenvalues and mode shapes the same as the first twenty modes of the undamped rod. This compensator had dimension 40. When we closed the loop with the 30-mode simulation model used for Table 6.2 and computed the closed-loop eigenvalues, we obtained virtually identical results to those for Compensator 1, except that this third closed-loop system had only half as many real eigenvalues because the corresponding states were not modelled in the compensator. Even for modes 18 and 19, all of the closed-loop eigenvalues produced by the third compensator matched to at least three digits the corresponding eigenvalues produced by Compensator 1.

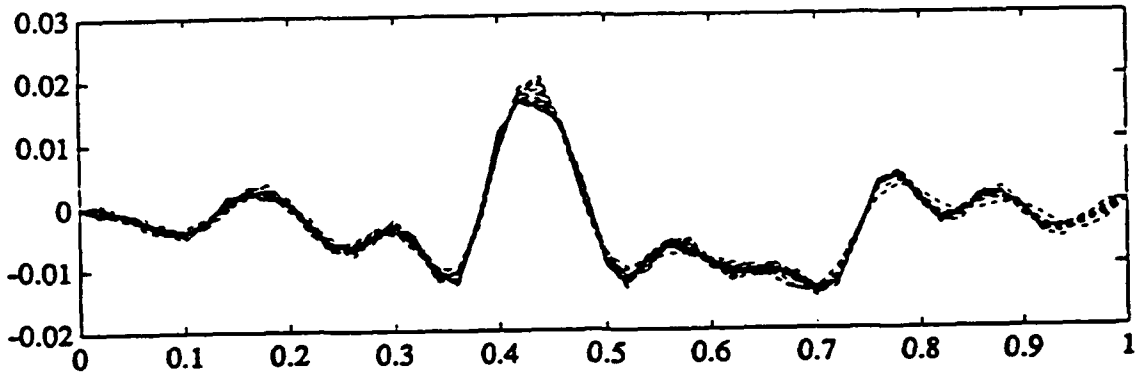

Figure 6.1a: Approximating Functional Control Gains $k^n_{1,1}$, $n = 18, 19, \ldots 33$

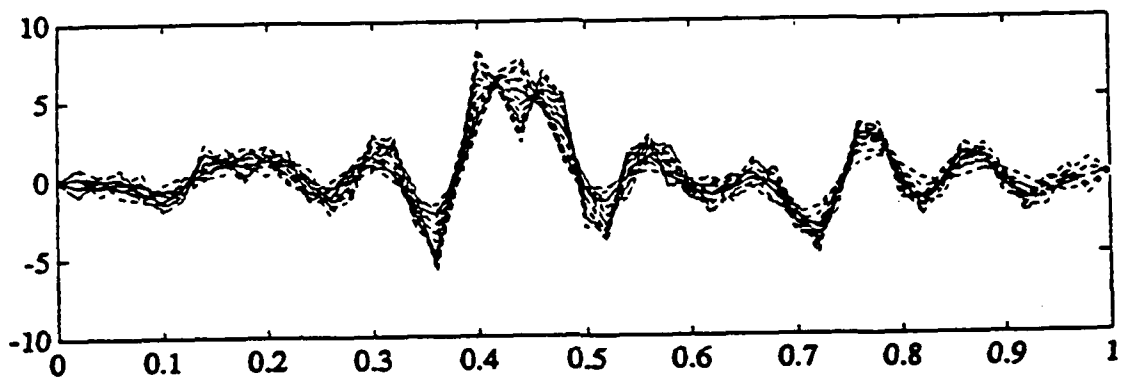

Figure 6.1b: Approximating Functional Control Gains $k^n_{1,2}$, $n = 18, 19, \ldots 33$

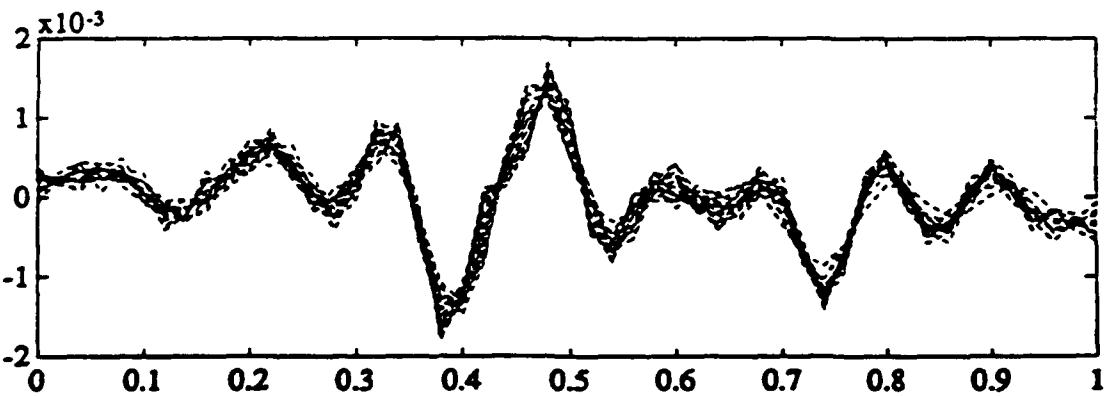

Figure 6.1c: Approximating Functional Control Gains $k^n_{1,3}$, $n = 18, 19, \ldots 33$

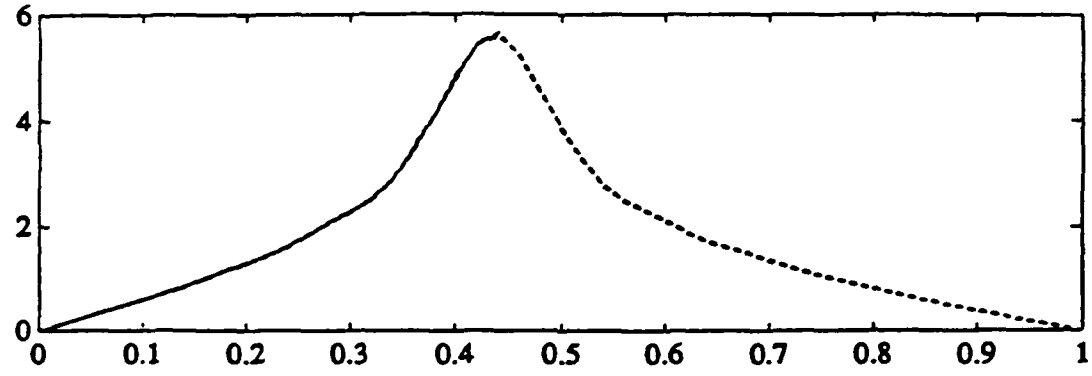

Figure 6.2a: Approximating Functional Estimator Gains $\hat{k}^n_{1,1}$, $n = 18, 19, \ldots 33$

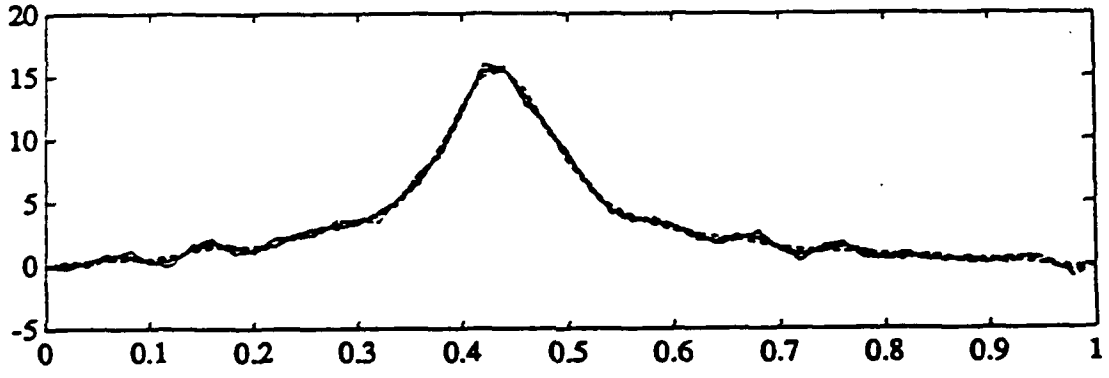

Figure 6.2b: Approximating Functional Estimator Gains $\hat{k}^n_{1,2}$, $n = 18, 19, \ldots 33$

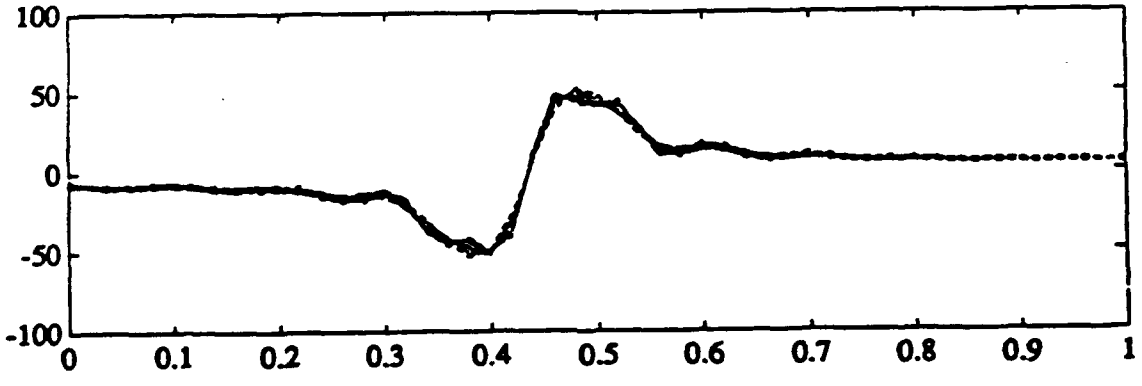

Figure 6.2c: Approximating Functional Estimator Gains $\hat{k}^n_{1,3}$, $n = 18, 19, \ldots 33$

Mode Number	Open-loop	Closed-loop with Compensator 1	Closed-loop with Compensator 2
1	$-2.30 \times 10^{-7} \pm i\,6.57 \times 10^{0}$ -1.30×10^{-4}	$-3.15 \times 10^{-1} \pm i\,6.57 \times 10^{0}$ $-1.44 \times 10^{0} \pm i\,6.89 \times 10^{0}$ -1.30×10^{-4} -1.30×10^{-4}	$-3.13 \times 10^{-1} \pm i\,6.58 \times 10^{0}$ $-1.45 \times 10^{0} \pm i\,6.87 \times 10^{0}$ -1.30×10^{-4} -1.31×10^{-4}
2	$-9.19 \times 10^{-7} \pm i\,1.31 \times 10^{1}$ -5.21×10^{-4}	$-1.26 \times 10^{-1} \pm i\,1.31 \times 10^{1}$ $-1.22 \times 10^{-1} \pm i\,1.31 \times 10^{1}$ -5.21×10^{-4} -5.21×10^{-4}	$-1.63 \times 10^{-1} \pm i\,1.31 \times 10^{1}$ $-8.50 \times 10^{-2} \pm i\,1.32 \times 10^{1}$ -5.21×10^{-4} -5.23×10^{-4}
3	$-2.07 \times 10^{-6} \pm i\,1.97 \times 10^{1}$ -1.17×10^{-3}	$-2.55 \times 10^{-1} \pm i\,1.97 \times 10^{1}$ $-3.45 \times 10^{-1} \pm i\,1.97 \times 10^{1}$ -1.17×10^{-3} -1.17×10^{-3}	$-2.17 \times 10^{-1} \pm i\,1.97 \times 10^{1}$ $-3.84 \times 10^{-1} \pm i\,1.96 \times 10^{1}$ -1.18×10^{-3} -1.17×10^{-3}
10	$-2.30 \times 10^{-5} \pm i\,6.57 \times 10^{1}$ -1.30×10^{-2}	$-1.82 \times 10^{-1} \pm i\,6.57 \times 10^{1}$ $-8.03 \times 10^{-2} \pm i\,6.57 \times 10^{1}$ -1.30×10^{-2} -1.30×10^{-2}	$-2.16 \times 10^{-1} \pm i\,6.56 \times 10^{1}$ $-4.66 \times 10^{-2} \pm i\,6.58 \times 10^{1}$ -1.30×10^{-2} -1.31×10^{-2}
14	$-4.50 \times 10^{-5} \pm i\,9.20 \times 10^{1}$ -2.55×10^{-2}	$-3.44 \times 10^{-2} \pm i\,9.20 \times 10^{1}$ $-3.41 \times 10^{-3} \pm i\,9.20 \times 10^{1}$ -2.55×10^{-2} -2.55×10^{-2}	$-3.76 \times 10^{-2} \pm i\,9.19 \times 10^{1}$ $-2.66 \times 10^{-4} \pm i\,9.20 \times 10^{1}$ -2.56×10^{-2} -2.55×10^{-2}
18	$-7.45 \times 10^{-5} \pm i\,1.18 \times 10^{2}$ -4.22×10^{-2}	$-1.53 \times 10^{-2} \pm i\,1.18 \times 10^{2}$ $-2.16 \times 10^{-3} \pm i\,1.18 \times 10^{2}$ -4.22×10^{-2} -4.22×10^{-2}	$-1.74 \times 10^{-2} \pm i\,1.18 \times 10^{2}$ $-9.75 \times 10^{-5} \pm i\,1.18 \times 10^{2}$ -4.22×10^{-2} -4.24×10^{-2}
19	$-8.30 \times 10^{-5} \pm i\,1.25 \times 10^{2}$ -4.70×10^{-2}	$-1.03 \times 10^{-2} \pm i\,1.25 \times 10^{2}$ $-1.98 \times 10^{-3} \pm i\,1.25 \times 10^{2}$ -4.70×10^{-2} -4.70×10^{-2}	$-1.22 \times 10^{-2} \pm i\,1.25 \times 10^{2}$ $-9.05 \times 10^{-5} \pm i\,1.25 \times 10^{2}$ -4.70×10^{-2} -4.72×10^{-2}
20	$-9.19 \times 10^{-5} \pm i\,1.31 \times 10^{2}$ -5.21×10^{-2}	$-2.51 \times 10^{-3} \pm i\,1.31 \times 10^{2}$ $-6.67 \times 10^{-4} \pm i\,1.31 \times 10^{2}$ -5.21×10^{-2} -5.21×10^{-2}	$-3.18 \times 10^{-3} \pm i\,1.31 \times 10^{2}$ $-9.33 \times 10^{-5} \pm i\,1.31 \times 10^{2}$ -5.21×10^{-2} -5.23×10^{-2}
21	$-1.01 \times 10^{-4} \pm i\,1.38 \times 10^{2}$ -5.75×10^{-2}	$-1.04 \times 10^{-4} \pm i\,1.38 \times 10^{2}$ -5.75×10^{-2}	$-1.04 \times 10^{-4} \pm i\,1.38 \times 10^{2}$ -5.75×10^{-2}
22	$-1.11 \times 10^{-4} \pm i\,1.45 \times 10^{2}$ -6.31×10^{-2}	$-1.34 \times 10^{-4} \pm i\,1.45 \times 10^{2}$ -6.31×10^{-2}	$-1.34 \times 10^{-4} \pm i\,1.45 \times 10^{2}$ -6.31×10^{-2}
Simulation Model: 30 Modal Subspaces, $\alpha_L = 1.29 \times 10^{-3}$ Compensator 1: 20 Modal Subspaces, $\alpha_L = 1.29 \times 10^{-3}$ Compensator 2: 20 Modal Subspaces, $\alpha_L = 0$			

Table 6.2: Typical Open-loop and Closed-loop Eigenvalues

7 Conclusions

The abstract formulation of distributed models and the approximation theory developed in this paper apply to a wide variety of thermoelastic control systems. The uniform exponential stability result in Section 5 applies to a large class of thermoelastic problems, but not to certain systems that are known to be uniformly exponentially stable [14].

The numerical study in Section 6 focussed on the effect of thermoelastic damping in optimal control of a flexible structure. The eigenvalue results demonstrate that, even though thermoelastic damping is small in common metals, a compensator based on a thermoelastic model of a flexible structure can produce significantly better response in high-frequency modes than a compensator based on an undamped model can produce.

The theory in Sections 2–4 also applies to thermoelastic control problems in which a thermal disturbance excites mechanical vibrations. This class of problems, which includes vibrations in flexible space structures caused by solar heating, might provide the most important applications for the theory developed here.

References

[1] J.A. Burns, E.M. Cliff, Z.Y. Liu, and R.E. Miller, "Control of a thermoviscoelastic system," in *Proceedings of 27th IEEE Conference on Decision and Control*, (Austin, TX), pp. 1249–1252, December 1988.

[2] J.A. Burns, Z.Y. Liu, and R.E. Miller, "Approximations of thermoelastic and viscoelastic control systems," 1990. *Journal of Numerical Functional Analysis and Optimization*, to appear.

[3] Z.Y. Liu, *Approximation and Control of a Thermoviscoelastic System*. PhD thesis, Virginia Polytechnic Institute and State University, Blacksburg, VA, 1989.

[4] J.E. Lagnese, "Boundary stabilization of thin plates," *SIAM Studies in Applied Mathematics*, vol. 10, 1989.

[5] J.E. Lagnese, "The reachability problem for thermoelastic plates," 1990. *Archive for Rational Mechanics and Analysis*, to appear.

[6] S.W. Hansen, "Exponential energy decay in a linear thermoelastic rod," 1990. *Journal of Mathematical Analysis and Applications*, to appear.

[7] J.S. Gibson, I.G. Rosen, and G. Tao, "Approximation in Control of Thermoelastic Systems," in *Proceedings of 1989 American Control Conference*, (Pittsburgh, PA), pp. 1171–1176, June 1989.

[8] J.S. Gibson, I.G. Rosen, and G. Tao, "Approximation in LQG Optimal Control of a Thermoelastic Rod," in *Proceedings of 3rd Annual Conference on Aerospace Computational Control*, (Oxnard, CA), August 1989.

[9] I.G. Rosen and C.H. Su, "An approximation theory for the identification of linear thermoelastic systems," 1990. *Journal of Differential and Integral Equations*, to appear.

[10] J.L. Walsh and P.B. Ulrich, "Thermal blooming in the atmosphere," in *Laser Beam Propagation in the Atmosphere*, (J.W. Strohnbehn, ed.), pp. 223–320, Berlin: Springer-Verlag, 1978.

[11] C.M. Dafermos, "On the existence and the asymptotic stability of solutions of the equations of linear thermoelasticity," *Archive for Rational Mechanics and Analysis*, vol. 29, pp. 241–271, 1968.

[12] M. Slemrod, "Global existence, uniqueness, and asymptotic stability of classical smooth solutions in one-dimensional non-linear thermoelasticity," *Archive for Rational Mechanics and Analysis*, vol. 76, pp. 97–133, 1981.

[13] J.A. Walker, *Dynamical Systems and Evolution Equations*. New York: Plenum, 1980.

[14] Jong Uhn Kim, "On the energy decay of a linear thermoelastic bar and plate," 1990. Preprint.

[15] R.E. Showalter, *Hilbert Space Methods for Partial Differential Equations*. London: Pitman, 1977.

[16] H. Tanabe, *Equations of Evolution*. London: Pitman, 1979.

[17] H.T. Banks and K. Ito, "A unified framework for approximation and inverse problems for distributed parameter systems," *Control Theory and Advanced Technology*, vol. 4, pp. 73–90, 1988.

[18] J.S. Gibson and A. Adamian, "Approximation theory for LQG optimal control of flexible structures," *SIAM Journal on Control and Optimization*, vol. 29, pp. 1–37, January 1991.

[19] A.V. Balakrishnan, *Applied Functional Analysis*, Second Edition. New York: Springer-Verlag, 1981.

[20] R.F. Curtain and A.J. Pritchard, *Infinite Dimensional Linear Systems Theory*. New York: Springer-Verlag, 1978.

[21] J.S. Gibson, "The Riccati Integral Equations for Optimal Control Problems on Hilbert Spaces," *SIAM Journal on Control and Optimization*, vol. 17, pp. 537–565, July 1979.

[22] J.S. Gibson and I.G. Rosen, "Computational Methods for Optimal Linear-Quadratic Compensators for Infinite Dimensional Discrete-Time Systems," in *Springer-Verlag Lecture Notes in Control and Information Sciences*, (Vorau, Austria), pp. 120–135, July 1986. Vol. 102.

[23] H.T. Banks and K. Kunisch, "The linear regulator problem for parabolic systems," *SIAM Journal on Control and Optimization*, vol. 22, pp. 684–696, September 1984.

[24] J.S. Gibson and I.G. Rosen, "Numerical approximation for the infinite-dimensional discrete-time optimal linear-quadratic regulator problem," *SIAM Journal Control and Optimization*, vol. 26, pp. 428–451, March 1988.

[25] T. Kato, *Perturbation Theory for Linear Operators*, Second Edition. New York: Springer-Verlag, 1984.

[26] D.E. Carlson, "Linear thermoelasticity," in *Handbuch der Physik*. Bd. Vla/2, (C. Truesdell, ed.), Berlin: Springer, 1972.

[27] E. P. Popov, *Introduction to Mechanics of Solids*. Englewood Cliffs, NJ: Prentice-Hall, 1968.

[28] A.D. Day, *Heat Conduction within Linear Thermoelasticity*. New York: Springer-Verlag, 1985.

[29] M. N. Ozisik, *Heat Conduction*. New York: Wiley, 1980.

[30] J.D. Roberts, "Linear model reduction and solution of the algebraic Riccati equation by use of the sign function," *International Journal of Control*, vol. 32, pp. 677–687, 1980.

[31] J.S. Gibson, "An Analysis of Optimal Modal Regulation: Convergence and Stability," *SIAM Journal on Control and Optimization*, vol. 19, pp. 686–707, September 1981.

Uniform Exponential Stability of Solutions to Abstract Linear Wave Equations with Coercive Damping

J.S. Gibson *
Mechanical, Aerospace and Nuclear Engineering
University of California, Los Angeles 90024

October 3, 1990

Abstract

This paper derives sufficient conditions for uniform exponential stability of solutions to abstract linear evolution equations that are second-order in time. The main problems motivating the paper involve sets of coupled partial differential equations with nonsymmetric damping. Such systems arise in acoustics problems when the interaction between compressible fluids and elastic boundaries produces a skew-symmetric damping term.

*This research was supported by AFOSR Grant 87-0373.

1 Introduction

By abstract wave equations, we mean evolution equations that are second-order in time. This class includes both classical wave and biharmonic equations. The evolution equations that are the primary motivation for the paper are sets of coupled partial differential equations that represent acoustic waves in a compressible fluid interacting with an elastic boundary.

This paper has two main objectives: first, to derive sufficient conditions for the solutions to abstract linear wave equations with coercive damping to be uniformly exponentially stable; second, to demonstrate that the class of coupled partial differential equations of greatest interest in this paper do indeed have the abstract second-order form treated here. Uniform exponential stability is important in active control of distributed systems [1,2,3], and having the abstract second-order form allows an extensive theory of approximation derived especially for control and estimation problems to be applied (see [1,2,3,4], for example).

The most interesting property of the equations motivating this paper is that the damping operator is not symmetric. A nonzero skew-symmetric damping operator makes the issue of uniform exponential stability more complicated than in the case of symmetric damping. In particular, when the damping operator is symmetric, it must only be coercive with respect to the kinetic-energy norm to guarantee uniform exponential stability. However, an example in Section 3 of this paper shows that, in general, more is needed when the damping is not symmetric. (While the operator in the term with the first-order time derivative in second-order evolution equations is referred to commonly as damping, the skew-symmetric part of this operator represents conservative energy transfer among different states, as opposed to dissipation.)

2 Abstract Linear Wave Equations

Throughout this paper, H or H_j $(j = 0, 1, 2)$ will be a Hilbert space with inner product $(\cdot,\cdot)$ or $(\cdot,\cdot)_j$ and corresponding induced norm $|\cdot|$ or $|\cdot|_j$. Also, V or V_j will be a Hilbert space with norm $\|\cdot\|$ or $\|\cdot\|_j$ and inner product $\langle\cdot,\cdot\rangle_V$ or $\langle\cdot,\cdot\rangle_{V_j}$. The continuous dual of V will be denoted by V', and

$$V \hookrightarrow H \hookrightarrow V' \tag{2.1}$$

will mean that V is embedded densely and continuously in H, which implies that H is embedded densely and continuously in V'. In this case, $(\cdot,\cdot)$ will denote both the H-inner product and the duality pairing on $V \times V'$.

For an operator $\mathcal{L} \in \mathcal{B}(V_i, V_j')$, we define $\mathcal{L}^* \in \mathcal{B}(V_j, V_i')$ (the Banach-space adjoint of $\mathcal{L}$) by

$$\langle v, \mathcal{L}^* w\rangle_i = \overline{\langle w, \mathcal{L} v\rangle}_j, \qquad v \in V_i,\ w \in V_j. \tag{2.2}$$

We say that $\mathcal{L} \in \mathcal{B}(V, V')$ is *symmetric* if $\mathcal{L} = \mathcal{L}^*$. We say that $\mathcal{L} \in \mathcal{B}(V, V')$ is nonnegative if

$$\mathrm{Re}\langle v, \mathcal{L} v\rangle \geq 0, \qquad v \in V, \tag{2.3}$$

and that $\mathcal{L}$ is *dissipative* if $-\mathcal{L}$ is nonnegative. We say that $\mathcal{L} \in \mathcal{B}(V, V')$ is *H-coercive* if there exists a positive real number μ such that

$$\mathrm{Re}(v, \mathcal{L} v) \geq \mu |v|^2, \qquad v \in V, \tag{2.4}$$

and that $\mathcal{L} \in \mathcal{B}(V, V')$ is *V-coercive* if there exists a positive real number μ such that

$$\mathrm{Re}\langle v, \mathcal{L} v\rangle \geq \mu \|v\|^2, \qquad v \in V. \tag{2.5}$$

We assume

$$V_0 \hookrightarrow H_0 \hookrightarrow V_0', \tag{2.6}$$

and we study evolution equations of the form

$$\ddot{w}(t) + \mathcal{D}_0 \dot{w}(t) + \mathcal{A}_0 w(t) = 0, \qquad t > 0, \tag{2.7}$$

where $\mathcal{D}_0, \mathcal{A}_0 \in \mathcal{B}(V_0, V_0')$ with $\mathcal{D}_0$ nonnegative and $\mathcal{A}_0$ equal to the Riesz map on V_0. Thus,

$$\langle v, w\rangle_{V_0} = (v, \mathcal{A}_0 w)_0, \tag{2.8}$$

and $\mathcal{A}_0$ is symmetric and V_0-coercive.

We define

$$V = V_0 \times V_0 \hookrightarrow H = V_0 \times H_0 \hookrightarrow V' = V_0 \times V_0'. \tag{2.9}$$

(We identify V_0 with V_0' in the first component of H only.) We define

$$\mathcal{A} = \begin{bmatrix} 0 & I \\ -\mathcal{A}_0 & -\mathcal{D}_0 \end{bmatrix} \in \mathcal{B}(V, V'). \tag{2.10}$$

If follows from

$$\mathcal{A}_1^{-1} = \begin{bmatrix} -\mathcal{A}_0^{-1}\mathcal{D}_0 & -\mathcal{A}_0^{-1} \\ I & 0 \end{bmatrix} \in \mathcal{B}(V_1', V_1) \tag{2.11}$$

that $\mathcal{A}$ is an isomorphism from V to V'. Now we define $A : \mathrm{Dom}(A) \subset H \to H$ by

$$\mathrm{Dom}(A) = \{(v, h) \in V : \mathcal{A}(v, h) \in H\}, \qquad A = \mathcal{A}|_{\mathrm{Dom}(A)}. \tag{2.12}$$

According to Lemma 2.1 in [3], A is a maximal dissipative operator on H. Hence A generates a strongly continuous contraction semigroup on H. (See [4,2,5] for similar approaches.)

3 Uniform Exponential Stability

Theorem 3.1 *If $\mathcal{D}_0$ is H_0-coercive and there exists a positive real number γ such that*

$$|\mathrm{Re}\langle v, \mathcal{D}_0 h\rangle_0| \le \gamma \|v\|_0 \cdot |\mathrm{Re}\langle h, \mathcal{D}_0 h\rangle_0|^{1/2}, \qquad v, h \in V_0, \tag{3.1}$$

then the semigroup generated on H by the operator A in (2.12) is uniformly exponentially stable.

Proof We define the following self-adjoint bounded linear operator on H:

$$Q = \begin{bmatrix} \sigma I & \mathcal{A}_0^{-1} \\ I & \sigma I \end{bmatrix} \tag{3.2}$$

where σ is a positive real number. For σ sufficiently large, Q is H-coercive. Also, $QV \subset V$. For $x = (v, h) \in \mathrm{Dom}(A) \subset V$,

$$\mathrm{Re}\,\langle Qx, Ax\rangle = \mathrm{Re}\,\langle Qx, \mathcal{A}x\rangle = -\|v\|_0^2 + |h|_0^2 - \sigma \mathrm{Re}\langle h, \mathcal{D}_0 h\rangle_0 - \mathrm{Re}\langle v, \mathcal{D}_0 h\rangle_0. \tag{3.3}$$

Since $\mathcal{D}_0$ is H_0-coercive, it follows from (3.1) and (3.3) that, for σ sufficiently large, there exists a positive real number μ such that

$$\mathrm{Re}\langle Qx, Ax\rangle \le -\mu |x|^2, \qquad x \in \mathrm{Dom}(A). \qquad \square \tag{3.4}$$

Remark 3.2 *A sufficient condition for the existence of a positive real number γ such that* (3.1) *holds is that $\mathcal{D}_0$ be V_0-coercive.*

Remark 3.3 *If $\mathcal{D}_0$ is H_0-coercive, the generalized Schwarz inequality and the fact that $\mathcal{D}_0 \in \mathcal{B}(V_0, V_0')$ imply that $|\mathrm{Re}\langle v, (\mathcal{D}_0 + \mathcal{D}_0^*)h\rangle_0|$ is bounded by the right side of* (3.1) *for some positive γ independent of v and h. Therefore, when $\mathcal{D}_0$ is H_0-coercive,* (3.1) *holds for some γ independent of v and h if and only if*

$$|\mathrm{Re}\,\langle v, (\mathcal{D}_0 - \mathcal{D}_0^*)h\rangle_0| \le \gamma \|v\|_0 \cdot |\mathrm{Re}\,\langle h, \mathcal{D}_0 h\rangle_0|^{1/2}, \qquad v, h \in V_0, \tag{3.5}$$

for some γ independent of v and h. When $\mathcal{D}_0$ is H_0-coercive, one sufficient condition for (3.5) *is that $\mathcal{R}(\mathcal{D}_0 - \mathcal{D}_0^*) \subset H_0$ (this includes the case $\mathcal{D}_0 = \mathcal{D}_0^*$).*

The following example shows that $\mathcal{D}_0$ being H_0-coercive without (3.1) or some other condition is not sufficient for the semigroup generated by A to be uniformly exponentially stable.

Let α be a negative real number, and let β_n and ω_n be sequences of positive real numbers such that

$$\omega_n \to \infty \qquad \text{and} \qquad \beta_n/\omega_n \to \infty \qquad \text{as} \quad n \to \infty \tag{3.6}$$

and

$$\sup_n \beta_n/\omega_n^2 < \infty. \tag{3.7}$$

Let H_0 be ℓ_2, let T_0 be the infinite-dimensional diagonal matrix with the sequence ω_n on the diagonal, let $V_0 = T_0^{-1} H_0$ with $\mathcal{A}_0 = T_0^2$, and let $\mathcal{D}_0$ be the infinite-dimensional diagonal matrix with the sequence $\alpha + i\beta_n$ on the diagonal.

The eigenvalues of the corresponding semigroup generator A are the solutions to a sequence of quadratic equations. Elementary analysis shows that these eigenvalues approach the imaginary axis as $n \to \infty$. Hence the semigroup generated on H by A is not uniformly exponentially stable.

4 Coupled Abstract Wave Equations

In this section, we assume that the Hilbert spaces H_0 and V_0 and the operators $\mathcal{A}_0$ and $\mathcal{D}_0$ have the forms

$$H_0 = H_1 \times H_2, \qquad V_0 = V_1 \times V_2, \tag{4.1}$$

$$\mathcal{A}_0 = \begin{bmatrix} \mathcal{A}_{11} & 0 \\ 0 & \mathcal{A}_{22} \end{bmatrix}, \tag{4.2}$$

$$\mathcal{D}_0 = \begin{bmatrix} \mathcal{D}_{11} & \mathcal{D}_{12} \\ -\mathcal{D}_{12}^* & \mathcal{D}_{22} \end{bmatrix}. \tag{4.3}$$

We assume that $\mathcal{A}_{ii}$ is the Riesz map for V_i, $i = 1, 2$, and that $\mathcal{D}_{ij} \in \mathcal{B}(V_j, V_i')$ with $\mathcal{D}_{ii}$ nonnegative.

We are particularly interested in problems where the wave equation on $V_1 \times H_1$ represents an elastic boundary condition for the wave equation on $V_2 \times H_2$. In this case, we have

$$\mathcal{R}(\mathcal{D}_{12}) \subset H_1. \tag{4.4}$$

We should note that (4.4) does *not* imply

$$\mathcal{R}(\mathcal{D}_{12}^*) \subset H_2. \tag{4.5}$$

We consider the domain of the semigroup generator A for the coupled system when (4.4) holds. It follows from (2.9)–(2.12) that $\mathrm{Dom}(A)$ is the set of all elements

$$(v_1, v_2, h_1, h_2) \in V = V_1 \times V_2 \times V_1 \times V_2 \tag{4.6}$$

such that

$$\mathcal{A}_{11} v_1 + \mathcal{D}_{11} h_1 \in H_1, \tag{4.7}$$

$$\mathcal{A}_{22} v_2 + \mathcal{D}_{22} h_2 - \mathcal{D}_{12}^* h_1 \in H_2. \tag{4.8}$$

From (4.7), we see that the conditions on v_1 and h_1 are independent of the coupling operator $\mathcal{D}_{12}$ and are the same as when the two wave equations are uncoupled. On the other hand, if $\mathcal{R}(D_{12}^*)$ is not contained in H_2, then the conditions on v_2 and h_2 do depend on $\mathcal{D}_{12}$. In most applications, $\mathcal{D}_{12}^*$ affects the 'natural boundary conditions' for v_2 and h_2.

To be more concrete, we take $T_2 \in \mathcal{B}(V_2, H_2)$ such that

$$\langle v, w \rangle_{V_2} = \langle v, \mathcal{A}_{22} w \rangle_2 = \langle T_2 v, T_2 w \rangle_2, \qquad v, w \in V_2, \tag{4.9}$$

and we take T_2^* to the Hilbert space adjoint of T_2 with respect to the H_2-inner product. It is a straightforward exercise to show that (4.8) is equivalent to

$$T_2 v_2 + T_2 \mathcal{A}_{22}^{-1} \mathcal{D}_{22} h_2 - T_2 \mathcal{A}_{22}^{-1} \mathcal{D}_{12}^* h_1 \in \mathrm{Dom}(T_2^*). \tag{4.10}$$

In many examples, it is easy to determine $T_2 \mathcal{A}_{22}^{-1} \mathcal{D}_{22}$ and $T_2 \mathcal{A}_{22}^{-1} \mathcal{D}_{12}^*$. If $\mathcal{R}(\mathcal{D}_{12}^*) \subset H_2$, the term $T_2 \mathcal{A}_{22}^{-1} \mathcal{D}_{22} h_2$ drops out of (4.10), but this is not the case in which we will be interested from here on.

Before considering an example, we will give a sufficient condition for solutions to the system of coupled abstract wave equations to be uniformly exponentially stable in $H = V_0 \times H_0$.

Theorem 4.1 *Let H_0, V_0, $\mathcal{A}_0$ and $\mathcal{D}_0$ have the forms in (4.1)–(4.3) with $\mathcal{D}_{ii}$ symmetric, $i = 1, 2$. Let (4.4) hold. If $\mathcal{D}_{11}$ is H_1-coercive and $\mathcal{D}_{22}$ is V_2-coercive, then the semigroup generated on H by the operator A in (2.9)–(2.12) is uniformly exponentially stable.*

Proof Since $\mathcal{D}_{12} \in \mathcal{B}(V_2, V_1')$, (4.4) implies $\mathcal{D}_{12} \in \mathcal{B}(V_2, H_1)$. For $v_1, h_1 \in V_1$ and $v_2, h_2 \in V_2$,

$$\begin{aligned} |\langle v_1, \mathcal{D}_{12} h_2 \rangle_1 + \langle v_2, \mathcal{D}_{12}^* h_1 \rangle_2| &= |\langle v_1, \mathcal{D}_{12} h_2 \rangle_1 + \overline{\langle h_1, \mathcal{D}_{12} v_2 \rangle_1}| \\ &\le \|\mathcal{D}_{12}\|_{\mathcal{B}(V_2, H_1)} (|v_1|_1 \cdot \|h_2\|_2 + |h_1|_1 \cdot \|v_2\|_2). \end{aligned} \tag{4.11}$$

Since $\mathcal{D}_{11}$ is symmetric and H_1-coercive, $\mathcal{D}_{22}$ is symmetric and V_2-coercive and the V_1-norm is stronger than the H_1-norm, it follows from (4.11) that (3.5) holds for some postive γ independent of $v = (v_1, v_2) \in V_0$ and $h = (h_1, h_2) \in V_0$. □

5 An Example from Acoustics

In this one-dimensional application, the wave equation on $V_2 \times H_2$ governs the velocity potential in a compressible fluid, and the wave equation on $V_1 \times H_1$ reduces to the equation of motion of a mass-spring-damper system on one boundary of the fluid. We assume zero velocity potential on the other boundary of the fluid.

We have

$$H_1 = V_1 = R^1, \tag{5.1}$$

$$H_2 = L_2(0,1), \qquad V_2 = \{\phi \in H^1(0,1) : \phi(1) = 0\}, \tag{5.2}$$

$$\mathcal{A}_{11} = 1 \tag{5.3}$$

$$\langle \phi, \mathcal{A}_{22}\psi \rangle_2 = \int_0^1 \phi'\psi'\, d\eta \qquad \phi, \psi \in V_2, \tag{5.4}$$

$$\mathcal{D}_{11} = \epsilon_1, \tag{5.5}$$

$$\mathcal{D}_{22} = \epsilon_2 \mathcal{A}_{22}, \tag{5.6}$$

$$\langle \beta, \mathcal{D}_{12}\psi \rangle_1 = -\beta\psi(0), \qquad \beta \in V_1,\ \psi \in V_2. \tag{5.7}$$

We have taken all physical constants to be 1, except the nonnegative real numbers ϵ_1 and ϵ_2.

The operator T_2 in (4.9) and (4.10) is given by

$$\mathrm{Dom}(T_2) = V_2, \qquad T_2\phi = \phi', \tag{5.8}$$

and its adjoint is given by

$$\mathrm{Dom}(T_2^*) = \{\phi \in H^1(0,1) : \phi(0) = 0\}. \qquad T_2^*\phi = -\phi'. \tag{5.9}$$

In this example, $T_2\mathcal{A}_{22}^{-1}\mathcal{D}_{12}^*$ is a function in $L_2(0,1)$. From (5.7), it follows that

$$(T_2\mathcal{A}_{22}^{-1}\mathcal{D}_{12}^*\beta)(\eta) = \beta, \qquad 0 < \eta < 1, \qquad \beta \in R^1. \tag{5.10}$$

Also,

$$\mathcal{A}_{22}^{-1}\mathcal{D}_{22} = \epsilon_2 I. \tag{5.11}$$

It follows from (4.6), (4.7) and (4.10), then, that $\mathrm{Dom}(A)$ is the set of all quadruples $(\alpha, \phi, \beta, \psi)$ satisfying

$$\alpha, \beta \in R^1, \tag{5.12}$$

$$\phi, \psi \in H^1(0,1), \qquad \phi(1) = \psi(1) = 0, \tag{5.13}$$

$$(\phi + \epsilon_2\psi - \beta)' \in H^1(0,1), \qquad \phi'(0) + \epsilon_2\psi'(0) - \beta = 0. \tag{5.14}$$

From (2.10)–(2.12) and the definitions of the various operators in this example, it follows that, for $(\alpha, \phi, \beta, \psi) \in \mathrm{Dom}(A)$,

$$A\begin{pmatrix} \alpha \\ \phi \\ \beta \\ \psi \end{pmatrix} = \begin{pmatrix} \beta \\ \psi \\ -\alpha - \epsilon_1\beta + \psi(0) \\ (\phi' + \epsilon_2\psi')' \end{pmatrix}. \tag{5.15}$$

We define $w(t) = (\alpha(t), \phi(t)) \in V_0 = V_1 \times V_2$ to be the solution to

$$\begin{pmatrix} w(0) \\ \dot{w}(0) \end{pmatrix} \in \mathrm{Dom}(A), \qquad \frac{d}{dt}\begin{pmatrix} w(t) \\ \dot{w}(t) \end{pmatrix} = A\begin{pmatrix} w(t) \\ \dot{w}(t) \end{pmatrix}, \qquad t > 0. \tag{5.16}$$

Equivalently, $\alpha(t)$ and $\phi(t) = \phi(t, \eta)$ satisfy

$$\ddot{\alpha}(t) + \epsilon_1 \dot{\alpha}(t) + \alpha(t) = \frac{\partial \phi}{\partial t}(t, 0) \qquad t > 0, \tag{5.17}$$

$$\frac{\partial^2 \phi}{\partial t^2}(t, \eta) - \frac{\partial}{\partial \eta}\left(\frac{\partial \phi}{\partial \eta} + \epsilon_2 \frac{\partial^2 \phi}{\partial \eta \partial t}\right)(t, \eta) = 0, \qquad 0 < \eta < 1, \quad t > 0, \tag{5.18}$$

$$\frac{\partial \phi}{\partial \eta}(t, 0) + \epsilon_2 \frac{\partial^2 \phi}{\partial \eta \partial t}(t, 0) = \dot{\alpha}(t), \qquad t \geq 0, \tag{5.19}$$

$$\phi(t, 1) = 0, \qquad t \geq 0. \tag{5.20}$$

If ϵ_1 and ϵ_2 are positive, then Theorem 4.1 says that the semigroup generated on H by A and consequently all solutions to (5.17)–(5.20) are uniformly exponentially stable. It is important to note that, to apply Theorem 4.1, we need the $\mathcal{D}_{22}$ in (5.6), or something similar, as opposed to, say, $\mathcal{D}_{22} = \epsilon_2 I$. The $\mathcal{D}_{22}$ in (5.6) is a realistic dissipation term for waves in a compressible fluid because it represents viscosity [6, page 315], [7].

6 Conclusions

It is straightforward to generalize the example here to wave equations in higher dimensions. For example, the wave equation on $V_1 \times H_1$ could represent an elastic membrane interacting with the waves in a three-dimensional volume of fluid, represented by the wave equation on $V_2 \times H_2$. In such cases, the product on the right side of (5.7) becomes an L_2-inner product on the elastic boundary.

In the higher-dimension problems, the damping operator $\mathcal{D}_{11}$ for the elastic boundary need be only H_1-coercive for uniform exponential stability, if $\mathcal{D}_{22}$ represents viscosity, as in the example here. This is important because many common damping models for flexible structures are H_1-coercive but not V_1-coercive.

Whether the hypotheses in Theorem 3.1 or the requirement in Theorem 4.1 that $\mathcal{D}_{22}$ be V_2-coercive can be weakened is an open and interesting question. The example at the end of Section 3 suggests that significantly weaker sufficient conditions than those given in this paper for uniform exponential stability might not exist.

References

[1] H. T. Banks and K. Kunisch, "The Linear Regulator Problem for Parabolic Systems," *SIAM Journal on Control and Optimization*, vol. 22, pp. 684–696, September 1984.

[2] J.S. Gibson and A. Adamian, "Approximation theory for LQG optimal control of flexible structures," 1991. To appear in *SIAM Journal on Control and Optimization*.

[3] J.S. Gibson, I.G. Rosen, and G. Tao, "Approximation in control of thermoelastic systems," 1990. Submitted to *SIAM Journal on Control and Optimization*.

[4] H. T. Banks and K. Ito, "A Unified Framework for Approximation and Inverse Problems for Distributed Parameter Systems," *Control Theory and Advanced Technology*, 1988.

[5] R.E. Showalter, *Hilbert Space Methods for Partial Differential Equations*. London: Pitman, 1977.

[6] Lord Rayleigh, *Theory of Sound*. Vol. II, New York: Dover, 1945 (Original Publication, 1877).

[7] W.C. Meecham, "Lecture notes on acoustics," 1988. Mechanical, Aerospace and Nuclear Engineering, UCLA.

A NEW UNWINDOWED LATTICE FILTER FOR RLS ESTIMATION

S. W. Chen and J. S. Gibson

Mechanical, Aerospace and Nuclear Engineering

University of California, Los Angeles 90024

ABSTRACT

Adaptive lattice algorithms are derived for solution of unwindowed least-squares estimation problems for AR and FIR models. The basic approach is to embed the unwindowed problem in a larger prewindowed problem and then eliminate superfluous terms in the lattice. Initializations are given to allow the lattice to use no initial parameter estimates or to include initial parameter estimates with desired weightings in the quadratic criterion for parameter estimation. A numerical example is given.

This research was supported by AFOSR Grant 870373

1. Introduction

This paper treats two initialization problems for unnormalized lattice implementation of recursive least-squares estimation of AR and FIR models. The first problem, usually called unwindowed estimation, is to obtain the exact least-squares fit to data when the data preceding the initial point used cannot be assumed to be zero. The second problem is to penalize deviation from initial parameter estimates. Although solutions to both problems are straight-forward in the classical recursive least-squares algorithm, solutions via lattices require not only special initializations but more complicated lattices than the common prewindowed lattice [1,2,3,4].

The terms prewindowed and unwindowed refer to how data is handled in estimation, rather than to the AR or FIR model. In prewindowed estimation, all data before some initial time is assumed to be zero. Although this assumption usually is not correct, it affects only the first few terms in the cumulative least-squares criterion, and therefore the affect on estimated parameters and predicted data fades as the number of processed data points increases. Whether the error caused by the prewindowing assumption, when it is incorrect, is tolerable depends on the application. This error is eliminated by unwindowed estimation, where the criterion to be minimized tries to fit only true data with the AR or FIR model. In unwindowed estimation, no assumption is made about data preceding that used.

Including initial parameter estimates makes practical sense only in unwindowed estimation. Initial parameter estimates can be included in prewindowed estimation, but their effect and that of the error induced by the prewindowing assumption fade at the same rate. Also, to include initial parameter estimates in a lattice filter for an AR model, the model must be embedded in an FIR model. This is necessary to preserve the shift structure of the recursion vectors for the AR lattice.

Both problems addressed in this paper have been addressed with previous lattice filters. Normalized lattices for unwindowed estimation were given in [5,6]. An unnormalized lattice for the scalar-channel (single experiment) unwindowed, or covariance problem was given in [2]. An unnormalized lattice and initializations for unwindowed RLS estimation with and without initial parameter estimates was proposed in [7], although, as discussed in Section 5 of this paper, we have concluded that the lattice and initializations in [7] do not solve unwindowed problems. While the lattice here and the initialization of parameter estimates are different from those in [7], the basic idea of using the initial parameter estimates as initial data for the output channel of an FIR model is common to Section 4 of this paper and [7].

The basic idea behind the unwindowed AR lattice in Section 3 of this paper is to use an artificial measurement channel in the prewindowed lattice in [3]. This idea is straightforward, and it has been explored previously (see [8]). However, the additional channel makes the lattice more complex. The most important objective in developing the AR lattice is to exploit the special structure associated with the artificial channel to reduce the expanded lattice to an efficient solution of the unwindowed least-squares estimation problem. In particular, expanding the lattice with the artificial channel increases the dimension of the coefficient matrices that must be inverted in the prewindowed lattice. By using the structure induced by the artificial channel and generalizing a well-known formula for low-rank updates of matrix inverses, we obtain an unwindowed lattice in which the matrices to be inverted have the same dimension as the corresponding matrices in the prewindowed lattice.

The authors of [8] concluded that the normalized lattice they derived using an artificial channel was not competitive in terms of computational requirements with the covariance lattice in [5], whereas we believe that the lattice developed here will be competitive with any unnormalized lattice for solving the unwindowed problem. These different conclusions about the two lattices based on the artificial-channel idea appear to stem in large part from the ability to reduce the dimension of the matrices that must be inverted in our lattice and the inability to reduce the dimension of the matrices of which square roots must be computed in the lattice in [8].

The remainder of the paper is organized as follows. Section 2 defines unwindowed and prewindowed estimation problems for an AR model, embeds the unwindowed problem in the prewindowed problem and reduces the prewindowed lattice to produce an efficient solution of the unwindowed problem. The basic algorithm for the entire paper is Algorithm 2.1, the residual-error lattice for the AR problem. Algorithm 2.2 is used to generate the estimated AR coefficients. Section 3 defines unwindowed and prewindowed estimation problems for an FIR model and develops the additional update equations that must be appended to the algorithms in Section 2. Section 4 shows how to include initial parameter estimates in the FIR problem. For this, the lattice algorithms in Sections 2 and 3 are used but the time-initializations are replaced with those in Section 4.

Section 5 presents an example to demonstrate the faster convergence of the unwindowed lattice versus the prewindowed lattice and the advantage of including initial parameter estimates in the presence of measurement noise. Section 6 presents our conclusions, and the Appendix contains the matrix inversion lemma that we use in Section 2.

2. The AR Problem

We consider an $m \times p$ measurement matrix

$$y(t) = [y^1(t) y^2(t) \ldots y^p(t)] \ , \tag{2.1}$$

where t is any integer and the i^{th} column $y^i(t)$ is a real m-vector, referred to as the i^{th} measurement channel. The k^{th} element of $y^i(t)$ is called the k^{th} measurement in the i^{th} channel. By an n^{th}-order AR model, we mean

$$y(t) = \sum_{j=1}^{n} y(t-j) A_{n,j} + \varepsilon_n(t) , \tag{2.2}$$

where the $A_{n,j}$'s are $p \times p$ matrices referred to as AR coefficients. We denote the i^{th} column of $A_{n,j}$ by $A^i_{n,j}$.

As in [3], we define the Hilbert space

$$\ell_2(R^m, \lambda) = \{ z = [x_1^T x_2^T x_3^T \ldots]^T : \text{each } x_j \in R^m \text{ and } |z|^2 = \langle z, z \rangle < \infty \} \ , \tag{2.3}$$

where

$$\langle z, \hat{z} \rangle = \sum_{j=1}^{\infty} \lambda^{j-1} x_j^T \hat{x}_j \tag{2.4}$$

and λ is a positive real number called the forgetting factor. Throughout the paper, $\langle \cdot , \cdot \rangle$ means the inner product in (2.4). For $k = 0, 1, 2, \ldots$, M_k is the subspace of $\ell_2(R^m, \lambda)$ such that each element of M_k has the form of z in (2.3) with the m-vector $x_j = 0$ for $j > k$, and

$$Q_k = \text{orthogonal projection of } \ell_2(R^m, \lambda) \text{ onto } M_k \ . \tag{2.5}$$

We denote the infinite history of $y(t)$ by

$$\psi(t) = [\psi^1(t) \psi^2(t) \ldots \psi^p(t)] = [y^T(t) y^T(t-1) y^T(t-2) \ldots]^T \tag{2.6}$$

so that $\psi^i(t)$, the i^{th} column of $\psi(t)$, is the infinite history of $y^i(t)$, and $\psi(t) \in \ell_2(R^m, \lambda)$. For any integer t, we define $H_0(t) = \{0\}$, which is the zero subspace of $\ell_2(R^m, \lambda)$, and

$$\begin{aligned} H_n(t) = \text{span} \{ & \psi^1(t-1) \ldots \psi^p(t-1) \ \psi^1(t-2) \ldots \psi^p(t-2) \\ & \ldots \psi^1(t-n) \ldots \psi^p(t-n) \} \ , \quad n = 1, 2, \ldots \ . \end{aligned} \tag{2.7}$$

For $k = 0, 1, 2, \ldots$, we define $H_{n,k}(t) = Q_k H_n(t)$. Hence $H_0(t) = H_{0,k}(t) = H_{n,0}(t) = \{0\}$. We use the projection operators

$$P_n(t) = \text{orthogonal projection of } \ell_2(R^m, \lambda) \text{ onto } H_n(t), \tag{2.8}$$

$$P_{n,k}(t) = \text{orthogonal projection of } \ell_2(R^m, \lambda) \text{ onto } H_{n,k}(t). \tag{2.9}$$

(We note $P_n(t)\psi(t) = [P_n(t)\psi^1(t) \ \dots \ P_n(t)\psi^p(t)]$ and $P_{n,k}(t)\psi(t) = [P_{n,k}(t)\psi^1(t) \ \dots \ P_{n,k}(t)\psi^p(t)]$.) Computing $P_{n,k}(t)\psi(t)$ is an unwindowed least-squares problem, and computing $P_n(t)\psi(t)$ when $\psi(t)$ has a finite number of nonzero entries is a prewindowed least-squares problem.

Throughout this paper, $y(t)$ will denote the $m \times p$ measurement matrix for unwindowed problems and $\tilde{y}(t)$ will denote the $m \times \tilde{p}$ measurement matrix for prewindowed problems. The histories of $y(t)$ and $\tilde{y}(t)$ are $\psi(t)$ and $\tilde{\psi}(t)$, respectively. The projections defined by (2.8) and (2.9) corresponding to $y(t)$ and $\psi(t)$ are $P_n(t)$ and $P_{n,k}(t)$; the projection defined by (2.8) corresponding to $\tilde{y}(t)$ and $\tilde{\psi}(t)$ is $\tilde{P}_n(t)$.

Problem 2.1. (Unwindowed AR Problem) For $t = 1, 2, \dots$, and $n = 0, 1, 2, \dots, t-1$, compute $P_{n,t-n}(t)\psi(t) = P_{n,t-n}(t)\, Q_{t-1}\psi(t)$; equivalently, (for $n = 1, 2, \dots, t-1$) find matrices $A_{n,j}(t)$ such that, for each i ($i = 1, \dots, p$), the i^{th} columns of the matrices $A_{n,j}(t)$ minimize

$$J_1^{i,n}(t) = \sum_{\tau=n+1}^{t} \lambda^{t-\tau} \left| y^i(\tau) - \sum_{j=1}^{n} y(\tau - j)\, A_{n,j}^i(t) \right|^2 , \tag{2.10}$$

where $|\cdot|$ is the Euclidean norm of an m-vector.

Problem 2.2. (Prewindowed AR Problem) Assume $\tilde{y}(t) = 0$ for $t < 0$. For $t = 0, 1, 2, \dots$, and $n = 0, 1, 2, \dots, t$, compute $\tilde{P}_n(t)\tilde{\psi}(t)$; equivalently, (for $n = 1, 2, \dots, t$) find matrices $\tilde{A}_{n,j}(t)$ such that, for each i ($i = 1, \dots, \tilde{p}$), the i^{th} columns of these matrices minimize

$$J_2^{i,n}(t) = \sum_{\tau=0}^{t} \lambda^{t-\tau} \left| \tilde{y}^i(\tau) - \sum_{j=1}^{n} \tilde{y}(\tau - j)\, \tilde{A}_{n,j}^i(t) \right|^2 . \tag{2.11}$$

We note that, in Problem 2.1, nonzero data for $t \le 0$ is allowed but not used, whereas in Problem 2.2, all data is assumed zero for $t < 0$. The initial times in Problem 2.1 and 2.2 are, of course, arbitrary. We denote them differently so that we can embed Problem 2.1 in Problem 2.2 most conveniently.

The lattice in [&JG1.] solves Problem 2.2. We will need the following definitions from [&JG1.]. For any integer t and any nonnegative integer n,

$$f_n(t) = [f_n^1(t) \ \dots \ f_n^{\tilde{p}}(t)] = [I - \tilde{P}_n(t)]\tilde{\psi}(t), \tag{2.12}$$

$$b_n(t) = [b_n^1(t) \ \dots \ b_n^{\tilde{p}}(t)] = [I - \tilde{P}_n(t+1)]\tilde{\psi}(t-n), \tag{2.13}$$

$$\tilde{e}_n(t) = \textit{top } m \textit{ rows of } f_n(t), \quad \textit{forward residual error}, \tag{2.14}$$

$$\tilde{r}_n(t) = \textit{top } m \textit{ rows of } b_n(t), \quad \textit{backward residual error}, \tag{2.15}$$

$$\tilde{K}_{n+1}(t) = \tilde{p} \times \tilde{p} \textit{ matrix whose } (i, j) \textit{ element is } \langle f_n^i(t), b_n^j(t-1)\rangle, \tag{2.16}$$

$$\tilde{R}_n^e(t) = \tilde{p} \times \tilde{p} \textit{ matrix whose } (i, j) \textit{ element is } \langle f_n^i(t), f_n^j(t)\rangle, \tag{2.17}$$

$$\tilde{R}_n^r(t) = \tilde{p} \times \tilde{p} \textit{ matrix whose } (i, j) \textit{ element is } \langle b_n^i(t), b_n^j(t)\rangle. \tag{2.18}$$

The matrices $\tilde{e}_n(t)$, $\tilde{r}_n(t)$, $\tilde{K}_n(t)$, $\tilde{R}_n^e(t)$ and $\tilde{R}_n^r(t)$ are used in the lattice in [3]. The matrices $f_n(t)$ and $b_n(t)$, whose columns are infinitely long, are used in deriving the lattice in [3] but not in the final algorithm. These infinite dimensional matrices are used to derive the lattices in this paper also.

To embed Problem 2.1 in Problem 2.2, we define

$$\tilde{y}(t) = 0, \quad t < 0, \tag{2.19}$$

$$\tilde{y}(0) = [\underset{m\times p}{0} \mid \underset{m\times m}{I}], \tag{2.20}$$

$$\tilde{y}(t) = [\underset{m\times p}{y(t)} \mid \underset{m\times m}{0}], \quad t = 1, 2, \dots. \tag{2.21}$$

Thus $\tilde{p} = p + m$. It is easy to verify

$$Q_{t-n}\tilde{P}_n(t)\tilde{\psi}(t) = [P_{n,t-n}(t)\psi(t) \quad 0], \quad t = 1,2, \dots, \quad n = 1,2, \dots, \quad t \geq n. \tag{2.22}$$

This shows that the first $(t-n)m$ rows of the first p columns of $\tilde{P}_n(t)\tilde{\psi}(t)$ are equal to the first $(t-n)m$ rows of $P_{n,t-n}(t)\psi(t)$. Since all rows of $P_{n,t-n}(t)\psi(t)$ past the first $(t-n)m$ are zero, (2.22) shows that the solution to Problem 2.1 for the sequence $y(t)$ is embedded in the solution to Problem 2.2 for the sequence $\tilde{y}(t)$. Therefore, we can solve Problem 2.1 with the lattice in [3].

To make this solution efficient, though, we must exploit the special structure of the prewindowed problem for $\tilde{y}(t)$. From (2.19)-(2.21), it follows that, for $t = 1, 2, \dots$, and $n = 0, 1, \dots$, the matrices $\tilde{K}_n(t)$, $\tilde{R}_n^e(t)$ and $\tilde{e}_n(t)$ can be written

$$\tilde{e}_n(t) = \underset{m\times p}{[e_n(t)} \mid \underset{m\times m}{0}\,], \qquad \tilde{K}_n(t) = \begin{bmatrix} K_n(t) \\ \hline 0 \end{bmatrix}_{m\times\tilde{p}}^{p\times\tilde{p}}, \qquad \tilde{R}_n^e(t) = \begin{bmatrix} R_n^e(t) & 0 \\ 0 & \lambda^t I \end{bmatrix}_{m\times m}^{p\times p}. \tag{2.23}$$

Also, the initializations in (2.24) and (2.25) are straightforward from (2.12)-(2.21). The residual-error lattice in Section III.B of [3] then becomes Algorithm 2.1 for Problem 2.1.

Initialization 2.1 (For Unwindowed AR Problem)

$$\tilde{r}_0(0) = \underset{m\times p}{[0} \mid \underset{m\times m}{I}\,], \qquad \tilde{R}_0^r(0) = \begin{bmatrix} 0 & 0 \\ 0 & I \end{bmatrix}_{m\times m}^{p\times p}, \quad G_0(0) = \underset{m\times m}{I}. \tag{2.24}$$

$$K_n(t) = 0, \qquad n > t \geq 0. \tag{2.25}$$

Algorithm 2.1 (Residual Error Lattice for the Unwindowed AR Problem)

For each $t \geq 1$,

$$\tilde{r}_0(t) = [e_0(t) \mid 0\,] = [y(t) \mid 0\,], \tag{2.26}$$

$$\tilde{R}_0^r(t) = \begin{bmatrix} R_0^e(t) & 0 \\ 0 & \lambda^t I \end{bmatrix} = \tilde{r}_0^T(t)\tilde{r}_0(t) + \lambda\tilde{R}_0^r(t-1), \qquad G_0(t) = I. \tag{2.27}$$

For $n = 0$ to $min\{t-1..N\}$ (where N is the maximum order),

$$K_{n+1}(t) = \lambda K_{n+1}(t-1) + e_n^T(t)\, G_n^{\#}(t-1)\,\tilde{r}_n(t-1) \tag{2.28}$$

$$G_{n+1}(t) = G_n(t) - \tilde{r}_n(t)\,\tilde{R}_n^{r\#}(t)\,\tilde{r}_n^T(t) \tag{2.29}$$

$$\tilde{R}_{n+1}^r(t) = \tilde{R}_n^r(t-1) - K_{n+1}^T(t)\, R_n^{e\#}(t)\, K_{n+1}(t) \tag{2.30}$$

$$R_{n+1}^e(t) = R_n^e(t) - K_{n+1}(t)\,\tilde{R}_n^{r\#}(t-1)\, K_{n+1}^T(t) \tag{2.31}$$

$$e_{n+1}(t) = e_n(t) - \tilde{r}_n(t-1)\,\tilde{R}_n^{r\#}(t-1)\, K_{n+1}^T(t) \tag{2.32}$$

$$\tilde{r}_{n+1}(t) = \tilde{r}_n(t-1) - e_n(t)\, R_n^{e\#}(t)\, K_{n+1}(t). \tag{2.33}$$

As in [3], $G_n(t)$ is an $m \times m$ matrix. For a matrix M, $M^{\#}$ means any matrix such that $MM^{\#}M = M$.

The residual-error lattice for the unwindowed AR problem has the same form as the residual-error lattice in [3] for the prewindowed problem, but in the lattice for the unwindowed problem the arrays $K_n(t)$, $\tilde{r}_n(t)$

and $\tilde{R}_n^r(t)$ are larger than the corresponding arrays in the prewindowed lattice. While the matrices $R_n^e(t)$ and $G_n(t)$ have the same respective dimensions as in the prewindowed problem, the matrix $\tilde{R}_n^r(t)$ in the unwindowed problem has dimension $(p+m)\times(p+m)$ as opposed to $p \times p$ for the corresponding matrix in the prewindowed problem. The unwindowed lattice should be more complex than the prewindowed lattice, but inverting the larger matrix $\tilde{R}_n^r(t)$ is both undesirable and unnecessary.

From the way in which $R_n^e(t)$, $\tilde{R}_n^r(t)$ and $K_n(t)$ arise in [3] (they are used in computing projections), it follows that $\mathcal{R}(K_{n-1}(t)) \subset \mathcal{R}(R_n^e(t))$ and $\mathcal{R}(K_{n-1}^T(t)) \subset \mathcal{R}(\tilde{R}_n^r(t-1))$. According to Lemma A.1 in the Appendix then, we can generate an $\tilde{R}_n^{r-}(t)$ directly with

$$\begin{aligned} \tilde{R}_{n+1}^{r-}(t) &= \tilde{R}_n^{r-}(t-1) + \tilde{R}_n^{r-}(t-1)\,K_{n+1}^T(t)\,R_{n+1}^{e+}(t)\,K_{n+1}(t)\,\tilde{R}_n^{r-}(t-1)\,, \\ \tilde{R}_0^{r-}(0) &= \tilde{R}_0^{r+}(0) = \tilde{R}_0^r(0)\,, \end{aligned} \tag{2.30'}$$

where M^- is the usual pseudo inverse of a matrix M [9]. For the initialization in (2.30'), recall (2.24). The $\tilde{R}_n^{r-}(t)$ generated by (2.30') is not $\tilde{R}_n^{r-}(t)$ in general.

In the most efficient version of Algorithm 2.1 then, (2.30') replaces (2.30) and $R_n^{e-}(t)$ is used for $R_n^{e-}(t)$ in (2.30). (This is true for solving the FIR problems in Sections 3 and 4, also.) Although it is not necessary, it is most natural to use $G_n^-(t)$ in (2.28).

Also, we normally do not compute $R_n^{e-}(t)$ and $G_n^-(t)$ exactly when these matrices are singular or near singular. Rather, we choose a small number δ and for $\det(R_n^e(t)) < \delta$ or $\det(G_n(t)) < \delta$, we use the approximation

$$(\alpha I + M^T M)^{-1} M^T \approx M^+ \tag{2.34}$$

for small positive α. Numerical studies in [10] show that using (2.34) to approximate $R_n^{e-}(t)$ and $G_n^+(t)$ produces negligible error in the lattice results. For the numerical results in Section 5, we used $\alpha = \delta = 10^{-10}$.

The AR coefficients $A_{n,i}(t)$ for problem 2.1 can be generated at any t by the following algorithm. Like Algorithm 2.1, Algorithm 2.2 is derived from the corresponding algorithm in [3] by embedding Problem 2.1 in Problem 2.2 and then eliminating the parts of the expanded prewindowed algorithm that are not need for the solution of Problem 2.1.

Algorithm 2.2 (AR Coefficients for the Unwindowed AR Problem)

For $n = 1, 2, \ldots, t-1$ and $j = 1, 2, \ldots, n$

$$C_{n+1,j}(t) = C_{n,j}(t) - B_{n,j}(t)\tilde{R}_n^{r=}(t)\tilde{r}_n^T(t), \tag{2.35}$$

$$B_{n+1,j+1}(t) = [B_{n,j}(t) - C_{n,j}(t)G_n^+(t)\tilde{r}_n(t)] - A_{n,j}(t)R_n^{e+}(t)K_{n+1}(t), \tag{2.36}$$

$$A_{n+1,j}(t) = A_{n,j}(t) - [B_{n,j}(t) - C_{n,j}(t)G_n^+(t)\tilde{r}_n(t)]\,\tilde{R}_n^{r=}(t-1)K_{n+1}^T(t), \tag{2.37}$$

The end conditions, for $n = 0, 1, \ldots, t-1$, are

$$A_{n+1,n+1}(t) = [\tilde{R}_n^{r=}(t-1)]_{p\times\tilde{p}}\,K_{n+1}^T(t), \tag{2.38}$$

$$B_{n+1,1}(t) = R_n^{e+}(t)K_{n+1}(t), \tag{2.39}$$

$$C_{n+1,n+1}(t) = [\tilde{R}_n^{r=}(t)]_{p\times\tilde{p}}\,\tilde{r}_n^T(t), \tag{2.40}$$

where $[\tilde{R}_n^{r=}(t)]_{p\times\tilde{p}}$ means the top $p \times \tilde{p}$ block in $\tilde{R}_n^{r\#}(t)$.

3. The FIR Problem (Joint Process Estimation)

Now we assume that, in addition to the sequence of $m \times p$ measurement matrices $y(t)$, we have a sequence of $m \times q$ measurement matrices

$$x(t) = [x^1(t)\, x^2(t) \ \ldots \ x^q(t)] . \tag{3.1}$$

By an n^{th}-order FIR model, we mean

$$x(t) = \sum_{j=1}^{n} y(t-j+1)\, \hat{A}_{n,j} + \varepsilon_n(t) , \tag{3.2}$$

where the $\hat{A}_{n,j}$'s are $p \times q$ matrices referred to as FIR coefficients, and the i^{th} column of $\hat{A}_{n,j}$ is denoted by $\hat{A}^i_{n,j}$. We denote the history of $x(t)$ by

$$\phi(t) = [\phi^1(t)\, \phi^2(t) \ \ldots \ \phi^q(t)] = [x^T(t)\, x^T(t-1)\, x^T(t-2) \ \ldots \ ]^T . \tag{3.3}$$

Problem 3.1. (Unwindowed FIR Problem) For $t = 1, 2, \ldots,$ and $n = 0, 1, \ldots, t$, compute $P_{n,t-1-n}(t+1)\,\phi(t) = P_{n,t-1-n}(t+1)\, Q_{t-1-n}\, \phi(t)$; equivalently, (for $n = 1, 2, \ldots, t$) find matrices $\hat{A}_{n,j}(t)$ such that, for each i ($i = 1, \ldots, q$), the i^{th} columns of these matrices minimize

$$J_3^{i,n}(t) = \sum_{\tau=n}^{t} \lambda^{t-\tau} \, | \, x^i(\tau) - \sum_{j=1}^{n} y(\tau-j+1)\, \hat{A}^i_{n,j}(t) \, |^2 . \tag{3.4}$$

Problem 3.2. (Prewindowed FIR Problem) Assume $x(t) = 0$ and $\tilde{y}(t) = 0$ for $t < 0$. For $t = 0, 1, 2, \ldots,$ and $n = 0, 1, \ldots, t+1$, compute $\tilde{P}_n(t+1)\,\phi(t)$; equivalently, (for $n = 1, 2, \ldots, t+1$) find matrices $\tilde{\hat{A}}_{n,j}(t)$ such that, for each i ($i = 1, \ldots, q$), the i^{th} columns of these matrices minimize

$$J_4^{i,n}(t) = \sum_{\tau=0}^{t} \lambda^{t-\tau} \, | \, x^i(\tau) - \sum_{j=1}^{n} \tilde{y}(\tau-j+1)\, \tilde{\hat{A}}^i_{n,j}(t) \, |^2 . \tag{3.5}$$

As in Section 2, we embed the unwindowed problem in the prewindowed problem by defining the measurement sequence $\tilde{y}(t)$ for the prewindowed problem in terms of the measurement sequence $y(t)$ for the unwindowed problem according to (2.19)-(2.21). We have

$$Q_{t+1-n}\, \tilde{P}_n(t+1)\,\phi(t) = [P_{n,t+1-n}(t+1)\phi(t) \ \ 0] , \quad t = 1, 2, \ldots, \quad n = 1, 2, \ldots , \tag{3.6}$$

so that the first $(t+1-n)m$ rows of the first q columns of $\tilde{P}_n(t+1)\phi(t)$ are equal to the first $(t+1-n)m$ rows (the only possibly nonzero rows) of $P_{n,t+1-n}(t+1)\phi(t)$. Therefore, the solution to Problem 3.1 for the sequences $x(t)$ and $y(t)$ is embedded in the solution to Problem 3.2 for the sequences $x(t)$ and $\tilde{y}(t)$.

To obtain a lattice for Problem 3.2, we must append some new update equations to the prewindowed lattice in [3]. For nonnegative integers t and n, we define

$$\hat{f}_n(t) = [\hat{f}_n^1(t) \ \ldots \ \hat{f}_n^q(t)] = [I - \tilde{P}_n(t+1)]\,\phi(t), \tag{3.7}$$

$$\hat{e}_n(t) = \textit{top } m \textit{ rows of } \hat{f}_n(t), \tag{3.8}$$

$$\hat{K}_{n+1}(t) = q \times \tilde{p} \textit{ matrix whose } (i, j) \textit{ element is } \langle \hat{f}_n^i(t),\ b_n^j(t) \rangle, \tag{3.9}$$

$$\hat{R}_n^e(t) = q \times q \textit{ matrix whose } (i, j) \textit{ element is } \langle \hat{f}_n^i(t),\ \hat{f}_n^j(t) \rangle, \tag{3.10}$$

where, as in Section 2, $\tilde{P}_n(t)$ is the orthogonal projection onto $H_n(t)$ when, in (2.7), p is replaced by $\tilde{p}$ and $\psi'(t-j)$ is replaced by $\tilde{\psi}'(t-j)$ for $i = 1, \ \ldots \ , \tilde{p}$.

To derive order updates, we define

$$P_n^b(t) = \textit{orthogonal projection onto } \textit{span}\{b_n^1(t) \ \ldots \ b_n^{\tilde{p}}(t)\} \tag{3.11}$$

with $b_n^i(t)$ defined as in (2.13). We have then

$$[I - \tilde{P}_{n+1}(t)] = [I - P_n^b(t-1)][I - \tilde{P}_n(t)]. \tag{3.12}$$

From (3.7), (3.9), (3.12) and (2.18), we obtain

$$\hat{f}_{n+1}(t) = \hat{f}_n(t) - P_n^b(t)\hat{f}_n(t) = \hat{f}_n(t) - b_n(t)\,\tilde{R}_n^{r\#}(t)\,\hat{K}_{n+1}^T(t). \tag{3.13}$$

It is straightforward to use (3.7)-(3.10) and (3.13) to derive Initialization 3.1 and the order updates in Algorithm 3.1. With the foregoing equations in this section, the derivations of the time update for $\hat{K}_n(t)$ and of Algorithm 3.2 are similar to those in Sections III.B and III.C of [3] (see [10]). The most difficult of these derivations is that for the time update of $\hat{K}_n(t)$.

Initialization 3.1 (For the Unwindowed FIR Problem, append this initialization to Initialization 2.1.)

$$\hat{R}_0^e(0) = x^T(0)x(0), \quad \hat{K}_1(0) = [\,0 \mid x^T(0)] \tag{3.14}$$

$$\hat{K}_{n+1}(t) = 0, \quad n > t \geq 0 \tag{3.15}$$

Algorithm 3.1. (For the Unwindowed FIR Problem, append this algorithm to Algorithm 2.1.)

For $t \geq 1$

$$\hat{e}_0(t) = x(t), \quad \hat{R}_0^e(t) = x^T(t)x(t) + \lambda \hat{R}_0^e(t-1). \tag{3.16}$$

For $n = 0$ to t

$$\hat{K}_{n+1}(t) = \lambda \hat{K}_{n+1}(t-1) + \hat{e}_n^T(t) G_n^+(t) \tilde{r}_n(t) \tag{3.17}$$

$$\hat{e}_{n+1}(t) = \hat{e}_n(t) - \tilde{r}_n(t) \tilde{R}_n^{r=}(t) \hat{K}_{n+1}^T(t) \tag{3.18}$$

$$\hat{R}_{n+1}^e(t) = \hat{R}_n^e(t) - \hat{K}_{n+1}(t) \tilde{R}_n^{r=}(t) \hat{K}_{n+1}^T(t). \tag{3.19}$$

Algorithm 3.2. (For the FIR problem, append this algorithm to Algorithm 2.2.)

For $n = 1, 2, \ldots, t$ and $j = 1, 2, \ldots, n$,

$$\hat{A}_{n+1,j}(t) = \hat{A}_{n,j}(t) - B_{n,j}(t) \tilde{R}_n^{r\#}(t) \hat{K}_{n+1}^T(t). \tag{3.20}$$

The end condition , for $n = 0, 1, \ldots, t$, is

$$\hat{A}_{n+1,n+1}(t) = [\tilde{R}_n^{r=}(t)]_{p\times\tilde{p}} \hat{K}_{n+1}^T(t). \tag{3.21}$$

Algorithms 3.1 and 3.2 with Initialization 3.1 solve Problem 3.1. When the solution to Problem 3.2 with arbitrary $\tilde{y}(t)$, $t \geq 0$, is desired, Algorithm 3.1 can be appended to the prewindowed lattice in [3]. For this case, the only change in Initialization 3.1 is that $\hat{K}_1(0) = x^T(0)\tilde{y}(0)$ must be used in (3.14). Algorithm 3.2 generates the full matrices $\tilde{\hat{A}}(t)$ for Problem 3.2 if $\hat{A}_{n,j}(t)$, $B_{n,j}(t)$ and $[\tilde{R}_n^{r\#}(t)]_{p\times\tilde{p}}$ are replaced by $\tilde{\hat{A}}_{n,j}(t)$, $\tilde{B}_{n,j}(t)$ and $\tilde{R}_n^{r\#}(t)$, where $\tilde{B}_{n,j}(t)$ is the matrix $B_{n,j}(t)$ generated by the algorithm in [3] for the AR coefficients.

4. Including Initial Parameter Estimates

The algorithms and initializations in the previous sections do not use initial parameter estimates. To include initial estimates of the FIR parameters corresponding to a given order N, we need only change Initializations 2.1 and 3.1.

Problem 4.1. (Unwindowed FIR Problem with Initial Parameter Estimates) For $t = 1, 2, \ldots$, and $n = 1, \ldots, N$, find matrices $\hat{A}_{n,j}(t)$ such that, for each $i (i = 1, \ldots, q)$, the i^{th} columns of these matrices minimize

$$J_5^{i,n}(t) = J_3^{i,n}(t) + \mu\lambda^{t+1} \sum_{j=1}^{n} \lambda^{n-j} \mid \hat{A}_{n,j}^{i}(t) - \overline{A}_{N,j}^{i} \mid_D^2 , \tag{4.1}$$

where $\overline{A}_{N,j}$ is the initial estimate of $\hat{A}_{n,j}$, $D = diag\{\delta_1, \delta_2, \ldots, \delta_p\} \geq 0$, $\mid a \mid_D^2 = a^T D a$ and $\mu \geq 0$.

Like Problems 2.1 and 3.1, Problem 4.1 can be embedded in a prewindowed problem. We define a prewindowed FIR problem similar to Problem 3.2 except that the nonzero data begins at $t = -pN$ instead of $t = 0$. For $j = 1, 2, \ldots, N$ and $k = 1, 2, \ldots, p$, we define

$$\alpha_{N,j,k} = \mu^{1/2} \delta_k^{1/2} \begin{bmatrix} row\ k\ of\ \overline{A}_{N,j} \\ \hline 0\ 0\ \ldots\ 0 \end{bmatrix}_{(m-1)\times q}^{1\times q}, \qquad \beta_k = \mu^{1/2} \delta_k^{1/2} \begin{bmatrix} \overset{k^{th}\ place}{0\ 0\ \ldots\ 1\ \ldots\ 0\ 0} \\ \hline 0\ 0\ \ldots\ 0\ \ldots\ 0\ 0 \end{bmatrix}_{(m-1)\times \tilde{p}}^{1\times \tilde{p}}, \tag{4.2}$$

$$x(j - 1 - Nk) = \lambda^{-(k-1)N/2} \alpha_{N,j,k}, \quad 1 \leq j \leq N, \quad 1 \leq k \leq p. \tag{4.3}$$

We replace (2.19) with

$$\tilde{y}(t) = \begin{cases} \lambda^{-(k-1)N/2} \beta_k, & t = -kN, \quad 1 \leq k \leq p, \\ 0, & all\ other\ t < 0. \end{cases} \tag{4.4}$$

For $t \geq 0$, $\tilde{y}(t)$ is defined by (2.20)-(2.21). It is straightforward to see that the prewindowed FIR problem for these histories of $x(t)$ and $\tilde{y}(t)$ is equivalent to Problem 4.1. Furthermore, for $t = 0$, the various matrices in (2.12)-(2.18) and (3.8)-(3.10) can be computed directly from the definitions of $x(t)$ and $\tilde{y}(t)$ to yield the following.

Initialization 4.1

$$\tilde{r}_0(0) = [\underset{m\times p}{0} \mid \underset{m\times m}{I}], \quad \tilde{r}_n(0) = 0 \quad n = 1, 2, \ldots, N-1 \tag{4.5}$$

$$\tilde{R}^r_0(0) = \begin{bmatrix} \overset{p\times p}{\mu\lambda^N D} & 0 \\ 0 & \underset{m\times m}{I} \end{bmatrix}, \quad \tilde{R}^r_n(0) = \begin{bmatrix} \overset{p\times p}{\mu\lambda^{N-n} D} & 0 \\ 0 & \underset{m\times m}{0} \end{bmatrix}, \quad n = 1, 2, \ldots, N-1 \tag{4.6}$$

$$K_{n+1}(0) = 0, \quad n = 0, 1, \ldots, N-2 \tag{4.7}$$

$$G_0(0) = I, \quad G_n(0) = 0, \quad n = 1, 2, \ldots, N-1 \tag{4.8}$$

$$\hat{R}^e_0(0) = \mu \sum_{j=1}^{N} \lambda^{N-j+1} \bar{A}^T_{N,j} D \bar{A}_{N,j} + x^T(0) x(0) \tag{4.9}$$

$$\hat{K}_1(0) = [\mu\lambda^N \bar{A}^T_{N,1} D \mid x^T(0)], \quad \hat{K}_{n+1}(0) = [\mu\lambda^{N-n} \bar{A}^T_{N,n+1} D \mid 0], \quad n = 1, 2, \ldots, N-1. \tag{4.10}$$

For the solution to Problem 4.1, Initialization 4.1 replaces Initializations 2.1 and 3.1. Algorithms 2.1, 2.2, 3.1 and 3.2 are used as they are stated, except that the maximum n in Algorithms 2.1 and 2.2 is $N-2$ and the maximum n in Algorithms 3.1 and 3.2 is $N-1$.

Note that for $\mu = 0$, Initialization 4.1 reduces to Initializations 2.1 and 3.1. On the other hand, for $\bar{A}_{N,j} = 0$, Initialization 4.1 is different from the previous initializations because they imply no initial parameter estimates, which is different from setting initial parameter estimates equal to zero.

5. Example

We used a sixth-order AR model with $m = p = 1$ to generate the data sequence $y(t)$, $t = 1, 2, \ldots, 100$, from nonzero initial conditions. The true parameters and initial conditions are given in Table 1. These AR coefficients represent a single measurement from a system of coupled, lightly damped oscillators sampled at the rate of 50 Hz.

TABLE 1

True AR Coefficients and Initial Data

j	$A_{6,j}$	$y(1-j)$
1	4.0021	0.27
2	−7.8919	0.18
3	9.6013	0.029
4	−7.5673	0.096
5	3.6927	0.35
6	−0.89871	0.50

First, we will compare results obtained with the unwindowed AR lattice in this paper and results obtained with the prewindowed lattice in [3]. Rather than show the estimates of the AR parameters, we plot in Figure 1 the three frequencies computed from the parameter estimates according to

$$\omega = Im((\log \zeta) \times 50), \tag{5.1}$$

where ζ is an eigenvalue of the AR model. The frequencies corresponding to the true parameters are

$$\omega_1 = 14.549, \quad \omega_2 = 40.743, \quad \omega_3 = 58.862. \tag{5.2}$$

Also, we plot in Figure 2 the one-step-ahead prediction error; at any time t, this is the error between $y(t)$ and the summation on the right side of (2.2) evaluated with the estimated parameters.

In Figures 1 and 2, solid curves correspond to parameters generated by the algorithms in Section 2 of this paper, and the dashed curves correspond to parameters generated with the prewindowed lattice in [3]. In both lattices, we used the forgetting factor $\lambda = .98$. All numerical results presented here are for $n = 6$. If enough data is used, the frequencies corresponding to the parameter estimates from the prewindowed lattice eventually will converge to the true frequencies. This convergence is faster for smaller values of λ,

but to make the convergence significantly faster, λ must be so small that the lattice filter becomes very sensitive to noise.

To illustrate the effect of setting initial parameter estimates with Initialization 4.1, we added zero-mean white noise to the data generated by the AR model for $30 \le t \le 50$. The standard deviation of the noise was .01, which is between 1.5% and 2% of the amplitude of $y(t)$. We generated two sequences of parameter estimates with the unwindowed FIR lattice (i.e., Algorithms 2.1, 2.2, 3.1 and 3.2) and Initialization 4.1 with $N = 6$. We obtained an FIR problem by setting $x(t) = y(t+1)$, $t \ge 1$. For the first sequence of parameter estimates, we started at $t = 1$ with $\mu = 0$ (i.e., no initial parameter estimates) and continued until $t = 100$. For the second sequence of parameter estimates, we also started at $t = 1$ with $\mu = 0$, but at $t = 30$, we re-initialized the FIR lattice, using $\mu = 100$, $D = I$ and $\overline{A}_{N,j} = A_{N,j}(29)$ in Initialization 4.1.

For each of these sequences of parameter estimates, Figure 3 shows the norm of the error between the estimated parameter vector and the true parameter vector. For $1 \le t \le 29$, the two sequences of parameter estimates are identical.

For $t \ge 30$, the measurement noise affects the parameter estimates generated with no resetting much more than it affects the parameter estimates generated after resetting, since the reinitialized FIR coefficients are held near the correct values at $t = 29$ by the heavy weighting μ. With smaller forgetting factor λ, the parameter estimates would return to true values faster after $t = 50$, but smaller λ would defeat the purpose of μ.

We compared the performance of the lattices in this paper, the prewindowed lattice in [3], and the unwindowed lattice in [7] on the current example. Since [7] did not indicate how to generate estimates of either AR or FIR parameters, we compared the values produced by our lattices for the forward residual errors $e_6(t)$ and $\hat{e}_6(t)$ to the corresponding quantities produced by the lattice in [7]. We made this comparison for the AR problem corresponding to Figures 1 and 2, so that $\hat{e}_6(t) = e_6(t+1)$. The quantities $e_m(t)$, $\hat{e}_m(t)$ and $R_m^e(t)$ should correspond, respectively, to the quantities $e_{m,k,k}$, $\varepsilon_{m,k-1,k}$ and $\alpha_{m,k,k}$ (with $k = t$) in [7].

The *Exact Initialization* in [7], with the nonzero value for x_0 indicated in [7], yielded values for the forward error $e_{6,k,k}$, the error $\varepsilon_{6,k-1,k}$ and squared error norm $\alpha_{6,k,k}$ all very close to the corresponding quantities from the prewindowed lattice. Both the lattice in [7] and the prewindowed lattice yielded values of $e_{6,k,k}$ and $\varepsilon_{6,k-1,k}$ on the order of 10^{-2} and values of $\alpha_{6,k,k}$ on the order of 10^{-1}. Our unwindowed lattice yielded values of $e_6(t)$ and $\hat{e}_6(t)$ on the order of 10^{-12} and values of $R_6^e(t)$ on the order of 10^{-14}. These results indicate that our unwindowed lattice was solving the unwindowed problem and that the lattice in [7] was not.

When we shifted all data for $k \geq 0$ forward by one step and set $x_0 = 0$ in the *Exact Initialization*, the lattice in [7] yielded $e_{6,k,k}$, $\varepsilon_{6,k-1,k}$ and $\alpha_{6,k,k}$ that agree with the corresponding quantities from the prewindowed lattice to nine digits, all that we printed. We also ran the lattice in [7] with the *Soft-Constraint Initialization* on page 368 in [7] and compared the results to those from our lattice with soft-contraint initialization. Again, the forward errors from the lattice in [7] were much larger than those from our lattice.

Our analysis of the derivations and algorithms in [7] indicates that, when all data is zero for $t \leq 0$, the lattice in [7] with the *Exact Initialization* solves the prewindowed problem, but the lattice in [7] with either initialization in [7] does not solve the unwindowed problem. These conclusions are confirmed by our numerical results.

6. Conclusions

The purpose of the paper has been to derive efficient lattice filters to solve Problems 2.1, 3.1 and 4.1. Problem 2.1, the unwindowed AR problem with no initial parameter estimates, is solved by Algorithms 2.1 and 2.2 with Initialization 2.1. The residual-error lattice, Algorithm 2.1, is recursive in both time and order. Algorithm 2.2, which generates the estimates of the AR coefficients, also has a lattice structure, but this algorithm is recursive in order only. It can be run at any time t, but it need not be run at every t. For Problem 3.1, the unwindowed FIR problem with no initial parameter estimates, Algorithms 3.1 and 3.2 and Initialization 3.1 are run along with Algorithms 2.1 and 2.2 and Initialization 2.1. The solution to Problem 4.1, the unwindowed FIR problem with initial parameter estimates, also requires Algorithms 2.1, 2.2, 3.1 and 3.2, but Initialization 4.1 replaces Initializations 2.1 and 3.1.

To make the lattices in this paper most efficient, the generalized inverse $R_n^{\#}(t)$ is generated directly with (2.30′); $R_n^{-1}(t)$ need not be generated and (2.30) need not be used. Lemma A.1, on which (2.30′) is based, is a generalization of a well known formula, whose diverse applications were surveyed recently in [11]. Lemma A.1 appears to be new.

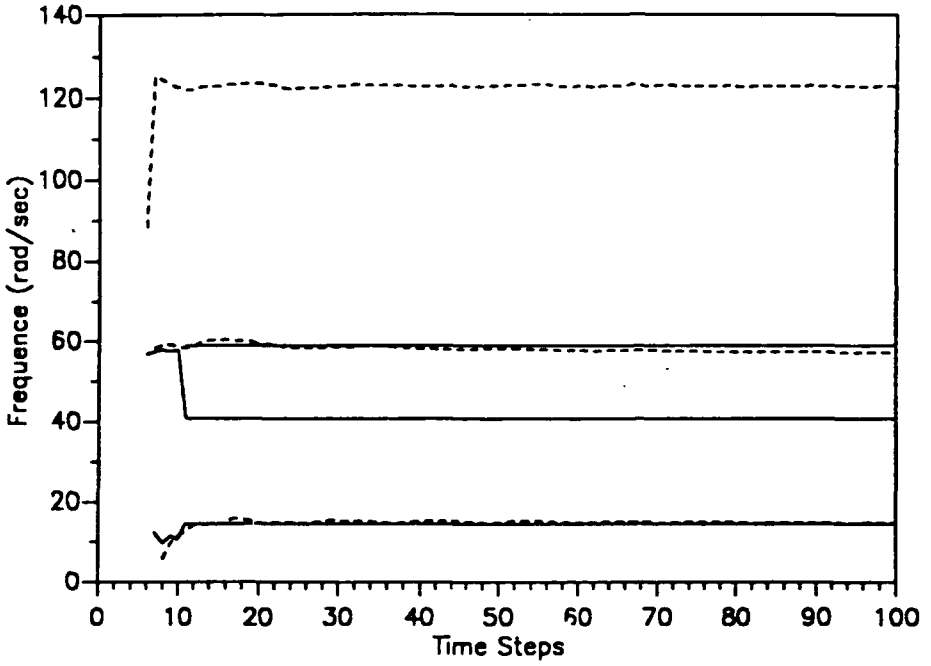

Figure 1: Frequency Estimates

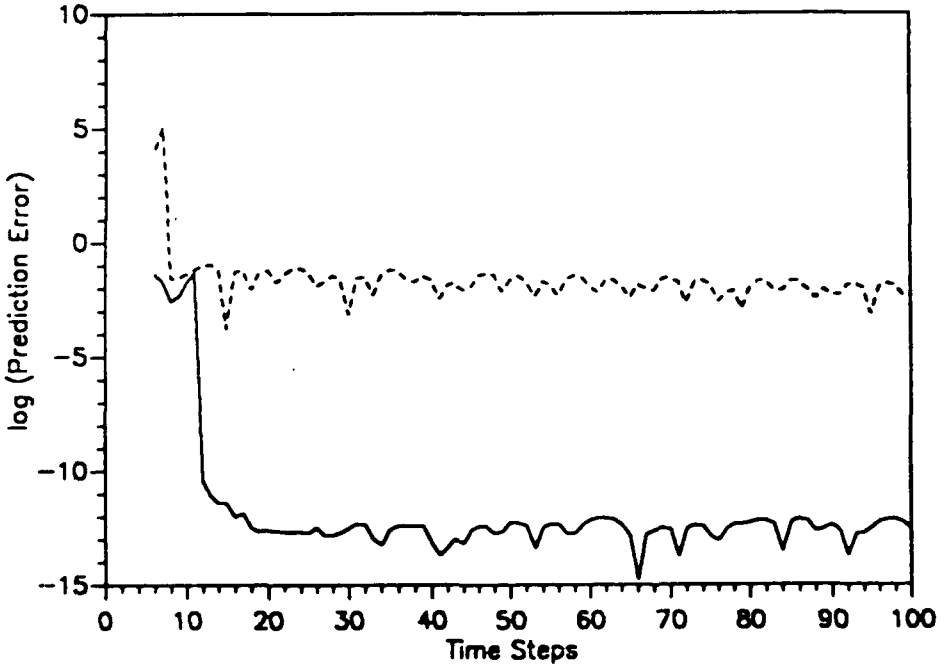

Figure 2: One-Step-Ahead Predition Errors

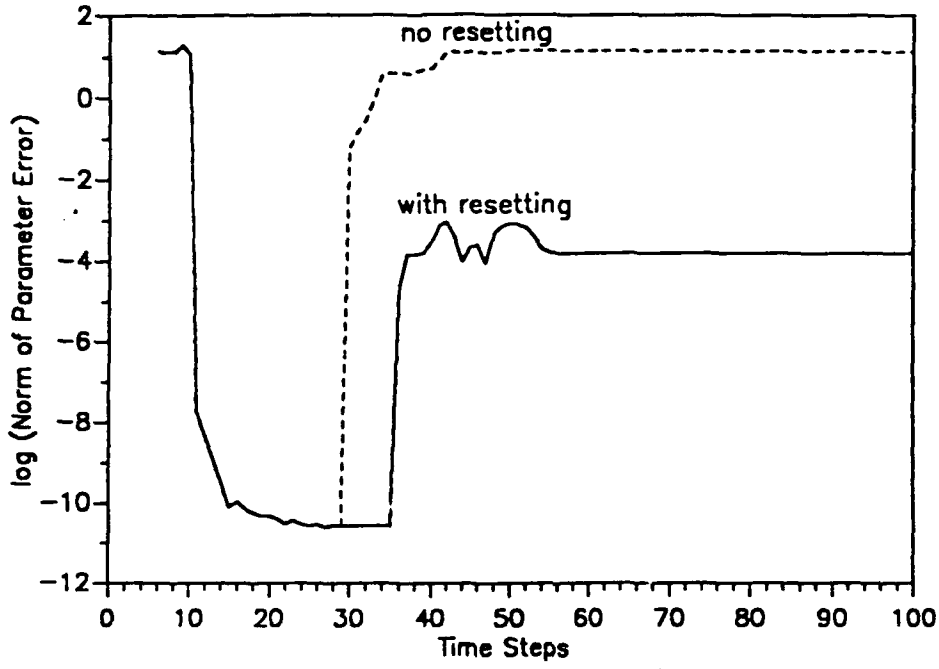

Figure 3: Norms of Parameter Errors

REFERENCES

1. Friedlander, B., "Lattice Filters for Adaptive Processing," *Proceedings of IEEE*, Vol. 70, No. 8, August 1982, pp. 829-867.

2. Honig, M. L., Messerschmitt, D. G., *Adaptive Filters*, New York: Kluwer Academic, 1982.

3. Jabbari, F., Gibson, J. S., "Vector-Channel Lattice Filters and Identification of Flexible Structures," *IEEE Transactions on Automatic Control*, Vol. 33, No. 5, May 1988, pp.448-456.

4. Ljung, L., Söderström, T., *Theory and Practice of Recursive Identification*, The MIT Press, Cambridge, Massachusetts, 1983.

5. Porat, B., Friedlander, B., Morf, M., "Square Root Covariance Ladder Algorithms," *IEEE Transactions on Automatic control*, Vol. AC-27, No. 4, August 1982, pp.813-829.

6. Porat, B., Kailath, T., "Normalized Lattice Algorithms for Least-Squares FIR System Identification," *IEEE Transactions on Acoustics, Speech, and Signal Processing*, Vol. ASSP-31, No. 1, Feb. 1983. pp.122-128.

7. Cioffi, J. M., "An Unwindowed RLS Adaptive Lattice Algorithm," *IEEE Transactions on Acoustics, Speech, and Signal Processing*, Vol. ASSP-36, No. 3. march 1988, pp.365-371.

8. Porat, B., Morf, M., Morgan, D. R., "on The Relationship among Several Square-Root Normalized Ladder Algorithms," *Proceedings of Conference on Information Sciences and Systems*, John Hopkins University, Baltimore, MD, March 1981, pp.495-501.

9. Golub, G. H., Van Loan, C. F., *Matrix Computations* , The Johns Hopkins University Press. Baltimore, Maryland, 1983.

10. Chen, S. W., *Unwindowed Lattice Filters and Application to Variable-order Adaptive Control*, Ph.D. Dissertation, Dept. of Mech., Aero. and Nucl. Engr., UCLA, 1991.

11. Hager, W. W., "Updating The Inverse of A Matrix," *SIAM Review*, Vol. 30, No. 2, June 1989. pp. 221-239.

APPENDIX

Lemma A.1 Let A, B and C be real $\tilde{p} \times \tilde{p}$, $\tilde{p} \times p$ and $p \times p$ matrices, respectively, with $\mathcal{R}(B) \subset \mathcal{R}(A)$, $\mathcal{R}(B^T) \subset \mathcal{R}(C)$, $\mathcal{N}(A) \subset \mathcal{N}(B^T)$ and $\mathcal{N}(C) \subset \mathcal{N}(B)$. Suppose that matrices $\overline{A}$, $\overline{C}$, $A^=$, $C^=$, $\overline{A}^=$ and $\overline{C}^=$ satisfy

$$\overline{A} = A - B C^= B^T, \tag{A.1}$$

$$\overline{C} = C - B^T A^= B. \tag{A.2}$$

$$\overline{A}^= = A^= + A^= B \overline{C}^= B^T A^=, \tag{A.3}$$

and

$$A A^= A = A, \quad C C^= C = C, \quad \overline{C}\,\overline{C}^=\overline{C} = \overline{C}. \tag{A.4}$$

Then

$$\overline{A}\,\overline{A}^=\overline{A} = \overline{A}. \tag{A.5}$$

Proof The inclusion $\mathcal{N}(A) \subset \mathcal{N}(B^T)$ and $A[A^= A - I] = 0$ imply

$$B^T A^= A = B^T. \tag{A.6}$$

Then

$$B^T A^= \overline{A} = B^T A^= A - B^T A^= B C^= B^T = C C^= B^T - B^T A^= B C^= B^T = \overline{C} C^= B^T. \tag{A.7}$$

Hence

$$\mathcal{R}(B^T A^= \overline{A}) \subset \mathcal{R}(\overline{C}). \tag{A.8}$$

Also, replacing A, $A^=$, B, C and $C^=$ in (A.7) and (A.8) with C, $C^=$, B^T, A and $A^=$, respectively, yields

$$B C^= \overline{C} = \overline{A} A^= B. \tag{A.9}$$

Now,

$$\begin{aligned} \overline{A}[A^= - A^= B \overline{C}^= B^T A^=]\overline{A} &= \overline{A} A^= \overline{A} + (\overline{A} A^= B)\overline{C}^= B^T A^= \overline{A} \\ &= \overline{A} A^= \overline{A} + B C^= \overline{C}\,\overline{C}^= B^T A^= \overline{A} = \overline{A} A^= \overline{A} + B C^= B^T A^= \overline{A} = A A^= \overline{A} = \overline{A}. \end{aligned} \tag{A.10}$$

The last identity in (A.10) follows from $\mathcal{R}(\overline{A}) \subset \mathcal{R}(A)$, which follows from $\mathcal{R}(B) \subset \mathcal{R}(A)$ and (A.1).

In general, $\overline{A}^= \neq \overline{A}^-$ (the pseudo inverse of $\overline{A}$), even when A^- and $\overline{C}^-$ are used for $A^=$ and $\overline{C}^=$, respectively, in the right side of (A.3). For example, if

$$A = \begin{bmatrix} 2 & 1 \\ 1 & 1 \end{bmatrix}, \quad B = \begin{bmatrix} 1 \\ 1 \end{bmatrix}, \quad C = 1, \tag{A.11}$$

then

$$\overline{A} = \overline{A}^+ = \begin{bmatrix} 1 & 0 \\ 0 & 0 \end{bmatrix}, \quad \overline{C} = \overline{C}^+ = 0, \tag{A.12}$$

and

$$\overline{A}^= = A^{-1} + A^{-1} B \overline{C}^+ B^T A^{-1} = A^{-1} = \begin{bmatrix} 1 & -1 \\ -1 & 2 \end{bmatrix}. \tag{A.13}$$

A VARIABLE-ORDER ADAPTIVE CONTROLLER FOR A MANIPULATOR WITH A SLIDING FLEXIBLE LINK

by

Y.-K. Kim and J.S. Gibson
Department of Mechanical, Aerospace and Nuclear Engineering
University of California
Los Angeles, CA 90024-1597

ABSTRACT

A digital adaptive controller for a robotic manipulator with a sliding flexible link is presented. The most important feature of the controller is its capability to vary the order of the control law adaptively. This capability results from using a lattice filter for adaptive parameter estimation. The superiority of the variable-order adaptive controller to a fixed-order adaptive controller is demonstrated by numerical simulations, in which the manipulator is represented by the nonlinear equations of motion for a finite element model of the manipulator.

This research was supported by AFOSR Grants 840309 and 870373.

1. INTRODUCTION

Adaptive control of robotic manipulators with rigid links has been studied by many authors [BDS1, DD1, K2, KG1, LE1, NT1, TH1, VK1]. While several authors have studied nonadaptive, usually optimal, control of manipulators with flexible links [BMW1, CS1, F2, UNM1], the literature contains only limited treatment of adaptive control of manipulators with flexible links. In [NM1, NMB1], an unknown payload was estimated on-line to update optimal control gains used to control a linear model of a flexible link. Parameters were identified in [RC1] and then used to design a steady-state linear-quadratic-Gaussian compensator, which was used to control a flexible one-link manipulator. In [CL1], a static elastic deflection was modeled in one simulation of adaptive pole placement for the Stanford arm. A discrete-time adaptive controller designed for a rigid link was applied to a flexible link in [Y1], and the adaptive controller did not appear to suppress all oscillations of the link about the final position.

This paper presents a digital adaptive controller for a manipulator with two links, the second of which is a flexible beam that slides out of the first link (i.e., there is a prismatic joint). The simulation model of the manipulator is nonlinear with time-varying coefficients, but the adaptive controller is based on a linear Auto Regressive-Moving Average (ARMA) model of the input/output characteristics of the plant. Both the parameters and the order of this ARMA model vary adaptively. Becasue the control law is based explicitly on the ARMA model, the adaptive control algorithm is indirect.

The most important feature of the adaptive controller in this paper is that its order can vary adaptively. This capability is important in the problem here because the flexible link abruptly ceases sliding and the associated large axial

deceleration has the effect of a lateral impulse on the link. The impulse excites previously unexcited elastic modes of vibration, so that the effective order of the plant increases. Such changes in plant order, which might result also from impacts or releasing payloads, are handled much better by a controller whose order can vary adaptively.

The order of the controller can vary adaptively because the parameter estimator is a least-squares lattice filter, which is an algorithm for least-squares parameter estimation that is recursive in both time and order. The lattice filter is more efficient than the standard least-squares method for large orders, and it is numerically stable [LL1]. Lattice filters have become prominent in adaptive signal processing [F1, GS1, HM1, LFM1, LMF1, LS1]. Their use in control and identification of flexible structures has been studied in [MS1, SM1, SM2, SM3, W1, WG1], and recently the capability of high-order lattices to identify many modes of very flexible structures has been demonstrated in [J1, JG1, JG2].

Recursive (in time) least-squares estimation is used widely in adaptive parameter identification. See [LS1, GS1] and many other references for the classical algorithm and its convergence properties. This method has one serious limitation for identification of systems like the manipulator in this paper: the classical recursive least-squares algorithm is based on a fixed-order input/output model. In a flexible system, different numbers of modes may be excited at different times, especially in problems with impulse phenomena. For such problems, determination of effective plant order is needed along with identification of parameters. With its order-recursive property, the lattice filter can identify the number of substantially excited modes of a flexible system as well as the parameters of a digital input/output model.

Section 2 describes the manipulator, the finite element model used for simulations, and the ARMA model on which the control law is based. Section 3 discusses the adaptive parameter estimation and presents the lattice filter algorithm. The adaptive control law is discussed in Section 4, along with the reference signal, learning period, control-torque bounds and the criterion for changing the order of the controller. Numerical simulations are presented and discussed in Section 5, and the paper's conclusions are stated in Section 6.

2. MANIPULATOR MODEL

Figure 2.1 shows the manipulator to be controlled, which consists of the rotor whose center is fixed at point O, the rigid link M_1 and the flexible link M_2. The rotor is modeled as a rigid disc and the rigid link is cantilevered to the rotor. The flexible link is a uniform Euler-Bernoulli beam that slides in the rigid link. The free end of the flexible link carries a payload, modeled as a point mass M_{PL}. As Table 2.1 indicates, the manipulator is unusually long and slender. This design is motivated by possible space applications of robotics and by the desire for a highly flexible, rather unwieldy manipulator to challenge the controller.

We assume that the radial motion of the flexible link is controlled by an actuator with sufficiently wide bandwidth and short time constant to make the flexible link follow a specified radial position profile r(t) exactly. Consequently, we treat r(t) and its derivatives as time-varying parameters. The control variable in this paper is a torque u that acts on the rotor at O.

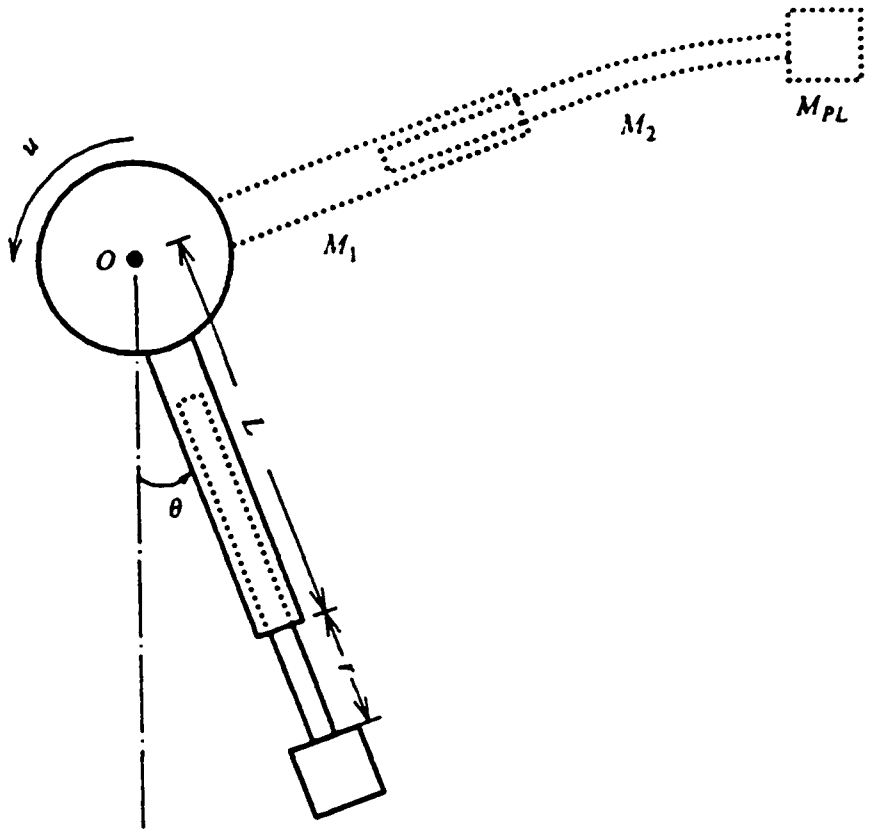

Figure 2.1: Robotic Manipulator with Sliding Flexible Link

TABLE 2.1

Manipulator Data

Combined Rotor and Rigid Link
Radius of rotor plus length of rigid link = $L = 3\,m$
Combined moment of inertia about rotor axis = $168.48\,Kg\,m^2$

Flexible Link(steel)
Length = $3\,m$
Length of segment outside of rigid link = r $(1\,m \le r \le 2\,m)$
Cross section = $0.02\,m \times 0.02\,m$
Mass per unit volume = $7.8 \times 10^3\ Kg/m^3$
Modulus of elasticity = E = $200 \times 10^9\ N/m^2$
Voigt-Kelvin damping coefficient = $c_0 = 0.001$
Fundamental cantilevered beam frequency:
For $r = 1\,m$, $f_1 = 16.356\,Hz$
For $r = 2\,m$, $f_1 = 4.089\,Hz$

In the dynamic model of the manipulator:

- first-order (linear) transverse deformations of the flexible link are modeled;
- axial elastic deformations are neglected;
- coupling between rigid-body angular velocity and elastic displacements is included;
- the contribution of the inertial axial load to bending stiffness is included;
- torques due to gravity are included.

For simulating the response of the manipulator, we use three finite elements of equal length to approximate the part of the flexible link outside the rigid link. Since this portion of the flexible link varies with time, the length r(t)/3 of each of the three elements must vary with time. We use cubic B-splines [S1] as basis functions. This means that we have three elastic degrees of freedom, which we take to be the transverse elastic displacements of nodes 2, 3 and 4. (Node 1 is the point on the flexible link at the end of the rigid link; node 4 is the end of the flexible link to which the payload is attached.) In all then, there are four degrees of freedom in our simulation model of the manipulator. We represent the rigid-body degree of freedom by the angle θ.

For the finite element model of the manipulator, the generalized displacement vector is $q = [\theta\ q_2\ q_3\ q_4]^T$ where q_2, q_3 and q_4 are the transverse elastic displacements of nodes 2-4 on the flexible link. Lagrange's equations for the finite element model have the form

$$M(t)\ddot{q} + D(t)\dot{q} + K(t)q = Q_g(t)g \sin\theta + Bu, \qquad (2.1)$$

where the 4x4 matrices M(t), D(t) and K(t) and the 4-vector $Q_g(t)$ have the forms

$$M(t) = M(q,r(t)), \tag{2.2}$$

$$D(t) = D_1(q,\dot{q},r(t)) + \dot{r}(t)D_2(q,r(t)), \tag{2.3}$$

$$K(t) = K_1(q,\dot{q},r(t),g) + \dot{r}(t)K_2(r(t)) + \ddot{r}(t)K_3(r(t)), \tag{2.4}$$

$$Q_g(t) = Q_g(r(t)), \tag{2.5}$$

$$B = [1 \quad 0 \quad 0 \quad 0]^T, \tag{2.6}$$

and g is the acceleration of gravity. Of course, the generalized coordinates q vary with time, but we want to emphasize that r(t) introduces time-varying coefficients into the equations of motion. We model small Voigt-Kelvin viscoelastic damping (See [CP1]) in the link, which means that the matrix D(t) contains c_0K_b where K_b is the part of K(t) that represents the bending stiffness of the flexible link and c_0 is a damping coefficient. For a complete derivation of the equations of motion, see [K1].

The flexible link slides out of the base link according to the length-versus-time profile in Figure 2.2. During the time between 0 and t_0, which will be used for preliminary parameter identification by the adaptive controller, the radial velocity $\dot{r}$ is zero and the rigid-body angle remains near zero (See Section 4.3). Between t_0 and t_1, the flexible link has the circular radial motion profile with positive $\dot{r}$ and $\ddot{r}$ indicated in Figure 2.2. Between t_1 and t_2, $\dot{r}$ is constant, and starting at t_2, $\dot{r}$ decreases according to the indicated circular radial motion profile until the sliding stops at time t_3. We chose the circular transition segments between t_0 and t_1 and between t_2 and t_3 in Figure 2.2 because the acceleration $\ddot{r}$ is proportional to ρ_1^{-1} and ρ_2^{-1}; we found this to be a convenient parameterization for studying the effects of the radial acce-

of action on the transverse vibration of the flexible link.

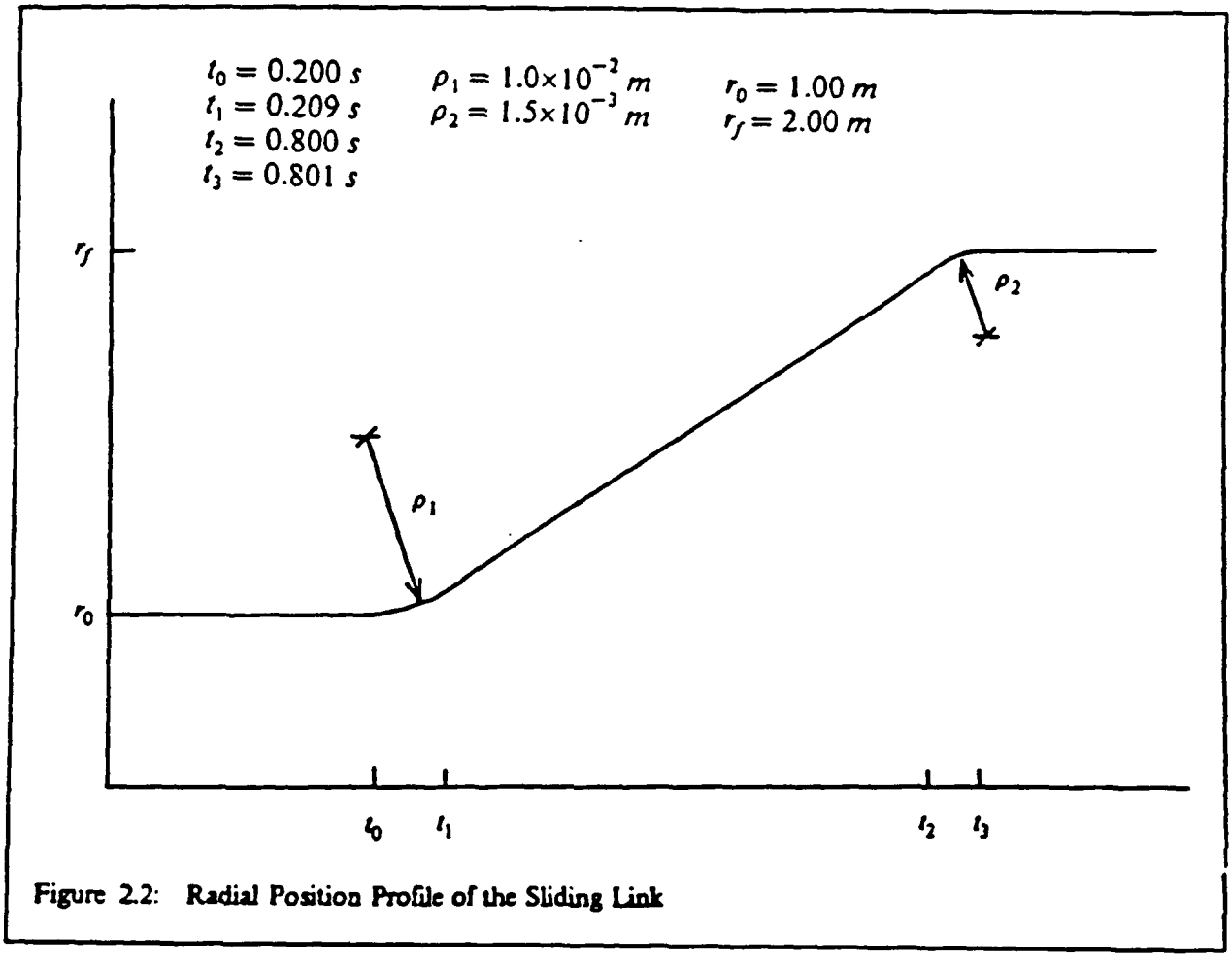

Figure 2.2: Radial Position Profile of the Sliding Link

One of the most important features of the application in this paper results from the fact that we specify that the radial velocity of the flexible link stop very quickly; i.e., $t_3 - t_2$ and ρ_2 are small and the radial acceleration $\ddot{r}(t)$ is very large between t_2 and t_3. With this large $\ddot{r}(t)$, the term $\ddot{r}(t)K_3(r(t))q$ in the equations of motion produces the equivalent of a lateral impulse on the flexible link, unless $q(t)$ is near zero between t_2 and t_3.

Two observations about (2.1) that are important for adaptive control can be made from the detailed equations of motion in [K1]. First, (2.1) can be written

$$M(t)\ddot{q} + D(t)\dot{q} + \tilde{K}(t)q = Bu, \tag{2.7}$$

where

$$\tilde{K}(t) = K(t) - Q_g(t)B^T g(\sin\theta(t))/\theta(t). \tag{2.8}$$

Second, for sufficiently small elastic vibration of the flexible link, no dominant terms in the matrices $M(t)$, $D(t)$ and $\tilde{K}(t)$ involve the elastic displacements q_2, q_3 and q_4 or their time derivatives. Hence the dominant terms in the coefficient matrices in (2.1) and (2.7) vary no faster than the rigid-body angle $\theta(t)$, the corresponding angular velocity, $\dot{r}(t)$ and $\ddot{r}(t)$. This conclusion follows from a tedious but straightforward examination of the detailed equations of motion in [K1]. It results essentially from the fact that we use a linearly elastic model for the flexible link, so that no significant terms in the equations of motion are more than first order in the elastic degrees of freedom.

Now we consider digital control of (2.1) and (2.7) by zero-order sample and hold; i.e., at the beginning of the k^{th} sampling interval ($k = 0, 1, 2, \ldots$), we sample an output vector $y(k)$ and apply a constant control vector $u(k)$ for the duration of the k^{th} sampling interval. We measure the rigid-body angle and the elastic deflection of the free end of the flexible link (the end holding the payload), so that

$$y(k) = \begin{pmatrix} \theta(k) \\ q_4(k) \end{pmatrix} = \begin{pmatrix} y_1(k) \\ y_2(k) \end{pmatrix}. \tag{2.9}$$

According to standard linear system theory, an input/output model for (2.7) with digital input and digital linear output has the form of the ARMA model

$$y(k) + \sum_{i=1}^{N} A_i(k)y(k-1) = \sum_{i=1}^{N} B_i(k)u(k-1) \tag{2.10}$$

where $A_1(k)$ and $B_1(k)$ are matrices of appropriate dimension and N depends on the number of excited flexible modes. In our application $A_1(k)$ is 2x2 and $B_1(k)$ is 2x1. For our simulations, N need not exceed 8 because our simulation model has four degrees of freedom. If the sampling rate is fast compared to the time rates of change of the dominant terms in the coefficient matrices in (2.7)(i.e., if the sampling rate is fast compared to the rigid-body angular velocity and acceleration and $\dot{r}$ and $\ddot{r}$), then the coefficient matrices in (2.10) can be considered to vary slowly. In this case, an adaptive parameter estimator should be able to track the coefficients in (2.10) and predict y(k) from data taken through time k - 1. Such prediction is the basis for the subsequent adaptive control algorithm.

The sampling rate used in the simulations in Section 5 is 100 Hz. Numerical results indicate that the slowly-varying-coefficients hypothesis is valid for our problem except between the times t_2 and t_3 when the impulsive effect of the large radial acceleration first excites higher flexible modes that usually are not excited, causing both the ARMA coefficients and the minimum ARMA order to change abruptly. Since $t_2 - t_3$ is only 10% of one sampling interval, the adaptive controller just sees a switch from one set of slowly varying coefficients to another. The numerical results in Section 5 demonstrate that it is important for the adaptive controller to be able to change both the ARMA coefficients and the ARMA order.

To shed further light on the system to be controlled, we consider the linearized open-loop dynamics of the manipulator with constant r, payload $M_{PL} = .1M_2$, and no gravity moment for the initial value of r = 1m and the final value of r = 2m. Table 2.2 gives the poles and zeros of the continuous-time transfer functions from the control torque to the two measurements. In the complex form

of poles and zeros, the frequency is given in rad/s; for the poles, the damping ratio ζ and the frequency f in Hertz are given in parentheses. We shall emphasize that the numbers in Table 2.2 were not present explicitly in the *nonlinear* finite-element model that we used for all simulations. We computed these poles and zeros after we linearized the simulation model.

As is common with flexible structures, we have a mimimum-phase transfer function for the sensor colocated with the actuator (i.e., the hub-rotation sensor). The transfer function for the noncolocated sensor, which measures the elastic tip deflection, is also minimum-phase after the double pole-zero cancellation. (The transfer function from the control torque to the absolute tip displacement for $r = 1m$ has a real zero at +175, but our controller does not use the absolute tip displacement.)

Another common feature in digital control of flexible structures is that, whatever the samp'ing rate, there will be some modes with frequencies above the Nyquist frequency. Thus we have selected the parameters in Table 2.1 so that, for $M_{PL} = .1M_2$ and $r = 1m$, the linearized plant has two frequencies above the Nyquist frequency (50 Hz in our problem) and, for $r = 2m$, there is one plant frequency above the Nyquist frequency. As illustrated by the simulations described in Section 5, the modes with the two nighest frequencies have sufficient open-loop damping that they are important in the control problem only after being excited by the internal impulse at t_2.

For any value of r, the continuous-time linearized system is controllable because there are no open-loop mode shapes in which the hub rotation is zero and there are no repeated open-loop eigenvalues besides zero, which corresponds to the rigid-body mode. For any constant value of r at which no frequency is a

multiple of 50 Hz, the discrete-time linear plus system (including the modes with frequency above 50 Hz) is controllable in the sense that the state vector can be driven to zero in a finite number of steps. With the positive damping modeled in the beam, even the nonlinear plant is stabilizable for any constant value of r. These conclusions are all easy to verify. We believe and all of our simulations indicate that similar statements about controllability and stabilizability hold for time-varying r, but we have not done the rigorous analysis.

While we have selected the parameters in the simulation model to produce plant characteristics that are common in control problems for flexible structures, this paper does not address the questions that arise when a sequence of finite element models with increasing dimensions is used for control design and simulation. Using more elements in the simulation model in this paper would add more high frequency modes above the Nyquist frequency, and under some excitations these additional modes might require the order of the controller to be larger than the maximum order used in the simulations here. The question of what order the finite element models used for controller design and simulation must have so that the controller can be guaranteed to work well for a distributed model of a flexible structure requires approximation theory and convergence analysis beyond the scope of this paper. Such issues have been addressed extensively for optimal control of flexible structures (see [GA1, GA2] for example), and corresponding theory for adaptive control of flexible structures is a focus of current research. The purpose of this paper is to demonstrate the desirability of a controller that can vary its order adaptively to account for modes that sometimes are excited and sometimes not, and to demonstrate how such a controller can be constructed.

TABLE 2.2

Continuous-Time Poles and Zeros for
$M_{PL} = 0.1 \times M_2$

r = 1m

Poles	(ζ, f)
0	
0	
-2.8 ± i 74.7	(.037, 11.9Hz)
-137.5 ± i 506.1	(.272, 80.5Hz)
-1278.7 ± i 960.4	(1.33, 152.9Hz)

Zeros Channel 1	Zeros Channel 2
	0
-2.3 ± i 67.8	0
-132.7 ± i 497.8	-173.5 ± i 563.0
-1263.7 ± i 960.6	-1135.4 ± i 990.8

r = 2m

Poles	(ζ, f)
0	
0	
-0.4 ± i 26.8	(.015, 4.3Hz)
-12.1 ± i 155.1	(.078, 24.7Hz)
-102.5 ± i 441.0	(.232, 70.2Hz)

Zeros Channel 1	Zeros Channel 2
	0
-0.3 ± i 22.8	0
-11.3 ± i 149.7	-15.6 ± i 176.2
-100.1 ± i 436.1	-86.7 ± i 407.2

3. PARAMETER IDENTIFICATION

For adaptive identification of the coefficient matrices $A_i(k)$ and $B_i(k)$ in (2.10) and determination of the ARMA order N, we use the least squares lattice algorithms in Tables 3.1 and 3.2. These algorithms are from [JG1], and similar algorithms can be found in [LMF1, F1, HM1] and other references.

We will discuss the structure of the lattice filter only briefly to indicate the most important points for the application here. For more detail see [F1, HM1, J1, JG1, LS1]. The lattice structure is based on two sets of vectors called forward and backward residual errors. The forward residual error vectors are obtained from projection of the most recent regression vectors onto the span of previous regression vectors. (Regression vectors contain measurement histories. In the lattice filter, both control system inputs and outputs must be treated as measurements.) The order of the lattice is the order of the ARMA model with which the lattice attempts to fit the data. The norm of the N^{th}-order forward residual error is the minimum value of the objective functional to be minimized by a least-squares estimate of the parameters in an ARMA model of order N. The backward errors are a set of Gram-Schmidt vectors that span the same space as the regression vectors. At each step, the filter updates the first element of each of the error vectors and the norms of the error vectors. The N^{th}-order lattice generates the equivalent of the least-squares fit to data for every ARMA order between 1 and N.

The main lattice algorithm, to be run at every time step, is listed in Table 3.1. The 1x3 matrices $e_N(k)$ and $r_N(k)$ are the first components of the forward and backward residual errors, respectively. See [JG1]. Also, $R_N^e(k)$, $R_N^r(k)$, $K_N(k)$ are 3x3 matrices and $G_N(k)$ is a scalar. The forgetting factor λ is

a positive real number less than or equal to 1, which (when $\lambda < 1$) reduces exponentially the effect of older data. For the simulations in Section 5, we used $\lambda = .99$.

The statement that the lattice is order recursive refers to the fact that the maximum lattice (ARMA) order can be increased by 1 at each time step, up to some limit determined by on-line computing capacity. In practice, N is increased until either it reaches the upper limit or some criterion involving the matrix $R_N^e(k)$ indicates that N need not be increased further.

The diagonal elements of the matrix $R_N^e(k)$ are the squares of the norms of the forward residual errors, which are related closely to prediction error (see [JG1]). These diagonal elements indicate the degree to which an N^{th}-order ARMA model fits the data, and they can be used to determine the order of the plant. In particular, the (1,1) element of $R_N^e(k)$ is a measure of the accuracy of the channel of the ARMA model corresponding to the rigid-body angle of our manipulator. We will use this number to determine the order of the ARMA model to be used for adaptive control, as discussed in Section 4.5.

The ARMA coefficients are obtained from the algorithm in Table 3.2, where $A_{N,1}(k)$, $B_{N,1}(k)$ and $C_{N,1}(k)$ are 3x3 matrices. For each N, the matrix $A_{N,1}(k)$ has the form

$$A_{N,1}(k) = \left[\begin{array}{c|c} -\hat{A}_1(k)^T & \begin{matrix} x \\ x \end{matrix} \\ \hline \hat{B}_1(k)^T & x \end{array}\right] \tag{3.1}$$

where $\hat{A}_1(k)$ and $\hat{B}_1(k)$ are the least-squares estimates at time k of the matrices in (2.10).

Initialize:

$$R_0^e(-1) = R_0^r(-1) = \sigma I, \quad K_{N+1}(k) = 0 \ \text{for} \ N+1 > k \geq 0$$

where σ is a small number (e.g., $\sigma = 10^{-7}$)

For each $k \geq 0$:

$$e_0(k) = r_0(k) = [y^T(k) \ \ u(k)], \quad G_0(k) = 1$$

$$R_0^e(k) = R_0^r(k) = e_0(k)^T e_0(k) + \lambda R_0^e(k-1)$$

For each $k \geq 1$, for $N = 0$ to $k-1$:

$$K_{N+1}(k) = \lambda K_{N+1}(k-1) + e_N^T(k) G_N^{-1}(k-1) r_N(k-1)$$

$$e_{N+1}(k) = e_N(k) - r_N(k-1) R_N^{-r}(k-1) K_{N+1}^T(k)$$

$$r_{N+1}(k) = r_N(k-1) - e_N(k) R_N^{-e}(k) K_{N+1}(k)$$

$$R_{N+1}^e(k) = R_N^e(k) - K_{N+1}(k) R_N^{-r}(k-1) K_{N+1}^T(k)$$

$$R_{N+1}^r(k) = R_N^r(k-1) - K_{N+1}^T(k) R_N^{-e}(k) K_{N+1}(k)$$

$$G_{N+1}(k) = G_N(k) - r_N(k) R_N^{-r}(k) r_N^T(k)$$

Table 3.1 Residual Error Lattice Algorithm

For $N = 1, k-1$ and for $i = 1, N$:

$$C_{N+1,i}(k) = C_{Ni}(k) - B_{Ni}(k) R_N^{-r}(k) r_N^T(k)$$

$$B_{N+1,i+1}(k) = [B_{Ni} - C_{Ni}(k) G_N^{-1}(k) r_N(k)] - A_{Ni}(k) R_N^{-e}(k) K_{N+1}(k)$$

$$A_{N+1,i}(k) = A_{Ni}(k) - [B_{Ni} - C_{Ni}(k) G_N^{-1}(k) r_N(k)] R_N^{-r}(k-1) K_{N+1}^T(k)$$

with

$$A_{N+1,N+1}(k) = R_N^{-r}(k-1) K_{N+1}^T(k)$$

$$B_{N+1,1}(k) = R_N^{-e}(k) K_{N+1}(k)$$

$$C_{N+1,N+1}(k) = R_N^{-r}(k) r_N^T(k)$$

Table 3.2 Algorithm For AR Coefficients

The adaptive controller in this paper is computationally efficient because the bulk of the computation is in the lattice filter and lattice filters are the fastest digital signal processing algorithms for recursive least-squares estimation. The signal-flow structure of the lattice lends itself particularly well to parallel architectures. These points are discussed widely in the digital signal processing literature (e.g., [F1, GS1, HM1, LMF1, LS1]).

4. ADAPTIVE CONTROL

4.1 Control Law

The adaptive control law is based on (2.10) with estimated coefficient matrices $\hat{A}_1(k)$ and $\hat{B}_1(k)$. For defining and computing the control law, the ARMA order N is assumed to be fixed; changing N adaptively is discussed in Section 4.5.

We set

$$\epsilon(k) = \sum_{i=1}^{N} \hat{A}_i(k)\, y(k-i) - \sum_{i=1}^{N} \hat{B}_i(k)\, u(k-i) - \gamma\, y(k-1) + (1+\gamma) y_r(k) \qquad (4.1)$$

where γ is a real number with magnitude less than 1 and $y_r(k)$ is a reference signal to be discussed later. We choose u(k-1) to minimize

$$J(k) = \epsilon(k)^T Q \epsilon(k) + \eta_0 u^2(k-1) \qquad (4.2)$$

where Q is the nonnegative matrix

$$Q = \begin{bmatrix} \eta_1 & 0 \\ 0 & \eta_2 \end{bmatrix} \qquad (4.3)$$

and η_0 is a nonegative real number. When $(\eta_0 + \hat{B}_1(k)^T Q \hat{B}_1(k)) > 0$, the unique control u(k-1) that minimizes (4.2) is

$$u(k-1) = \frac{\hat{B}_1^T(k) Q \{ \sum_{i=1}^{N} \hat{A}_i(k)\, y(k-i) - \sum_{i=2}^{N} \hat{B}_i(k)\, u(t-i) - \gamma\, y(k-1) + (1+\gamma) y_r(k) \}}{\eta_0 + \hat{B}_1^T(k) Q \hat{B}_1(k)} \qquad (4.4)$$

The objective J(k) is motivated by the fact that if $\epsilon(k) = 0$, then (4.1) and (2.10) yield

$$y(k) + \gamma\, y(k-1) = (1+\gamma) y_r(k). \tag{4.5}$$

Since in our problem y(k) and $y_r(k)$ are 2-vectors and u(k-1) is a scalar, it is almost never possible to obtain $\epsilon(k) = 0$. On the other hand, if $\eta_1 > 0$ and $\eta_2 = \eta_0 = 0$, the first element of $\epsilon(k)$ will be zero, so that (4.5) will hold with y(k) and $y_r(k)$ replaced by their respective first elements. (The first element of B_1 is nonzero in our problem.)

The adaptive control law in (4.4) is a variation on a family of model reference schemes discussed in [GS1, Section 6.3]. For a plant that can be represented exactly by (2.10) with fixed order N and constant coefficients, stability results for the closed-loop system produced by the adaptive controller here are similar to stability results in [GS1, Chapters 5 and 6]. In particular, if the first element of B_1 is nonzero, $\eta_1 > 0$ and $\eta_2 = \eta_0 = 0$, then the adaptive controller here reduces to a one-step-ahead model reference adaptive controller for a SISO system. In that case, a sufficient condition for asymptotic stability is that all plant zeros lie inside the open unit disc.

While (2.10) with constant coefficients cannot represent the manipulator in our problem exactly, we have considered linearized motion about the final equilibrium position for asymptotic stability analysis. (In this case, the flexible link no longer slides, and the control torque is perturbed about the appropriate static torque.) A root locus analysis in [K1] shows how the (discrete-time) zeros of the open-loop ARMA model that relates torque perturbations to perturbations in the rigid-body angle depend on the viscoelastic damping in the flexible link. All of these zeros lie on the unit circle when no

damping is modeled in the open-loop manipulator, and all of these zeros move inside the unit circle when damping is modeled in the flexible link. This root locus analysis is straight forward. The analogous distributions of continuous-time zeros for flexible structures with colocated actuators and sensors is well known.

For controlling the manipulator, we take $\eta_1 = 1000$ and $\eta_2 = 1$. Hence the control law in (4.4) almost amounts to SISO control of the rigid-body angle, except near the final position, where the relatively small penalty on the elastic tip deflection slightly improves settling. Also, we take $\eta_0 = 5\times10^{-9}$ in (4.2) and (4.4) so that the control law will be determined uniquely, and because a root locus analysis in [K1] indicates that values of η_0 on the order of 10^{-9}, as opposed to $\eta_0 = 0$, improve the asymptotic stability of the closed-loop system without producing measurable steady-state error.

During the first 10 steps when the manipulator starts to rotate (i.e., after the learning period), we set $\gamma = 0$ to get the manipulator moving rapidly. Then we set $\gamma = 0.96$ for the remainder of the motion so that the controller does not try to eliminate the error between $y(k)$ and $y_r(k)$ unrealistically fast.

4.2 Reference Signal

We are most interested in commanding the absolute position of the manipulator tip, which lies on a circle of radius $L + r$. Since $r(k)(k = 0,1,2, \ldots)$ is already specified by Figure 2.2, we concern ourselves with the tip position $y_{tip}(k)$ measured as arc length along the circle of radius $L + r(k)$. Since

$$y_{tip}(k) = \theta(k)(L+r(k)) + y_2(k), \tag{4.6}$$

we command $y_{tip}(k)$(whose desired profile is shown in Figures 5.1-5.6) indirectly through the reference signal $y_r(k)$ for the output vector in (2.9).

In $\theta_r(t)$, the commanded rigid-body angle, we must account for the static tip deflection due to gravity. We cannot determine this deflection off-line without using the exact data for the flexible link and the exact payload. Therefore, to give the control system the capability to adapt to unknown link characteristics, different payloads and different desired final positions, we use an estimate of the static tip deflection in the reference signal. We construct this estimate, denoted by $\hat{y}_2(k)$, with the low-pass filter

$$\hat{y}_2(k+1) + a\hat{y}_2(k) = (1+a)v(k),$$

$$v(k) = \text{sign}(y_2(k)) \cdot \min \{|y_2(k)|, \Delta_y\}, \tag{4.7}$$

which attenuates oscillations in $y_2(k)$. The constants in (4.7) are $a = -0.986$ and $\Delta_y = 0.1$ m. During the large-angle motion, it is important only that $\hat{y}_2(k)$ be small; near the final position $\hat{y}_2(k)$ should approximate closely the steady-state tip deflection.

We denote the polar coordinates of the desired final tip position by (θ_f, L_f) where $L_f = L + r_f$ and r_f is the final value of r. The reference signal for the output vector in (2.9) is

$$y_r(k) = \begin{pmatrix} \theta_r(k) \\ \hat{y}_2(k) \end{pmatrix} \tag{4.8}$$

with

$$\theta_r(k) = [\theta_f L_f(1-e^{-.05k}) - \hat{y}_2(k)]/(L+r(k)). \tag{4.9}$$

This definition of $\theta_r(k)$ is motivated by and equivalent to

$$\theta_f L_f(1-e^{-.05k}) = \theta_r(k)(L+r(k)) + \hat{y}_2(k), \tag{4.10}$$

which is obtained from (4.6) by replacing $y_2(k)$ with the estimate $\hat{y}_2(k)$ and

replacing $y_{tip}(k)$ by the desired tip position $\theta_f L_f(1-e^{-.05k})$.

We acknowledge that the reference signal here is unusual because it includes implicitly a sensor measurement. We see no way to avoid this feature if the control system is to be truly adaptive.

4.3 Learning Period

To allow the lattice filter to obtain initial parameter estimates before the manipulator starts to move significantly, we use an initial learning period of 0.2 sec, or 20 samples. During this period, the control torque is

$$u_{learn}(k) = 10e^{-.001k}\cos(.4\pi k) \text{ Nm.} \tag{4.11}$$

Because of the frequency of this input, the manipulator does not move significantly from its initial position at $\theta = 0$. We do not attempt to identify the plant order or parameters precisely during this learning period because the ARMA model will begin to change as the flexible link begins to slide and nonlinear terms involving the angular velocity build up during the fast rigid-body rotation. Since the flexible modes are not excited significantly when the manipulator starts to rotate at .2 sec, we use the ARMA order 2 during and immediately after the learning period. Therefore, we need only a simple input for a short learning period to obtain parameter estimates sufficient for beginning the rigid-body motion.

4.4 Bound on Control Magnitude

In the simulations in Section 5, we impose the bound $u_{max} = 5\text{x}10^4$ Nm on the magnitude of the control torque to demonstrate that the algorithm is robust with respect to actuator saturation. This means that if the magnitude of the control

torque in (4.4) exceeds u_{max}, then u_{max} times the sign of the expression on the right side of (4.4) is used for u(k-1).

The torque limit $5x10^4$ Nm is approximately the torque required to produce the angular acceleration associated with the reference signal in the simulations. It is not clear whether such a torque limit is realistic for robot actuators; however, our objective in the simulations is to demonstrate an adaptive control algorithm that can control fast slewing in the presence of elastic vibrations and a variable-order plant. If lower torque limits on available actuators dictate slower angular accelerations, the adaptive control problem should be less challenging because the slower rigid-body motion will excite the elastic modes less than in our simulations.

4.5 Changing the Order of the ARMA Model

As we said in Section 3, the size of the diagonal elements of $R_N^e(k)$(which must be nonnegative) indicates how well an ARMA model of order N fits the input-output data taken through time k. In [JG1], data from a simulated flexible structure was used to demonstate how $R_N^e(k)$ indicates the number of excited modes when small measurement noise is present. The idea is to increase N and look for large drops in the diagonal elements of $R_N^e(k)$. It might appear then that $R_N^e(k)$ should be examined to determine the plant order detected by the lattice filter, and that that ARMA order should be used for adaptive control. However, order determination for adaptive control is not so simple, for two reasons. First, an ARMA model with constant coefficients cannot fit exactly the nonlinear, time-varying manipulator to be controlled here (even without measurement noise), so that we should not expect the kind of sharp drop in $R_N^e(k)$ at the correct order that was seen in [JG1]. Second, as demonstrated in [JG2] with data from an experimental flexible structure, the lattice filter can detect very marginally

excited flexible modes, which usually do not need to be controlled actively. Our simulations have indicated repeatedly that using an ARMA order that corresponds to the total number of modes in the plant leads to poor identification and control if some of the modes are only marginally excited. While marginally excited modes were identified in [JG1, JG2], much longer data records were required than an adaptive controller has time to process before the control law must be computed and executed.

Our criterion for choosing the ARMA (lattice) order adaptively after the learning period combines information in $R_N^e(k)$ with a measure of the control system performance to obtain an indication of the order of the ARMA model needed for effective control. The (1,1) element of $R_N^e(k)$, denoted by $R_N^e(k,1,1)$, is the term in $R_N^e(k)$ most closely related to the accuracy of one-step-ahead prediction for the rigid-body measurement in our problem (again, see [JG1]), and most pertinent for our controller because of the relative weighting in the matrix Q. At each sampling time, the following test indicates whether to change N:

$$e(k) = \frac{c}{[\Delta_0 + \sum_{j=0}^{k} |y(j) - y_r(j)|^2]} \; ; \tag{4.12}$$

$$\begin{aligned} &R_N^e(k,1,1) < e(k) - \Delta_1 \longrightarrow N = N - 1, \\ &R_N^e(k,1,1) > e(k) + \Delta_1 \longrightarrow N = N + 1. \end{aligned} \tag{4.13}$$

We have chosen the constants $c = 50.0$, $\Delta_0 = 1.0 \times 10^{-5}$, and $\Delta_1 = 0.005$ empirically.

This order-change criterion is admittedly ad hoc, and further research might produce a more sophisticated criterion. However, the test here has two

features that we believe will be important in any criterion for changing the order of an adaptive controller: 1) the model-fit-to-data error can remain large if the control system achieves the desired response; 2) the dead band represented by Δ_1 reduces chattering of the ARMA order significantly (although the simulations in Section 5 show that order chattering has not been eliminated entirely). Because magnitudes of desired and true responses and number of sampling points for a typical motion vary with the application, we suspect that any criterion with features 1) and 2) will have constants that must be adjusted empirically for each application.

5. SIMULATION

In the simulations, the nonlinear equations of motion (2.1) were solved numerically with the control torque generated by the adaptive control law in (4.4) and the reference signal given in Section 4.2. (See [K1] for details of the numerical integration). The parameters in the ARMA model (2.10) were estimated with the lattice algorithms in Tables 3.1 and 3.2, and the order of the adaptive controller (i.e., the order of the ARMA model upon which the control law is based) was determined adaptively by the criterion in Section 4.5. Also, the learning period and control torque bounds in Sections 4.3 and 4.4 were used.

Representative examples of the numerous simulations in [K1] are presented in Figures 5.1-5.6. For these figures, the initial position is the vertical position corresponding to $\theta = 0$ in Figure 2.1. In the final position, illustrated by the all-dotted position in Figure 2.1, the polar coordinates of the manipulator tip are $\theta_f = 2$ rad and $L_f = 5$m (recall Section 4.2). In the figures, TIP POSITION is the y_{tip} in (4.6) and DESIRED TIP POSITION at time k is $\theta_f L_f(1-e^{-.05k})$(recall (4.9) and (4.10)). TIP POSITION is in meters, and TIME is

in seconds. CONTROL TORQUE in the figures is the control u divided by the bound u_{max}.

For all six figures here, the same adaptive controller was used (i.e., all the same constants in the equations in Section 4), except that in Figures 5.2 and 5.4, the order N of the adaptive controller was fixed at 2. For Figures 5.1, 5.3, 5.5, and 5.6, the maximum allowable order of N was 8. To emphasize the role that the lattice filter plays in adjusting the order of the controller, the order of the controller is labeled LATTICE ORDER in the figures.

The gravitational moment on the manipulator was included in the simulation model for Figures 5.1-5.4, but no gravity was modeled for Figures 5.5 and 5.6. In other words, the manipulator moved in a vertical plane for Figures 5.1-5.4 and in a horizontal plane for Figures 5.5 and 5.6. Thus a steady-state control torque equal to approximately 1% of the maximum control torque is required in Figures 5.1-5.4 to offset the torque due to gravity. The steady-state control torque in Figures 5.5 and 5.6 is zero.

Figures 5.1 and 5.2 compare the variable-order adaptive controller with an adaptive controller of fixed order 2 for a payload M_{PL} equal to 10% of the mass of the flexible link. Until the effective lateral impulse at 0.8 sec produced by the sudden halt of the radial motion, the second-order adaptive controller is sufficient. The impulse greatly excites transient elastic vibration in the manipulator and the lattice (ARMA) order in Figure 5.1 is adjusted automatically (in six steps) to the maximum order N = 8. When most of the vibration is taken out of the system, the lattice order is decreased back to 2.

It is not surprising that a second-order controller produces poor transient response in the presence of significant vibrations of the flexible link. A more

interesting question is whether we should not just fix the order of the controller at 8 throughout the motion. We have simulated the response for fixed-order controllers with N = 8 and other orders between 2 and 8, and the simulations almost always show a response that becomes unstable before .8 sec, when the higher order is needed in the controller. It appears that when the order of the ARMA model is higher than that needed to fit the input/output data for the plant, the estimates of the redundant parameters are so poor that the adaptive prediction upon which the control law is based is very poor.

Figures 5.3 and 5.4 compare the variable and fixed-order adaptive controllers for a payload equal to 50% of the mass of the flexible link. While the superiority of the variable-order controller is still clear from Figures 5.3 and 5.4, these and other simulations in [K1] show that the difference between the performance produced by the variable-order controller and that produced by the fixed-order controller decreases with increasing payload. With a payload equal to 70% of the mass of the flexible link, both the variable and the fixed-order controllers produce a response very similar to that in Figure 5.3 (when the gravitational moment is present).

We are not certain why the change in controller order is less important for heavier payloads. The need to increase the controller order is greatest when the internal impulse at 0.8 sec has its greatest effect on the transverse vibrations of the flexible link, and the magnitude of this impulse is proportional to the magnitude of the elastic deformation at the time of the impulse. More extensive data in [K1] indicates that, for the commanded motion in the simulations here, the elastic deformation with the larger payloads is small at 0.8 sec. For heavier payloads, when we time the internal impulse to coincide with larger elastic deformation, the improvement made by the variable-order control-

ler over the fixed-order controller becomes larger; however, in most simulations the difference between variable-order and fixed-order controllers is still greater for lighter payloads.

The control constants η_0, η_1, η_2, etc. in the adaptive control law were selected empirically to produce good response for a wide range of payloads when the manipulator moves in a vertical plane under the influence of gravity. Figures 5.5 and 5.6 demonstrate that the variable-order adaptive controller is sufficiently robust to continue to stabilize the manipulator about the desired final position when the gravitational torque is removed from the simulation model, although the response does degrade. The control constants can be adjusted to optimize the response in the horizontal plane, but using the same controller for all of the Figures here better demonstrates the adaptive capability of the controller.

Figures 5.1 and 5.5 show some chatter in the lattice order. The criterion in Section 4.5 for order-determination has eliminated most such chatter. A better criterion might eliminate the chatter entirely. We have no simulations with the order determination criterion here in which this chatter appears to degrade the response of the manipulator.

6. CONCLUSIONS

The motion of the manipulator, in both the horizontal and vertical planes, can be controlled adaptively for a wide range of payloads. Because of the internal impulse associated with the sudden halt in sliding of the flexible link, the capability of the controller to vary its order adaptively is very important. The lattice filter used for the on-line parameter estimation pro-

vides the variable-order capability, which the standard least-squares algorithm and other parameter estimation schemes commonly used in adaptive control do not provide. Also, since a lattice of order N generates parameter estimates for ARMA models of all orders between 1 and N, the additional computation required for the controller capable of varying its order between 1 and N, as opposed to a controller of fixed order N, is only the minor computation required for the order determination criterion in Section 4.5.

REFERENCES

BDS1 Balestrino, A., De Maria, G., and Sciavicco, L., "An Adaptive Model Following Control for Robotic Manipulator," *ASME J. of Dyn. Sys. Meas. and Control*, Vol. 105, Sept. 1983, pp. 145-151.

BMW1 Book, W.J., Maizza-Neto, O., and Whitney, D.E., "Feedback Control of Two Beam, Two Joint Systems with Distributed Flexibility," *ASME J. of Dyn. Sys. Meas., and Control*, Vol. 97, No. 4, Dec. 1975.

CL1 Chung, C.H., and Leininger, G.G., "Adaptive Self-Tuning Control of Manipulators in Task Coordinate System," *Proceedings, International Conference on Robotics*, Atlanta, Georgia, March 12-15, 1984, pp. 608-612.

CP1 Clough, R.W., and Penzien, J., *Dynamics of Structures*, McGraw Hill, New York, 1975.

CS1 Cannon, R.H., and Schmitz, E., "Initial Experiments on the End-Point Control of a Flexible One-Link Robot," *Int. J. of Robotics Research*, Vol. 2, No. 3, 1985, pp. 73-88.

DD1 Dubowsky, S., and Des Forges, D.T., "The Application of Model Referenced Adaptive Control to Robotic Manipulators," *ASME J. of Dyn. Sys. Meas., and Control*, 101, 1979.

F1 Friedlander, B., "Lattice Filters for Adaptive Processing," *Proceedings of IEEE*, Vol. 70, No. 8, Aug. 1982, pp. 829-867.

F2 Fukuda, T., "Flexibility Control of Elastic Robotic Arms," *J. of Robotic Systems*, 2(1). 1985, pp. 73-88.

GS1 Goodwin, G.C., and Sin, K.S., *Adaptive Filtering Prediction and Control*, Prentice-Hall, Inc., Englewood Cliffs, New Jersey, 1984.

HM1 Honig, M.L., and Messerschmitt, D.G., *Adaptive Filters*, Kluwer Academic Publishers, 1984.

J1 Jabbari, F., *Vector-Channel Lattice Filters and Identification of Flexible Structures*, Ph.D. dissertation, UCLA, 1986.

JG1 Jabbari, F., Gibson, J.S., "Vector-Channel Lattice Filters and Identification of Flexible Structures," *IEEE Trans. on Automatic Control*, Vol. 33, No. 5, May 1988, pp. 448-456.

JG2 Jabbari, F., Gibson, J.S., "Adaptive Identification of a Flexible Structure by Lattice Filters," *AIAA J. Guidance, Control and Dynamics*, Vol. 12, No. 4, July-August 1989, pp. 548-554.

K1 Kim, Y.-K., *Adaptive Control of a Robotic Manipulator with a Sliding Flexible Link*, Ph.D. dissertation, UCLA, 1988.

K2 Koivo, A.J., "Self-Tuning Manipulator Control in Cartesian Base Coordinate System," *ASME J. of Dyn. Sys. Meas., and Control*, Vol. 107, Dec. 1985.

KG1 Koivo, A.J., and Guo, T.H., "Adaptive Linear Controller for Robotic Manipulators," *IEEE Trans. on Automatic Control*, Feb. 1983.

LE1 Lim, K.Y., and Eslami, M., "Adaptive Controller Designs for Robotic Manipulator Systems Yielding Reduced Cartesian Error," *IEEE Trans. on Automatic Control*, Vol. AC-32, No. 2, Feb. 1987, pp. 184-187.

LFM1 Lee, D.T.L., Friedlander, B., and Morf, M., "Recursive Ladder Algorithms for ARMA Modeling," *IEEE Trans. on Automatic Control*, Aug. 1981, pp. 753-764.

LL1 Ljung, S., Ljung, L., "Error Propagation of Recursive Least-Squares Adaptation Algorithms," *Automatica*, Vol. 21, 1985, pp. 157-167.

LMF1 Lee, D.T.L., Morf, M., Friedlander, B., "Recursive Least Squares Ladder Estimation Algorithms," *IEEE Trans. on ASSP*, June 1981, pp. 627-641.

LS1 Ljung, L., Soderstrom, T., *Theory and Practice of Recursive Identification*, The MIT Press, 1983.

MS1 Montgomery, R.C., and Sundararajan, N., "Identification of a Two Dimensional Grid Structure Using Least Squares Lattice Filters," *J. of the Astronautical Sciences*, Vol. 33, 1985, pp. 33-47.

NM1 Nelson, W.L., and Miltra, D., "Load Estimation and Load Adaptive Optimal Control for a Flexible Robot Arm," *1986 IEEE International Conference on Robotics and Automation*, pp. 206-211.

NMB1 Nelson, W.L., Miltra, D., and Boie, R.A., "End Point Sensing and Load Adaptive Control of a Flexible Robotic Arm," *1985 American Control Conference*, June 1985, pp. 1410-1415.

NT1 Nicosia, S., and Tomei, P., "Model Reference Adaptive Control Algorithms for Industrial Robots," *Automatica*, Vol. 20, No. 5, 1984, pp. 635-644.

RC1 Rovner, D.M., and Cannon, R.H., "Experiments Toward On-Line Identification and Control of a Very Flexible One-Link Manipulator," *International J. Robotics Research*, Vol. 6, No. 4, Winter 1987, pp. 3-19.

S1 Schultz, M.H., *Spline Analysis*, Englewood Cliffs, New Jersey, Prentice-Hall, 1973.

SM1 Sundararajan, N., Montgomery, R.C., "Identification of Structural Dynamics Systems Using Least Squares Lattice Filters," *AIAA J. Guidance, Control and Dynamics*, Vol. 6, 1983, pp. 374-381.

SM2 Sundararajan, N., Montgomery, R.C., "Adaptive Modal Control of Structural Dynamics Systems Using Recursive Lattice Filters," *AIAA J. Guidance, Control and Dynamics*, Vol. 8, 1985, pp. 223-229.

SM3 Sundararajan, N., Montgomery, R.C., "Experiments Using Lattice Filters to Identify the Dynamics of a Flexible Beam," *J. of Dyn. Sys. Meas. and Control*, Vol. 107, Sept. 1985.

TH1 Tomizuka, M., and Horowitz, R., "Model Reference Adaptive Control of Mechanical Manipulators," *IFAC Adaptive Systems in Control and Signal Processing*, San Francisco, 1983, pp. 27-32.

UNM1 Usoro, P.B., Nadira, R., Mahil, D., "Control of Light Weight Flexible Manipulators: A Feasibility Study," *Proc. of 1984 American Control Conference*, San Diego, 1984, pp. 1209-1216.

VK1 Vukobratovic, M., and Kireanski, N., "An Approach to Adaptive Control of Robotic Manipulators," *Automatica*, Vol. 21, No. 6, 1985, pp. 639-647.

W1 Wiberg, D.M., "Frequencies of Vibration Estimated by Lattice," *J. of the Astronautical Sciences*, Vol. 33, 1985, pp. 48-60.

WG1 Wiberg, D.M., and Gillis, J.T., "Estimation of Frequencies of Vibration Using Lattices," *Proc. of 24th IEEE-CDC, Ft. Lauderdale, FL.*, Dec. 1985.

Y1 Yuh, J., "Application of Discrete-Time Model Reference Adaptive Control to a Flexible Single-Link Robot," *Journal of Robotic Systems*, 4(5), Oct. 1987, pp. 621-630.

GA1 Gibson, J.S., and Adamian, A., "Approximation Theory for Linear--Quadratic-Gaussian Optimal Control of Flexible Structures," *SIAM J. Contr. Opt.*, Vol. 29, No. 1, January 1991, pp.1-37.

GA2 Gibson, J.S., and Adamian, A., "A Comparison of Three Approximation Schemes for Optimal Control of a Flexible Structure," to appear, *SIAM Frontiers Edition on Control and Identification of Distributed Systems*, 1991.

A LYAPUNOV ROBUSTNESS BOUND FOR LINEAR SYSTEMS WITH PERIODIC UNCERTAINTIES

U.L. Chen and J.S. Gibson
Mechanical, Aerospace and Nuclear Engineering
University of California, Los Angeles 90024

ABSTRACT

For linear systems involving uncertain parameters with known, constant nominal values and uncertain perturbations that vary sinusoidally with time, Lyapunov robustness analysis is used to determine a stability bound, or margin, for the amplitudes of the parameter perturbations. This bound is the size of a hypercube in parameter space for which asymptotic stability is guaranteed. The bound, which is based on a quadratic Lyapunov function that depends linearly on parameter perturbations, varies with the frequency of the uncertain parameter perturbations. The bound is asymptotically proportional to the square root of this frequency as it becomes large.

This research was supported by the United States Air Force under AFOSR Grant 870373.

1. Introduction

Numerous recent papers [B1-KBH1, PT1-ZK2] have used quadratic Lyapunov functions to develop robustness bounds for linear systems with uncertain parameters. Some papers [HB2, PT1, Y1-ZK1] have dealt with robustness analysis only, while some [B1, HB1, KBH1, P1, PH1, ZK2] have used Lyapunov-based robustness analysis as a basis for design of robust controllers. A common feature of the references just cited and most related work is that a single Lyapunov function is used for the entire set of parameters for which stability is guaranteed. Because of this, the Lyapunov robustness analysis applies to time-varying uncertain parameters (although the nominal plant must be constant). However, the robustness bounds, or margins, produced by such analysis involve only the magnitude of parameter variations; the analysis cannot detect how the allowable magnitude of uncertain time-varying parameters depends on their frequency.

In [L1, LG1], a quadratic Lyapunov function was developed that varies linearly with uncertain plant parameters. Because of the linear dependence on parameters, the method in [L1, LG1] is called a first-order method. For all but one example to date, this first-order method has yielded larger robustness bounds than the sharpest possible method based on parameter-independent Lyapunov functions (see [L1, LG1]). The first-order method in [L1, LG1] does not apply to problems with time-varying uncertainties, though.

This paper extends the approach in [L1, LG1] to linear systems in which the nominal system is time-invariant but the perturbations in uncertain coefficients vary sinusoidally with time. As in [L1, LG1], the Lyapunov function here varies linearly with uncertain parameters. The first-order term in the Lyapunov matrix satisfies a differential equation in which the forcing term contains the sinusoidal perturbations from the nominal plant. As a

result, the Lyapunov function and the resulting robustness margin depend on the frequency of the parameter perturbations. In general, the robustness margin is proportional to the square root of the frequency of the perturbations at large frequencies.

2. Preliminaries

We consider the system

(2.1) $\dot{x}(t) = A(t)\, x(t)$

where $x(t)$ is a real n-vector and the n x n matrix $A(t)$ has the form

(2.2) $A(t) = A(t,p) = A_0 + G(p) \sin\omega t$

where the real matrix $G(p)$ is a linear function of the constant parameter vector $p = [p_1\ p_2\ \ldots\ p_m]^T \in R^m$ and the real matrix A_0 is constant and independent of p.

Definition 2.1. A real n x n matrix function $P(t)$ is a *Lyapunov matrix* for $A(t)$ if i) $P(t)$ is periodic with period $2\pi/\omega$; ii) $P(t)$ is symmetric and positive definite for each t, its maximum eigenvalue is bounded uniformly in t and its minimum eigenvalue is bounded away from 0 uniformly in t; iii) $P(t)$ is piecewise continuously differentiable and the real symmetric matrix

(2.3) $Q(t) = -[\dot{P}(t) + A(t)^T P(t) + P(t) A(t)]$

is nonnegative. Furthermore, $P(t)$ is a *strict Lyapunov matrix* for $A(t)$ if $Q(t)$ is positive definite with its minimum eigenvalue bounded away from 0 uniformly in t.

Theorem 2.2. (Standard Result) The system (2.1) is uniformly exponentially stable if and only if there exists a strict Lyapunov matrix for A(t).

We assume that the eigenvalues of A_0 all have negative real parts, so that for each positive definite symmetric real n x n matrix Q_0 there exists a unique positive definite symmetric real n x n matrix P_0 satisfying

$$A_0^T P_0 + P_0 A_0 = -Q_0. \tag{2.4}$$

We will factor Q_0 uniquely as

$$Q_0 = LL^T \tag{2.5}$$

where L is a real n x n lower triangular matrix with positive diagonal elements.

3. The First-order Method

We define

$$P(t,p) = P_0 + P_1(t,p) \tag{3.1}$$

where, for each value of the parameter vector p, $P_1(t,p)$ is the unique periodic solution to

$$\dot{P}_1(t,p) + A_0^T P_1(t,p) + P_1(t,p) A_0 = -[G^T(p) P_0 + P_0 G(p)] \sin\omega t. \tag{3.2}$$

That (3.2) has exactly one periodic solution follows from the fact that the eigenvalues of A_0 all have negative real parts. The matrix $P_1(t,p)$ is a linear function of the parameter vector p, since G(p) is. Furthermore, $P_1(t,p)$ has the form

$$P_1(t,p) = P_a(p) \cos\omega t + P_b(p) \sin\omega t \tag{3.3}$$

where the real symmetric nxn matrices $P_a(p)$ and $P_b(p)$ are the unique nxn matrices that solve the equations

$$(3.4) \qquad -\omega P_a(p) + A_0^T P_b(p) + P_b(p) A_0 = -[G^T(p)\ P_0 + P_0\ G(p)]$$

$$(3.5) \qquad \omega P_b(p) + A_0^T P_a(p) + P_a(p) A_0 = 0.$$

To motivate our terminology, we note that, if the solution P(t,p) to (2.3) for fixed $Q = Q_0$ is expanded as a Taylor series in p, the zero-order term is P_0 and the first-order term is $P_1(t,p)$.

Next, we define some quantities that will be useful in determining whether P(t,p) is a Lyapunov matrix for A(t,p). First,

$$(3.6) \qquad W(t,p) = L^{-1}[G^T(p)\ P_1(t,p) + P_1(t,p)\ G(p)]\ L^{-T} \sin\omega t$$

where L is the matrix in (2.5). For a matrix M:

(3.7) $\sigma_{max}(M)$ = maximum singular value of M;

(3.8) $\lambda_{max}(M) = \max\{|\lambda|: \lambda \text{ is an eigenvalue of } M\}$ (for square M).

Since P_0 is a strict Lyapunov matrix for A_0, the following two conditions, together, are sufficient for P(t,p) to be a strict Lyapunov matrix for A(t,p) for a given p:

Condition 3.1. $\lambda_{max}(P_0^{-1} P_1(t,p))$ is bounded strictly below 1 uniformly in t.

Condition 3.2. $\sigma_{max}(W(t,p))$ is bounded strictly below 1 uniformly in t.

Definition 3.3. (Hypercube in R^m). For $s \geq 0$,

$$C(s) = \{p = [p_1\ p_2\ \ldots\ p_m]^T: \max_i |p_i| \leq s\}.$$

We note that C(s) is the convex hull of its 2^m vertices.

Definition 3.4. If f is a real-valued function defined on C(1), then

$$\mu_1(f) = \max \{f(p): p \text{ is a vertex of } C(1)\}.$$

Lemma 3.5. Let $\{\xi_1, \xi_2, \ldots \xi_k\}$ be a finite collection of points in a linear space, let S be the convex hull of $\{\xi_1, \xi_2, \ldots \xi_k\}$, and let f be a convex function defined on S. Then $\max \{f(\xi): \xi \in S\} = f(\xi_j)$ for some j.

The proof of this lemma is elementary. See [L1].

We recall that $\sigma_{max}(\cdot)$ is a norm for any space of finite dimensional matrices. Hence $\sigma_{max}(\cdot)$ is a convex function on any such space. Also, for a fixed matrix M, $\lambda_{max}(M^TMN) = \sigma_{max}(MNM^T)$ is a convex function on the space of symmetric matrices N of a given dimension. We will use these facts, along with Lemma 3.5, to estimate the largest hypercube C(s) such that, for each p in the interior of C(s), P(t,p) is a strict Lyapunov matrix for A(t,p).

Since $P_a(p)$ and $P_b(p)$ are linear in p and since a convex function of a linear function is convex, Lemma 3.5 yields

$$\lambda_{max}(P_0^{-1}P_a(sp)) - s\lambda_{max}(P_0^{-1}P_a(p)) \le s\,\mu_1(\lambda_{max}(P_0^{-1}P_a)), \quad p \in C(1) \text{ and } s \ge 0, \tag{3.9}$$

and similarly for $P_b(p)$. Then, since a sum of convex functions is convex and since the square of a nonnegative convex function is convex,

$$\lambda_{max}(P_0^{-1}P_1(t,sp)) \le s\,\sigma_{0max}(Q_0), \quad p \in C(1), \quad s, t \ge 0, \tag{3.10}$$

where

$$\sigma_{0max}(Q_0) = \mu_1([\lambda_{max}(P_0^{-1}P_a)^2 + \lambda_{max}(P_0^{-1}P_b)^2]^{1/2}). \tag{3.11}$$

We factor G(p) as

$$G(p) = G_0G_1(p) \tag{3.12}$$

where G_0 is independent of p and $G_1(p)$ is linear in p. Since $[L^{-1}P_a(p)G_0]$ and $[G_1(p)L^{-T}]$ are linear functions of p, $\sigma_{max}(L^{-1}P_a(p)\ G_0)$ and $\sigma_{max}(G_1(p)L^{-T})$ are convex functions of p, and similarly for $P_b(p)$. Therefore, Lemma 3.5 and elementary properties of $\sigma_{max}(\cdot)$ yield

$$\sigma_{max}(W(t,p)) \le 2\ \mu_1(\sigma_{max}(L^{-1}P_1(t,p)G_0\sin\omega t)) \cdot \mu_1(\sigma_{max}(G_1L^{-T})), \quad p \in C(1). \tag{3.13}$$

(Recall $\mu_1(\cdot)$ from Definition 3.4.). From

$$2\ (P_a(p)\cos\omega t + P_b(p)\sin\omega t)\sin\omega t = P_b(p) + P_a(p)\sin 2\omega t - P_b(p)\cos 2\omega t, \tag{3.14}$$

it follows that

$$2\ \sigma_{max}(L^{-1}P_1(t,p)G_0\sin\omega t) \le \sigma_{max}(L^{-1}P_b(p)G_0) + [\sigma_{max}(L^{-1}P_a(p)G_0)^2 + \sigma_{max}(L^{-1}P_b(p)G_0)^2]^{1/2}. \tag{3.15}$$

Hence (3.13), (3.15) and Lemma 3.5 yield

$$\sigma_{max}(W(t,sp)) \le s^2\ \sigma_{1max}(Q_0)\ \sigma_{2max}(Q_0), \quad p \in C(1), \quad s, t \ge 0, \tag{3.16}$$

where

$$\sigma_{1max}(Q_0) = \mu_1(\sigma_{max}(L^{-1}P_bG_0)) + \mu_1([\sigma_{max}(L^{-1}P_aG_0)^2 + \sigma_{max}(L^{-1}P_bG_0)^2]^{1/2}) \tag{3.17}$$

and

$$\sigma_{2max}(Q_0) = \mu_1(\sigma_{max}(G_1L^{-T})). \tag{3.18}$$

Now we define

$$s_1(Q_0) = 1/\max\{\sigma_{0max}(Q_0),\ (\sigma_{1max}(Q_0) \cdot \sigma_{2max}(Q_0))^{1/2}\}. \tag{3.19}$$

For p in the interior of $C(s_1(Q_0))$, it follows from (3.10)-(3.11) that Condition 3.1 holds and it follows from (3.16)-(3.18) that Condition (3.2)

holds. Therefore, we have the following theorem, which is the main result of the paper.

Theorem 3.6. For each p in the interior of $C(s_1(Q_0))$, $P(t,p)$ is a strict Lyapunov matrix for $A(t,p)$.

From (3.3)-(3.5), it follows that $P_1(t,p)$ is proportional to $1/\omega$ for large ω. From (3.11) and (3.17) then, it follows that $\sigma_{0max}(Q_0)$ and $\sigma_{1max}(Q_0)$ are asymptotically proportional to $1/\omega$. Since $\sigma_{2max}(Q_0)$ is independent of ω, $(\sigma_{1max}(Q_0) \cdot \sigma_{2max}(Q_0))^{1/2}$ dominates $\sigma_{0max}(Q_0)$ for large ω, so that $s_1(Q_0)$ is proportional to $\omega^{1/2}$ for large ω.

4. Numerical Solution of the Lyanpunov Equations

Eliminating $P_b(p)$ from (3.4) and (3.5) yields

$$(4.1)\quad \omega^2 P_a(p) + A_0^{T2} P_a(p) + P_a(p) A_0^2 + 2A_0^T P_a(p) A_0 = \omega [G^T(p) P_0 + P_0 G(p)].$$

The Bartels-Stewart algorithm [BS1] for solving standard Lyapunov algebraic equations can be generalized in the following way to solve (4.1) for $P_a(p)$. Let U be a real unitary matrix such that $U^T A_0 U = A_s$ where A_s has quasi Schur form. Then premultiplying (4.1) by U^T, postmultiplying by U and inserting UU^T where needed yields

$$(4.2)\quad \omega^2 \tilde{P}_a(p) + A_s^{T2} \tilde{P}_a(p) + \tilde{P}_a(p) A_s^2 + 2A_s^T \tilde{P}_a(p) A_s = \omega U^T [G^T(p) P_0 + P_0 G(p)] U$$

where $\tilde{P}_a(p) = U^T P_a(p) U$. The various 1x1, 1x2, 2x1 and 2x2 blocks of (4.2) can be solved recursively as in [BS1].

5. Example

The matrices A_0 and $G(p)$ in (2.2) are the following 4x4 matrices:

$$(5.1) \qquad A_0 = \begin{vmatrix} 0 & I \\ -K_0 & -D \end{vmatrix} \qquad G(p) = \begin{vmatrix} 0 & 0 \\ -K_1 & 0 \end{vmatrix}$$

where

$$(5.2) \qquad K_0 = \begin{vmatrix} 1 & 0 \\ 0 & 4 \end{vmatrix} \qquad D = .05\, K_0 \qquad K_1 = \begin{vmatrix} p_1 & p_2 \\ p_2 & p_3 \end{vmatrix}.$$

Figure 1 shows $s_1(I)$ as a function of ω for $G(p)$ factored as in (3.12) with

$$(5.3) \qquad G_0 = \begin{vmatrix} 0 \\ I \end{vmatrix} \ (4x2), \qquad G_1(p) = \begin{vmatrix} -K_1 & 0 \end{vmatrix} \ (2x4),$$

and for $G(p)$ not factored (i.e., $G_0 = I$ and $G_1(p) = G(p)$). That $s_1(I)$ is asymptotically proportional to $\omega^{1/2}$, as predicted in Section 3, is clear from Figure 1.

Perhaps more interesting are the local minima at $\omega = 1$, 2, 3 and 4. We recall a classical result for the undamped Mathieu equation (see [NM1] or other standard references): a parametric excitation of frequency twice that of the nominal system makes the solution to the equation unstable. Thus the local minima at $\omega = 2$ and $\omega = 4$ (twice the natural frequencies of the nominal system) might be expected. Furthermore, results in [NM1, Chapter 5] for a multi-degree-of-freedom Mathieu equation indicate additional instabilities produced by parametric excitation frequencies equal to sums and/or differences of natural frequencies of the nominal system. (For the one-degree-of-freedom damped Mathieu equation obtained by taking A_0 and $G(p)$ to be 2x2 matrices of the forms in (5.1) and (5.2) with $K_0 = 1$ and $K_1 = p_1$, we have obtained an $s_1(I)$ plot similar to Figure 1 but with only the local minimum at $\omega = 2$.)

References

[B1] D.S. Bernstein, "Robust static and dynamic output feedback stabilization: deterministic and stochastic perspectives," *IEEE Trans. AC*, Vol. AC-32, No. 12, pp. 1076-1084, December 1987.

[BS1] R.H. Bartels and G.W. Stewart, "Solution of the equation AX + XB = C," *Comm. Assoc. Comp. Mach., 15*, pp. 820-826, 1972.

[HB1] W.M Haddad and D.S. Bernstein,"Robust reduced-order modeling via the optimal projection equations with Peterson-Hollot bounds," *IEEE Trans. AC*, Vol. AC-33, No. 7, pp. 692-695, July 1988.

[HB2] D.C. Hyland and D.S. Bernstein, "The majorant Lyapunov equation: a nonnegative matrix equation for robust stability and performance of large scale systems," *IEEE Trans. AC*, Vol. AC-32, No. 11, pp. 1005-1013, November 1987.

[KBH1] L.H. Keel, S.P. Bhattacharyya, and J.W. Howze, "Robust control with structured perturbations," *IEEE Trans. AC*, Vol. AC-33, No.1, pp. 68-78, January 1988.

[L1] M.A. Leal, *Objective and constraint functions for the analysis and design of robust control systems*, PhD dissertation, UCLA, 1988.

[LG1] M.A. Leal and J.S. Gibson, "Lyapunov robustness bounds for linear systems with uncertain parameters," submitted to *IEEE Trans. AC*.

[NM1] A.H. Nayfeh and D.T. Mook, *Nonlinear Oscillations*, Wiley, New York, 1979.

[PT1] R.V. Patel and M. Toda, "Quantitative measures of robustness for linear state space models," *Proc. Joint Automatic Control Conference*, Paper TP8-A, San Francisco, CA, 1980.

[P1] I.R. Peterson, "Stabilization of an uncertain linear system in which uncertain parameters enter into the input matrix," *SIAM J. Contr. Opt.*, Vol. 26, No. 6, pp. 1257-1264, November 1988.

[PH1] I.R. Peterson and C.V. Hollot, "A Riccati equation approach to the stabilization of uncertain linear systems," *Automatica*, Vol. 22, pp. 397-411, 1986.

[Y1] R.K. Yedavalli, "Improved measures of stability robustness for linear state space models," *IEEE Trans. AC*, Vol. AC-30, No. 6, pp. 557-579, June 1985.

[YL1] R.K. Yedavalli and Z. Liang, "Reduced conservatism in stability robustness bounds by state transformation," *IEEE Trans. AC*, Vol. AC-31, No. 9, pp. 863-866, September 1986.

[ZK1] K. Zhou and P.P. Khargonekar, "Stability robustness bounds for linear state-space models with structured uncertainty," *IEEE Trans. AC*, Vol. AC-32, No. 7, pp. 621-623, July 1987.

[ZK2] K. Zhou and P.P. Khargonekar, "On the stabilization of uncertain linear systems via bound invariant Lyapunov functions," *SIAM J. Contr. Opt.*, Vol. 26, No. 6, pp. 1265-1273, November 1988.

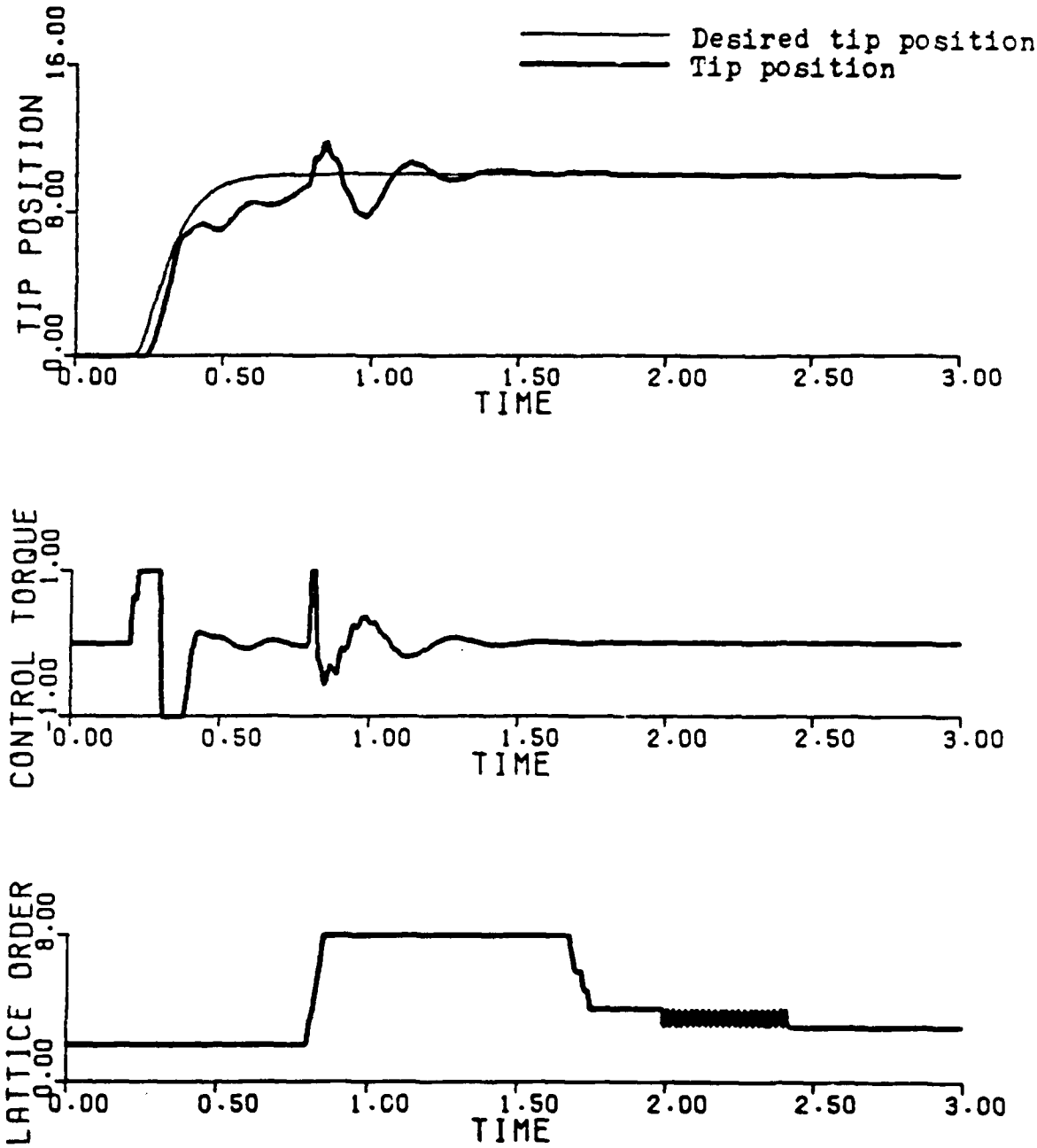

Figure 5.1. Controller Order Variable
Payload Mass = 0.1 x Flexible Link Mass
Gravity Included

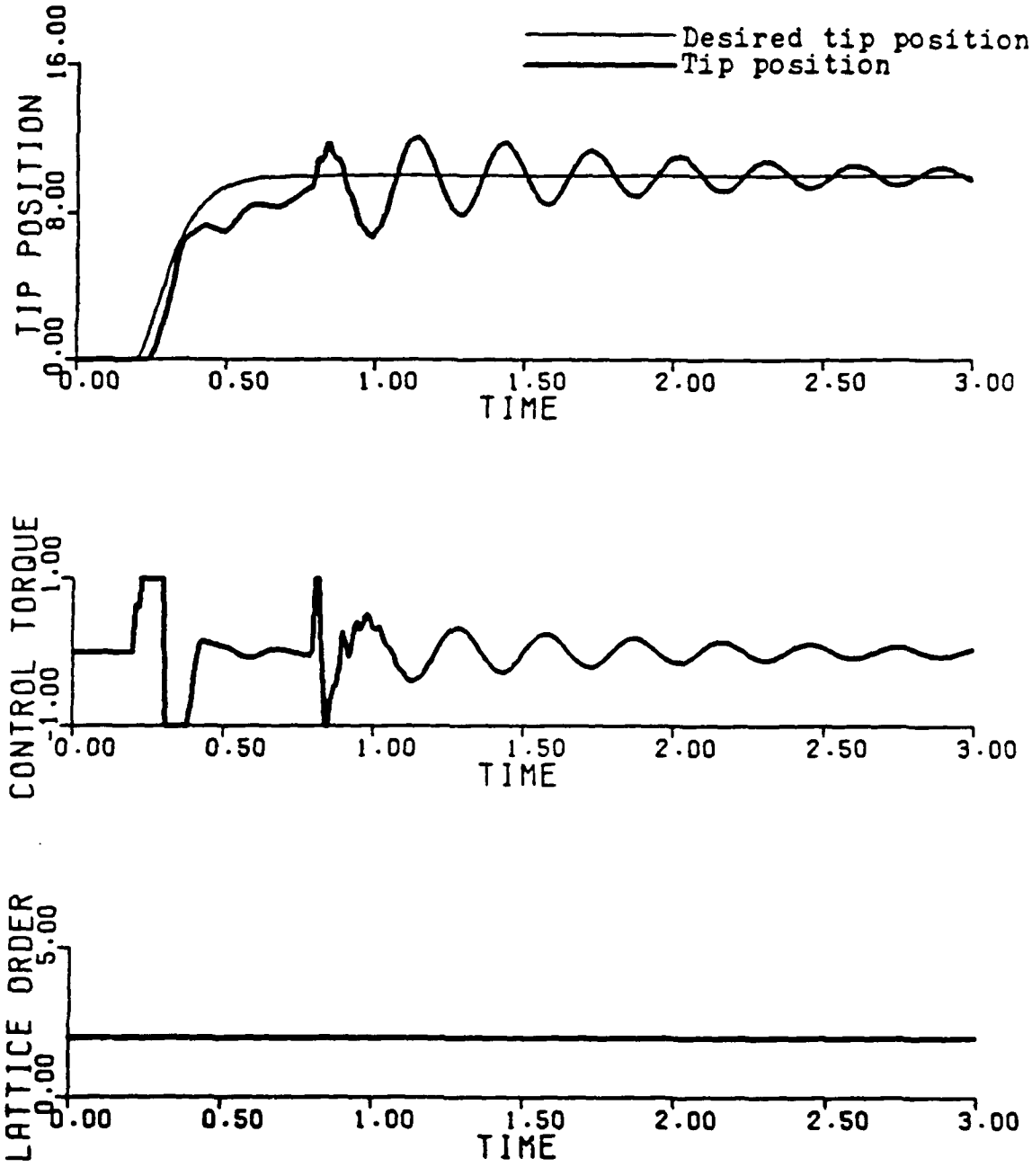

Figure 5.2. Controller Order Fixed, $N = 2$
Payload Mass = 0.1 x Flexible Link Mass
Gravity Included

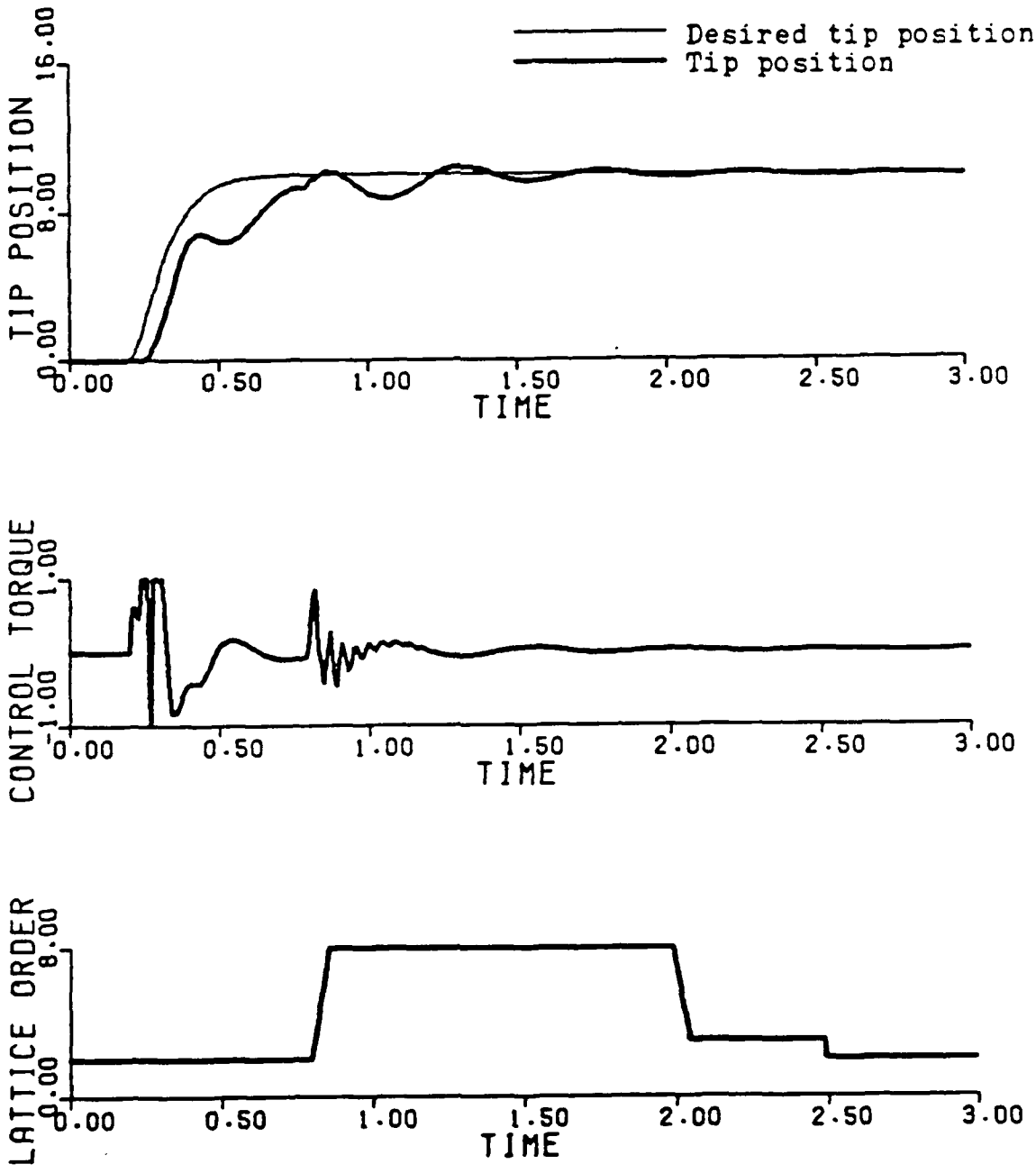

Figure 5.3. Controller Order Variable
Payload Mass = 0.5 x Flexible Link Mass
Gravity Included

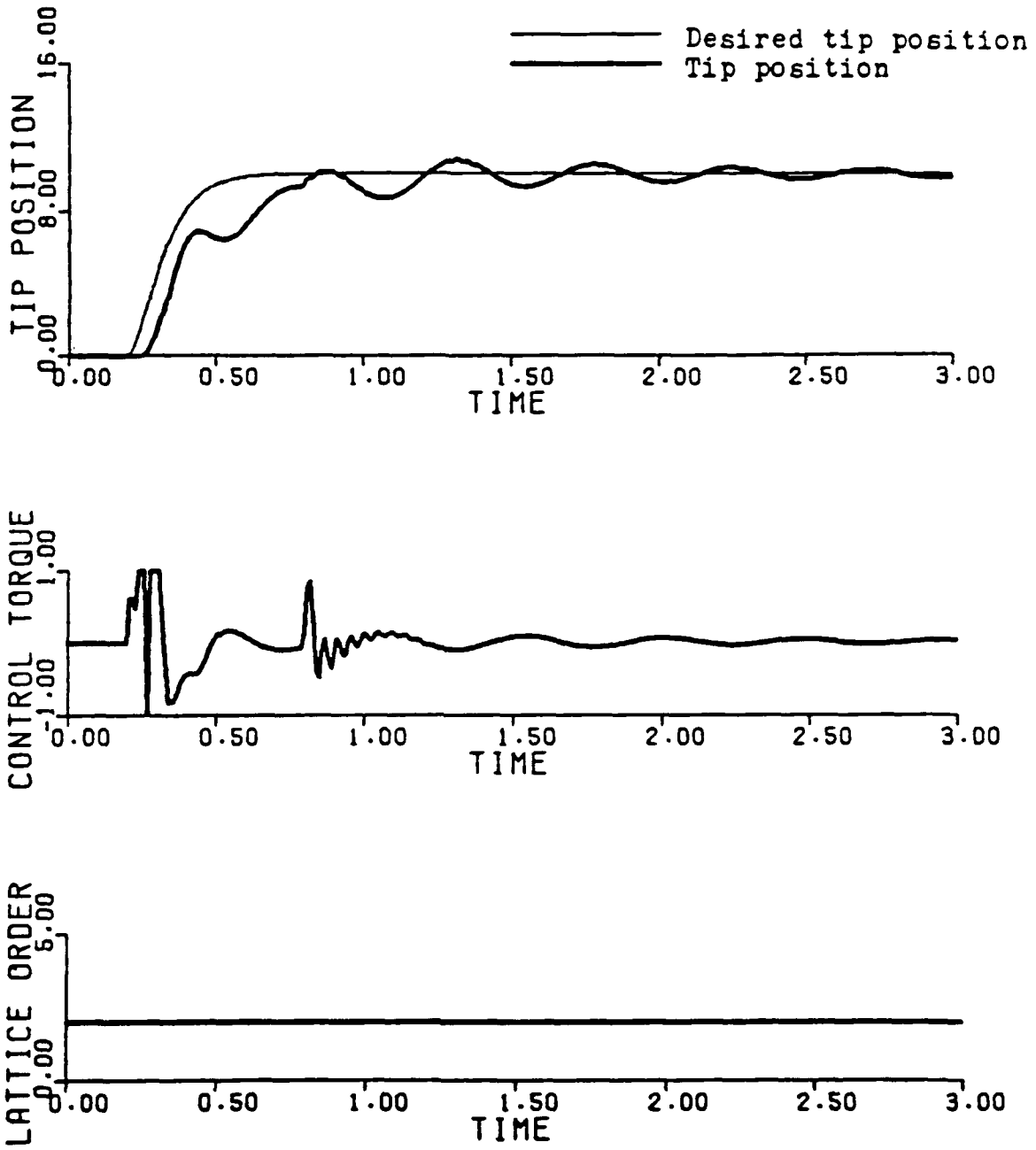

Figure 5.4. Controller Order Fixed, $N = 2$
Payload Mass = 0.5 x Flexible Link Mass
Gravity Included

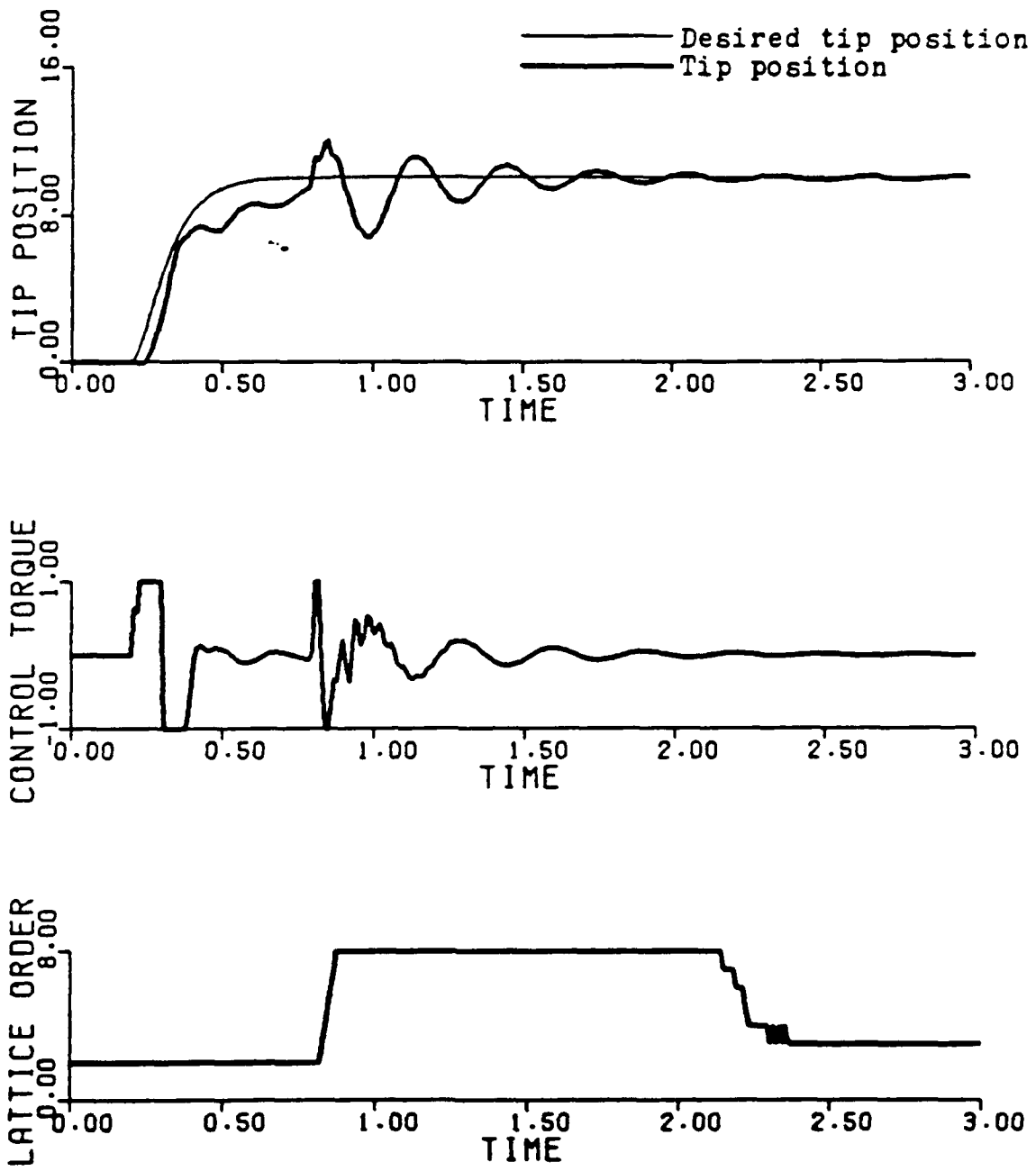

Figure 5.5. Controller Order Variable
Payload Mass = 0.1 x Flexible Link Mass
Gravity Not Included

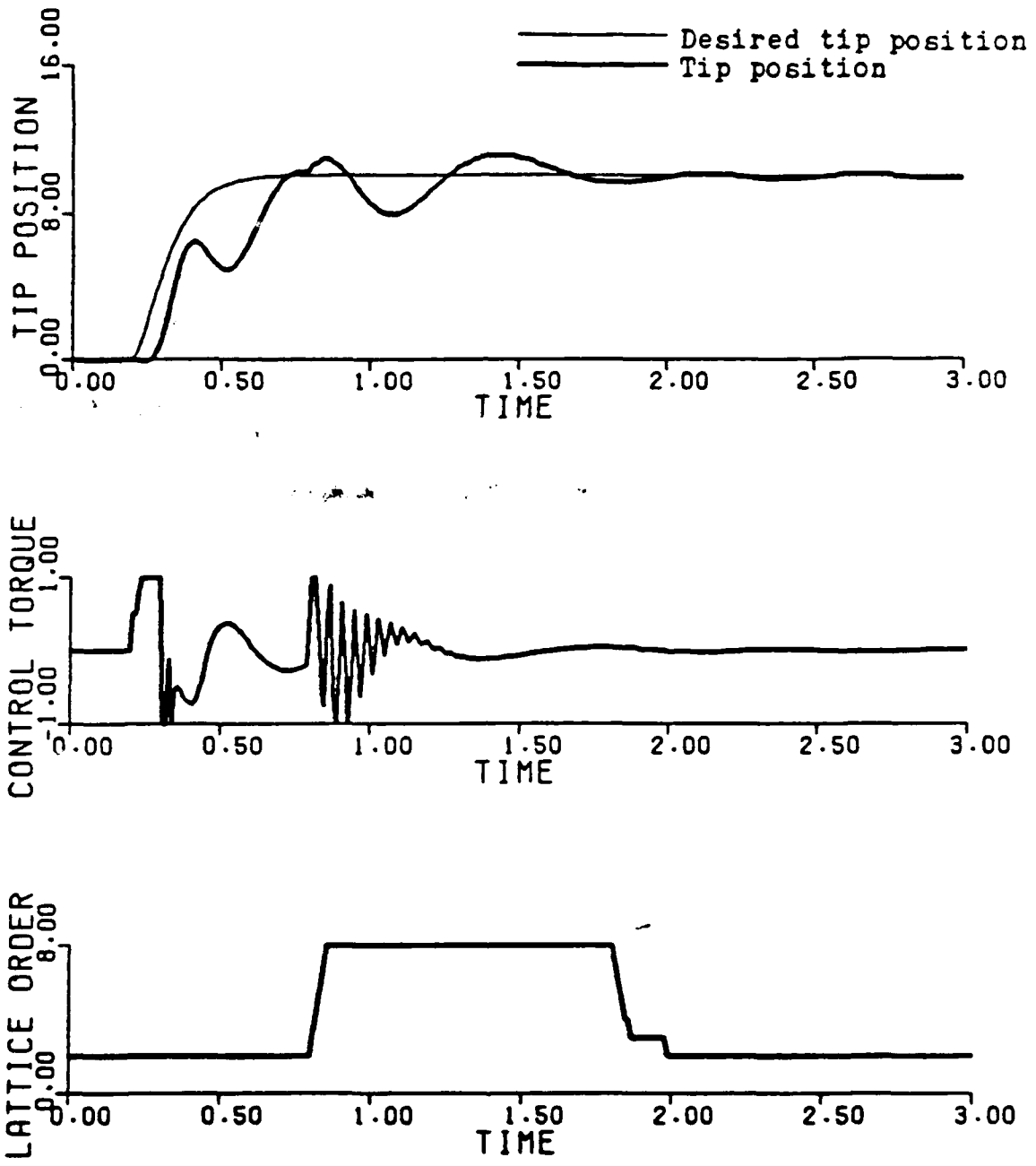

Figure 5.6. Controller Order Variable
Payload Mass = 0.7 x Flexible Link Mass
Gravity Not Included